Syracuse University

SURFACE

Theses - ALL

December 2017

INCREASED STRIATAL VULNERABILITY TO 3-NITROPROPIONIC ACID IN MALE, BUT NOT FEMALE, MICE LACKING INTERLEUKIN-1R1

Matthew Frederick Allen
Syracuse University

Follow this and additional works at: https://surface.syr.edu/thesis

 Part of the Life Sciences Commons

Recommended Citation

Allen, Matthew Frederick, "INCREASED STRIATAL VULNERABILITY TO 3-NITROPROPIONIC ACID IN MALE, BUT NOT FEMALE, MICE LACKING INTERLEUKIN-1R1" (2017). *Theses - ALL*. 190.
https://surface.syr.edu/thesis/190

This Thesis is brought to you for free and open access by SURFACE. It has been accepted for inclusion in Theses - ALL by an authorized administrator of SURFACE. For more information, please contact surface@syr.edu.

Abstract

Interleukin-1β (IL-1β), classically considered as a pro-inflammatory cytokine, has proven essential to cellular defense in nearly all tissues (Kaur et al., 2014, Ren and Torres, 2009). In brain, studies suggest that IL-1β has pleiotrophic effects. It acts as a neuromodulator, has been implicated in the pathogenic processes associated with a number of CNS diseases, but has also been shown to provide protection to the injured CNS. With respect to the latter, IL-1β signalling appears to mitigate pathology and motor symptoms in a mouse model of Huntington's disease (HD), a progressive neurodegenerative condition that targets the striatum. Specifically, HD mice bred onto an IL-1R1 null background demonstrate greater pathological striatal HTT aggregation that coincides with increased severity of motor symptoms (Wang et al., 2010). Of interest for this thesis, mitochondrial dysfunction and subsequent reactive oxygen species (ROS) generation appear to precipitate neuropathology in HD (Emerit et al., 2004). Also of interest, is research from this laboratory demonstrating that IL-1β can protect neural cells against oxidant-induced injury (He et al., 2015) (Chowdhury, unpublished observations). Thus, in this thesis, I explored whether IL-1β signalling could protect against oxidative stress-generated brain damage *in vivo* by employing a chemical model of HD. Toward this end, both male and female mice (16-18 wks) that were either null or wild-type for the IL-1β signalling receptor, IL-1R1, were treated systemically with 3-nitropropionic acid (3-NP), a phyto/fungal mitochondrial toxin (Pedraza-Chaverrí et al., 2009), for a total cumulative dose of 920mg/kg. Comparisons of the histological striatal injury and extent of behavioral symptomatology were made. Motor symptoms —including reduced general locomotor activity, hind limb and truncal

dystonia, and postural instability —increased progressively with increasing days of dosage with 3-NP, in both sexes regardless of genotype, demonstrating no observable difference in response during treatment. Despite this, histological analysis of the striatum, measured over seven levels ranging from +1.22 to -0.18 from bregma, revealed that IL-1R1 null male, but not female, mice had a greater incidence of striatal lesions that were also larger in size compared to their wild-type littermate controls. These results indicate that endogenous IL-1β signalling mitigated 3-NP induced structural, but not functional, striatal injury in male but not female mice.

INCREASED STRIATAL VULNERABILITY TO 3-NITROPROPIONIC ACID IN MALE, BUT NOT FEMALE, MICE LACKING INTERLEUKIN-1R1

by

Matthew Frederick Allen

B.S., The University of Huddersfield, 2015

Thesis
Submitted in partial fulfillment of the requirements for the degree of
Master of Science in *Biology*.

Syracuse University
December 2017

Copyright © Matthew Frederick Allen 2017

All Rights Reserved

Acknowledgments

This work could not have been completed without the advice and assistance of Dr. Sandra Hewett (advisor), Dr. James Hewett, Dr. Frank Middleton (research committee) and all members of the Hewett Laboratory.

Specific acknowledgement must be given to Dr. Yan He, for assistance with the assay of Succinate Dehydrogenase.

Table of Contents

List of Illustrative Materials

List of Abbreviations

3-NP	3-Nitropropionic acid
AALAC	American Association for Laboratory Animal Care
ATP	Adenosine Triphosphate
BBB	Blood brain barrier
GSH	Glutathione
HD	Huntington's Disease
HTT	Huntingtin
IACUC	Institutional Animal Care and Use Committee
ICE	Interleukin-1 converting enzyme
IKK	IκB kinase
IL-1R1	Interleukin-1 receptor type 1
IL-1R2	Interleukin-1 receptor type 2
IL-1Ra	Interleukin-1 receptor antagonist
IL-1RAcP	Interleukin-1 receptor accessory protein
IL-1α	Interleukin-1α
IL-1β	Interleukin-1β
IRAK	Interleukin-1 receptor associated kinase
IκB	Nuclear factor of kappa light polypeptide gene enhancer in B-cells inhibitor
JAX	The Jackson Laboratory
MAP	Microtubule-associated protein
MyD88	Myeloid differentiation primary response 88
NEMO	NF-κB essential modifier
NF-κB	Nuclear factor kappa-light-chain-enhancer of activated B cells
NIH	National Institute of Health
NIK	NF-κB-inducing kinase
PCD	Programmed cell death
RIP1	Receptor-interacting protein 1
ROS	Reactive oxygen species
SOD	Superoxide dismutase
t-BOOH	t-butyl hydroperoxide
TRAF	TNF receptor associated factor

1. CHAPTER ONE

1.1. Interleukin-1 Family of Proteins

The interleukin-1 family consists of many cytokines and associated proteins, such as IL-1α, IL-1β, IL-1Ra, IL-1RAcP, IL-18, IL-36Ra, IL-36α, IL-37, IL-36β, IL-36γ, IL-38, IL-33, IL-1R1, IL-1R2, IL-18Rα, and IL-1Rrp2. The term cytokine is derived from the ancient Greek cyto, meaning cell and kinesis (movement). Cytokines are therefore intra-cellular signalling molecules that initiate a cellular response when bound to a cell surface receptor. Interleukin-1 family proteins have been widely studied for many years and are considered to play a key role in many inflammatory diseases, although recent evidence points to it having pleiotropic effects. It is not practical to fully detail each member of the Interleukin-1 family, therefore further discussion will be restricted to the proteins most relevant to this study. For an extensive review of the Interleukin-1 family see (Sims and Smith, 2010, Garlanda et al., 2013, Palomo et al., 2015).

1.2. Discovery and Structure of IL-1β

Inflammation is a common occurrence during infection or after physical insult and its role in the resolution of injury has long been the subject of medical research. Research into the molecular factors of inflammation by Menkin and Beeson in 1943 first identified aspects that could stimulate inflammation that were deemed endogenous pyrogens (Dinarello, 1984). The work by Menkin and Beeson was limited by the assays available at the time. A radioimmunoassay was developed in the 1970's, enabling the purification of a specific pyrogen (Dinarello et al., 1977). Purification was achieved by using human blood samples to isolate a crude extract of human monocytes *in vitro*. Anti-serum for the pyrogens could be produced by

utilizing the immune system of a rabbit. Harvested antibodies could then be used in combination with gel filtration to separate proteins from the extract. The proteins could then be radio-labeled with a heavy isotope before further purification by gel filtration and ion exchange chromatography (Dinarello et al., 1977, Dinarello, 1984).

The successful purification of proteins enabled more detailed studies of the inflammation-inducing factors. The factor that became an interest of study was named Interleukin-1, for the leukocytes it was derived from. Nucleotide sequencing, of both human and murine cDNA, was published in two studies sequentially in November and December of 1984 (Lomedico et al., 1984, Auron et al., 1984). The two sequences only demonstrated 26% homology, but analysis of both associated polypeptides indicated Interleukin-1 is expressed as a precursor protein. A subsequent study identified two human DNA sequences, one of which had a high degree of similarity to the mouse sequence published in 1984 (March et al., 1985). The two proteins where named Interleukin1 – α (IL-1α) and Interleukin1 – β (IL-1β). IL-1α and IL-1β were characterized as inflammatory regulators, and have since been the focus of further study (Dinarello, 1988). The interleukin family of proteins have been well characterized, and expanded on since the discovery of IL-1α and IL-1β.

IL-1β is the protein of interest for this study. IL-1β is synthesized in an immature form, which is cleaved to produce the mature 'active' form. IL-1β converting enzyme (ICE) is a cysteine protease which was found to cleave the immature form of IL-1β (Black et al., 1989). ICE is a homologue of the *C.elegans* gene CED-3 and may be referred to as caspase 1 (Wilson et al., 1994, Martinon and Tschopp, 2007). ICE was later fully characterized and demonstrated to be

activated when cleaved from a larger protein, p45. ICE is solely able to produce mature IL-1β (Thornberry et al., 1992, Cerretti et al., 1992).

IL-1β is a globular protein for which x-ray crystallography studies have demonstrated the complete structure (Priestle et al., 1988, Treharne et al., 1990). At 3Å resolution, IL-1β can be demonstrated to be comprised of 12 β-sheets, forming a tetrahedral tertiary structure in which the edges consist of anti-parallel β-sheets (Priestle et al., 1988). The core of IL-1β is stabilized by hydrophobic side chain interactions, resulting in a tightly packed core in a small compact molecule. Connecting the β-sheets are 11 domain loops, which provide some structural flexibility for the molecule binding site to interact with its receptor (Priestle et al., 1988). Site specific mutagenesis was used to identify the binding site of IL-1β for the type 1 IL-1β receptor (IL-1R1) in a murine model. Seven amino acids (Arg-4, Leu-6, Phe-46, Ile-56, Lys-93, Lys-103 and Glu-105) form a discontinuous binding site, the loss of which produces a hundred-fold loss of binding to IL1-R1 (Labriola-Tompkins et al., 1991). Other than the discontinuous binding site, the most highly conserved residues are within the core of the molecule, whereas variations are present in the externally facing residues and the connecting loops. The conservation of IL-1β across species indicates the importance of the compact core for positioning the binding residues, while flexibility can be maintained by interchangeable polar residues. A second binding site was later found (Vigers et al., 1997). Both sites interact with IL-1R1 which wraps IL-1β with three immunoglobulin like domains.

1.3. Interleukin-1 Signalling Process

IL-1β signalling is highly regulated by extended members of the Interleukin family. IL-1β lacks the traditional leader sequence directing secretion of the polypeptide (Dinarello, 1994). IL-1β must be cleaved by ICE, which itself competes with antagonist pseudo-ICE (Druilhe et al., 2001), and is transported out of the cell after ATP mediated activation of the $P2X_7$ receptor (Solle et al., 2001). IL-1β signals through IL-1R1, which is expressed ubiquitously throughout brain tissue (Kasukawa et al., 2011). Equally, the presence of the type 2 IL-1β receptor (IL-1R2) further regulates signalling. IL-1R2 binds IL-1β with a ten times higher affinity than IL-1R1. However, the type two receptor lacks the intracellular domains required for signal transduction and therefore acts as a decoy (Peters et al., 2013). Interleukin 1 receptor antagonist (IL-1Ra) competes with IL-1β to bind IL-1R1, further suppressing signalling. IL-1β requires the accessory protein, IL-1RAcP, to actively signal. This provides an additional requirement and therefore further dependency on the cellular environment for signalling to occur (Casadio et al., 2001). The multiple levels of control present on IL-1β signal transduction are necessary as signal amplification means a small number of molecules effectively signalling can produce a significant cellular response. Intracellularly, IL-1R1 is in complex with MyD88, as well as IRAK and TRAF modifying proteins. The signal can be transduced through multiple pathways, including the canonical NF-κB pathway and various non-canonical MAP Kinase pathways (Rothwell and Luheshi, 2000). Signal transduction results in alteration of nuclear transcription and some evidence indicates a role in mRNA stabilization. It is to be determined the full effect and extent of IL-1β signalling through MAPK pathways. However, the NF-κB pathway has been extensively studied.

The NF-κB pathway is a highly involved and complicated pathway, associated with many different cellular processes. NF-κB was discovered in 1986 as one of three nuclear factors found in a study using an electrophoretic mobility shift assay to identify DNA bound proteins in the immune system. NF-κB was found to associate with an immunoglobulin κ enhancer, but only in B cells (Sen and Baltimore, 1986a). A follow up study clarified that NF-κB is present in cells that transcribe immunoglobulin κ light chain genes and not limited to B cells. The study was also able to determine that NF-κB is an inducible protein (Sen and Baltimore, 1986b). Since the discovery of NF-κB, associated proteins and the functional mechanism have been revealed. NF-κB exists as either a hetero- or homodimer of any of the associated class 1 or 2 proteins except for RELB which is only capable of forming a heterodimer (Nabel and Verma, 1993, Gilmore, 2006). All of the NF-κB proteins maintain a highly conserved amino terminal that contains a nuclear localization signal and allows for dimerization. The variation of the different dimerization partners enables NF-κB to act on downstream targets in a multitude of different cell types. In addition to the five members of the NF-κB family, there are a number of inhibitor proteins, called inhibitor of κB (IκB) proteins, which are activated by an IκB kinase (IKK) and an essential modifier, called NF-κB essential modifier (NEMO) (Perkins, 2006). NF-κB inducing kinase (NIK) can activate NF-κB, under appropriate circumstances independently of NEMO (Shih et al., 2011). The key components of NF-κB signalling have a multitude of functions that operate in different ways producing a large degree of variability.

During an inflammatory event, other extracellular signalling molecules, such as pathogen-associated molecular patterns and danger associated molecular patterns, may in addition to IL-1β, stimulate NF-κB response through binding receptors (Maverakis et al., 2015,

Shih et al., 2011). In order for NF-κB to be activated, IκB needs to be phosphorylated by an IKK leading to degradation of IκB (Hayden and Ghosh, 2004), but ubiquination of IKK is needed for activation (Perkins, 2006). Ubiquination of NEMO occurs, which enables recruitment of IKKβ and IKKα to form an activation complex. The specific sites that are ubiquinated can alter this fate. For example, K48 linked polyubiquination can lead to protein degradation, while K63 linked polyubiquination does not have this effect (Perkins, 2006). The activation complex is then able to phosphorylate IκB, signalling the protein's degradation, and the NF-κB proteins are able to relocate to the nucleus (Hayden and Ghosh, 2004).

The extent of the different NF-κB components gives an indication of the extent of the variation possible in NF-κB signalling. The variation and complexity of NF-κB pathway identifies many biological factors that may produce a cellular response after cascade activation from IL-1β. The cellular environment may affect any one of these factors to alter or mediate the cellular response. Understanding of this cascade indicates the extent of the molecular web in which IL-1β operates, demonstrating how the cellular environment can vary its response.

1.4. DNA binding and potential consequences of NF-κB activation

The different possible combinations of NF-κB class 1 and 2 proteins will alter the DNA binding targets once inside the nucleus. NF-κB recognises a degenerate consensus sequence, 5'-GGGRNWYYCC-3'; in which R indicates A or G, N indicates any nucleotide, W indicates A or T, and Y indicates C or T (Gilmore, 2006). The degeneracy in the binding site allows the site to appear at a high frequency with relation to multiple genes. IL-1β activates the NF-κB pathway

and NF-κB promotes further expression of IL-1β (Hiscott et al., 1993, Cogswell et al., 1994). Such interactions between NF-κB activity and the inflammation inducing factors, like IL-1β, indicate the possibility of inflammation being a feedforward process. Inflammation is a protective function, however, it can become harmful in excess. Excessive signalling can be further complicated as some components of the NF-κB signalling pathway have some unconventional functions that can have unwanted effects. For example, IKKα has been shown to be capable of phosphorylating serine 10 of histone H3 in NF-κB dependent promoters (Espinosa et al., 2015), demonstrating that components can alter gene expression in ways other than direct NF-κB binding. NEMO has been found to possess unorthodox functions, specifically by inhibiting programmed necrosis and therefore altering finely tuned programmed cell death (PCD) pathways. NEMO affects a change to necrosis by binding to ubiquinated receptor interacting protein 1 (RIP1) to prevent RIP1 from initiating necrotic death (O'Donnell et al., 2012). Any change to the abundance of NEMO could alter the rate and manner at which cells undergo PCD. Such variation in one of multiple pathways in which IL-1β can signal, indicates just how the single cytokine can have differing effects doth beneficial and detrimental.

1.5. Pleiotropic effects of IL-1β in the Central Nervous System

The extent of the factors controlling IL-1β signalling and the inherent complexity of the NF-κB pathway in which the IL-1β signal is transduced demonstrate the extent at which the effect of IL-1β signalling can be dependent on the cellular environment in which it is induced. In the central nervous system (CNS), IL-1β and IL-1R1 are expressed throughout the rodent brain at low basal levels and both are increased on induction of inflammation (Gayle et al., 1997,

French et al., 1999, Lechan et al., 1990). Classically, IL-1β has been thought of as a harmful factor in disease response. However, it is now clear that IL-1β can also protect CNS tissue from insult. This dichotomy is exemplified by the differing contribution of IL-1β to stroke and Huntington's disease.

1.5.1. IL-1β and Stroke

Cerebral ischemia or stroke occurs when blood flow to an area of the brain is blocked by a blood clot. Several studies have demonstrated that IL-1β contributes to ischemic infarct in murine stroke models (Relton and Rothwell, 1992, Yang et al., 1998, Basu et al., 2005). Examination of IL-1R1 expression, following stroke, has shown upregulation in multiple brain regions, including the striatum (Wang et al., 1997). Such upregulation occurs in a time dependent manner after insult. Further *in vivo* experimentation has demonstrated that treatment with IL-1ra, the naturally occurring IL-1R1 receptor antagonist, minimizes damage resulting from middle cerebral artery occlusion in rat (Relton and Rothwell, 1992, Yang et al., 1998), a result that is supported by experiments utilizing the same technique with IL-1R1 null mice (Fogal et al., 2007). Of import, IL-1Ra has been tested in drug trials as a possible treatment in stroke (Schulz et al., 1999, Lakhan et al., 2009). In a phase two medical study administering IL-1ra to human stroke patients, there were no adverse effects and those treated had significantly better health outcomes than those treated with a placebo (Emsley et al., 2005).

1.5.2 IL-1β in Huntington's Disease (HD)

HD is a condition named after George Huntington who described the condition in 1872. The disease was originally named Huntington's chorea because of stereotypical movements associated with HD. Patients suffering with chorea had long been studied by the time George Huntington published, however, the identification of an hereditary chorea, only present in later life, predominantly contracted by males and degenerative until death was novel at the time (Huntington, 1872). Huntington first described the observable symptoms of the disease as consistent shaking and twitching, unlike the sudden debilitating fits observed in epilepsy. Following advances in scientific understanding, the symptoms of HD have been more explicitly defined. Early symptoms of HD are commonly difficult to diagnose. Initially patients will experience mild loss of fine motor skills, muscle stiffness and irritability (Squitieri et al., 2000). Early stage symptoms can be missed, but upon rapid progression consist of uncontrollable muscle twitch/chorea like movement, muscle rigidity, dystonia, loss of motor control, psychosis, obsessive-compulsive disorder, depression and anxiety (Ross and Tabrizi, 2011). Physical deterioration along with symptom progression in HD was described in George Huntington's original characterisation and has been supported by subsequent studies. Current evidence indicates death typically occurs in HD patients due to respiratory failure 15-20 years after the onset of symptoms (Ross and Tabrizi, 2011, Walker, 2007).

HD is defined genetically as an autosomal dominant disorder, a result of an expanded 5'-CAG-3' repeat in the gene, which encodes the protein Huntingtin (HTT), mapped to chromosome 4p16.4 (MacDonald et al., 1993). Age of onset of HD is dependent on the number of CAG repeats. Directly associating the severity of mutation to the severity of phenotype, the

higher the number of CAG repeats present in an individual's HTT gene, the earlier in life the disease is likely to manifest (Ross and Tabrizi, 2011). Evidence directly linking the number of CAG repeats was collected by conducting linkage marker analysis on samples collected from 150 families with large pedigrees available for testing. Findings indicated that the number of repeats present in a healthy individual are between 11-34 repeats whereas people who displayed the diseased phenotype possessed 37-86 repeats (Duyao et al., 1993). Recently, diagnosis and screening has increased identification of people with HD, and it has been determined that 36-40 repeats are likely to lead to incomplete penetrance and mild symptoms, while greater than 40 repeats almost always leads to development of HD (Bates et al., 2015). Further clarification of the predominance of HD occurrence in males is provided by genome analysis demonstrating a higher rate of repeat instability during spermatogenesis (Duyao et al., 1993). Repeat instability occurs due to a phenomenon called replication slippage, which occurs more frequently in stretches of di- or tri-nucleotide repeats. Trinucleotide repeats, such as the CAG repeat seen in HD, commonly appear in eukaryotic genomes, in both coding and non-coding regions. Replication slippage occurs due to DNA polymerase pausing during replication of the repeat region causing the enzyme to disassociate from the DNA strand and bind back to the DNA strand at a different location within the repeat region (Viguera et al., 2001). A replication slippage event will cause the repeat region to be lengthened or shortened depending on where the DNA polymerase enzyme re-joins the strand. Repeat instability in HD has a higher rate of occurrence in spermatogenesis with the most severe mutations occurring post meiosis (Yoon et al., 2003, Duyao et al., 1993, Petruska et al., 1998).

IL-1β levels are increased in some Huntington's patients (Ona et al., 1999). Further, the inhibition of ICE delays the development of symptoms in a mouse model (Ona et al., 1999, Li et al., 1995). Such findings might indicate a detrimental function of IL-1β signalling in HD progression. However, it is important to note that ICE (aka caspase 1) is involved in the intrinsic apoptosis pathway (Nagata, 1997). Therefore, inhibition of ICE may result in greater survival for reasons not associated with IL-1β. Research into the specific function of IL-1β in HD is still relatively limited and predominately focuses on the presence of mature IL-1β as a marker of inflammation and not on a specific function of the cytokine (Olejniczak et al., 2015). However, one study utilizing R-1 HD mice that were cross-bred with IL-1R1 null mice demonstrated gene-dependent protection from IL-1R1 signalling. Using animals expressing the mutant HTT protein and wild type IL-1R1 as a baseline, animals heterozygous or null for IL-1R1 demonstrated progressively greater HTT aggregate accumulation and incrementally worse motor deficit (Wang et al., 2010). Such findings are consistent with IL-1 signalling being protective in HD. Given the spectrum of molecular events associated with IL-1β signalling, that are highly dependent on cellular environment, further research is clearly needed to address the function of IL-1β signalling in HD.

The pathology of HD has been the focus of research for many years. At a physiological level HD results in distinct loss of medium spiny neurons in the dorsal region of the putamen and in the caudate nucleus, regions of the human brain that are referred to collectively as the striatum in the mouse (Vonsattel et al., 1985, Vonsattel et al., 2011). The definitive molecular cause of HD has yet to be fully elucidated; however there are numerous possible events that are associated with neuronal loss in HD. Studies utilizing a *Drosophila* model have shown that

the poly-glutamine tract, which results from the extended CAG repeats, aggregates to block vesicle transport along axons (Lee et al., 2004). Interruption of axonal transport starves the mitochondria resulting in metabolic dysfunction and axonopathy, an irreversible process in the CNS (Chevalier-Larsen and Holzbaur, 2006, Spencer and Schaumburg, 1977). It is reasonable to relate the length of the poly-glutamine tract with the rate at which HTT aggregates and subsequently blocks axonal transport. Neuronal loss through inhibition of axonal transport would fit with the data regarding the age of onset and number of CAG repeats. It is possible that disruption to axonal transport is only a contributory factor and other molecular mechanisms are in effect during HD.

Indeed, an increase in oxidative stress have been shown to occur in human patients with HD. Post mortem analysis has demonstrated an increase in protein oxidation in the brain tissue of those affected (Sorolla et al., 2008). Similar increases in markers of oxidative stress markers have been identified in cell culture and animal models (Browne et al., 1999, Wyttenbach et al., 2002). Further, greater reactive oxygen species (ROS) production has been measured in multiple HD mouse models, when compared to their wild type controls (Perez-Severiano et al., 2004). Further, mitochondrial dysfunction has been associated with HD. Post mortem analysis of HD patients has demonstrated severe disruption of complex two and complex three of the electron transport chain (Tabrizi et al., 1999). Finally, study of the proteomic changes in HD mice has demonstrated an increase in expression of mitochondrial proteins associated with protection from ROS (Deschepper et al., 2012). Such findings are consistent with the generation of ROS and mitochondrial dysfunction being present in both human HD patients and HD models.

1.6. IL-1β and ROS

Many neurodegenerative diseases, including HD, demonstrate are associated with an increase in ROS production (Emerit et al., 2004). This could occur through disruption of the electron transport chain (mitochondrial damage) or inhibition of oxidative phosphorylation (energy deprivation) (Li et al., 2013). The ROS commonly resulting from such dysfunction is superoxide anion, which is rapidly converted by different forms of SOD to hydrogen peroxide, also a mediator of cell death (Clément et al., 1998). Hydrogen peroxide can be converted into highly reactive secondary free radicals in the presence of heavy metals via the Fenton reaction. Such free radicals result in DNA damage, lipid peroxidation and protein dysfunction (Yakes and Van Houten, 1997, Cabiscol et al., 2000, Ray et al., 2012). Further, the generation of ROS has been linked to the increase of IL-1β (Brabers and Nottet, 2006, Troy et al., 1996), and the presence of antioxidants, which redress a redox imbalance, have been linked with lessening IL-1β presence (Min et al., 2003).

Previously, we found that IL-1β enhanced the expression and functional activity of the cystine/glutamate transporter (system x_c^-) in astrocytes (Fogal et al., 2007). Interestingly, this transporter is vital for the uptake of cystine for the synthesis of the neuroprotective antioxidant molecule glutathione (GSH) (Bannai and Tateishi, 1986). This raised the intriguing possibility that IL-1β may upregulate processes that fundamentally protect against oxidative stress. Indeed, we found that interleukin-1β protected neural cells against oxidant-induced injury via an NFκB-dependent upregulation of GSH synthesis (He et al., 2015) (Chowdhury, unpublished observations). Thus, to further study the potential protective role of IL-1β *in vivo*, a chemical — 3-nitropropionic acid —was utilized. 3-nitropropionic acid is a naturally occurring phyto/fungal

mitochondrial toxin that has been shown to induce ROS and produce HD like symptoms associated with selective striatal lesions (Fontaine et al., 2000).

1.7. 3-Nitroproprionic Acid as a Model of HD

3-nitroprionic acid (3-NP) is a mitochondrial toxin produced by both plant species in the *Astragalus* genus and by fungi in the *Aspergillus* genus (Ludolph et al., 1991). It was first identified as a natural toxin in the legume, *Indigofera endecaphylla* (Morris et al., 1954). Multiple incidents of 3-NP poisoning, demonstrating toxicity in humans, have occurred. Between 1972 and 1985, 148 outbreaks of acute neurological poisoning caused by ingestion of moldy sugarcane were documented in China. The causative agent was 3-NP. In total, 726 people were affected and 64 fatalities. Many more cases may have gone unreported. Symptoms incurred were variable and attributed to inconsistency in exposure, with children documented to have the most severe symptoms (He et al., 1995). Exposed individuals would experience headaches and nausea initially with more severely affected patients slipping into a coma. Those who recovered from the coma would develop dystonia between four and forty days after exposure. On autopsy, non-surviving patients were shown to have lesions in their striatum similar to that seen in HD patients (He et al., 1995). The similarity of striatal lesion and evident dystonia would lead to the use of 3-NP as a chemical Huntington's model.

Later studies demonstrated 3-NP to be an irreversible inhibitor of succinate dehydrogenase (SDH) (Coles et al., 1979). The enzymatic activity of SDH requires the addition of an FAD cofactor (Kim et al., 2012). 3-NP acts as a succinate analogue resulting in neutrophilic attack on the N5 super oxidized form of the flavinylated cofactor covalently bonding and

inactivating the active site (Alston et al., 1977, Coles et al., 1979). The inhibition of the Krebs cycle in neurons, but not glial cells, has been shown by labelling succinate and measuring it's accumulation after administration of 3-NP (Hassel and Sonnewald, 1995). SDH, in addition to acting in the Krebs cycle, forms a subunit of complex 2 of the electron transport chain providing further opportunity for the disruption of energy disruption by 3-NP. Multiple studies have demonstrated a decrease in ATP after administration of 3-NP and an increase in ROS. Further, the administration of ROS inhibitors has been shown to attenuate damage from exposure to 3-NP (Pedraza-Chaverrí et al., 2009, Márquez-Valadez et al., 2012). The depletion of ATP and increase in ROS mimics that observed in HD (Tunez et al., 2010). Despite the long history of study of 3-NP, its precise mode of action continues to be revealed (Francis et al., 2013).

Nevertheless, systemic 3-NP exposure has a clearly demonstrated effect on striatal tissue. Lesion does occur in other regions of the brain, however the striatum remains the most vulnerable, being the first and most affected region. The specificity for striatum has been attributed to multiple factors. In the striatum there is a convergence of glutamatergic and dopaminergic afferents (Kötter, 1994). Energy deprivation through the disruption of oxidative phosphorylation results in membrane depolarization, which makes cells susceptible to secondary excitotoxicity (Albin and Greenamyre, 1992). Such disruption of ATP production by 3-NP would result in greater vulnerability to extracellular glutamate. Generation of ROS can occur as dopamine is easily oxidized by ferric ion to produce highly reactive electron deficient products, such as DOPA-quinone and DA-quinone (Meiser et al., 2013). Dopamine related ROS products are known to inhibit glutamate vesicle transport (Berman and Hastings, 1997). In turn, glutamate can inhibit the release of dopamine in the presence of hydrogen peroxide

(Avshalumov et al., 2003). The striatum may be further vulnerable as the endothelial cells constituting the blood brain barrier (BBB) of the lateral branches of the lenticulo-striate artery have a high density of amino acid transporters. Indeed, the administration of a glutamate transporter inhibitor has been shown to minimize the effect of 3-NP (Nishino et al., 2000).

1.8 Project Aim

Classically viewed as a pro-inflammatory mediator, in the brain IL-1β appears to have pleiotropic effects. It acts as a neuromodulator in the healthy CNS, has been implicated in the pathogenesis of a number of CNS diseases, and it may also provide protection to the injured CNS [for review see (Hewett et al., 2012)]. Of interest for this project, a recent study demonstrated increased Huntingtin aggregation and severity of Huntington's disease (HD) symptoms in an HD mouse bred and maintained into an IL-1R1 null background (Wang et al., 2010), demonstrating a potential protective role for IL-1β.

Aggregates of mutant Huntingtin protein are known to affect mitochondrial dynamics and function (Choo et al., 2004, Chang et al., 2006), with evidence suggesting that abnormal mitochondrial energetics contributes to the progression of HD in both humans and in rodent models (Browne et al., 1999). This is further implicated by the observation that animals and humans exposed to the phyto/fungal mitochondrial toxin, 3-NP, exhibit neurological symptoms and neuropathological outcomes similar to HD patients (Ludolph et al., 1991, Sipione and Cattaneo, 2001, Rubinsztein, 2002).

Abnormal energy metabolism not only leads to a decrease in cellular ATP levels, but also to an increase in the production of ROS (Lin and Beal, 2006). We recently demonstrated that IL-

1β increases astrocytic glutathione production and protects these cells from oxidant injury *in vitro* (He et al., 2015). The question of whether IL-1β may provide protection in HD by mitigating oxidative stress, forms the basis of this study.

This hypothesis was tested by comparing 3-NP-induced lesion, in striatal tissue, in mice wild-type or null for IL-1R1, the receptor for IL-1β. Oxidative stress and cell loss leading to impairment of motor function are generated by 3-NP through the irreversible inhibition of SDH (Borlongan et al., 1997a, Borlongan et al., 1997b, Borlongan et al., 1997c).

Specific Aim: Test the consequence of loss of IL-1β signalling on behavioral and histological toxicity of 3-Nitroproprionic acid.

To determine whether IL-1β is a protective molecule in the face of oxidative stress *in vivo*, we compared the extent of 3-NP injury between IL-1R1 (-/-) mice and their wild-type (+/+) littermates systemically treated twice per day, over a twelve-day period, with a total cumulative dose of 920mg/kg 3-NP. Behavioral tests assessing motor function or muscular strength were made daily to monitor toxicity progression. Following euthanasia, the pattern and extent of striatal injury was determined via histological analysis.

2. CHAPTER TWO

2.1. Rationale of Pilot Study

Early characterization of the effects of 3-NP, identified the development of striatal lesions and Huntington's like symptoms (Beal, 1994, Ludolph et al., 1992, Beal et al., 1993). However, the use of 3-NP as a Huntington's model demonstrated clear variability in results. Early work with rats produced clear strain differences and a wide variety of striatal lesions (Guyot et al., 1997), making it possible to categorize the animals as vulnerable or resistant. Vulnerability to 3-NP was associated with a rapid loss of SDH activity, whereas resistant animals, although experiencing the same final level of inhibition of SDH, demonstrated more gradual loss of activity. Such findings indicate that cell death in a 3-NP model is a cause of secondary factors which, when accrued in rapid succession, result in death but not as a direct result of SDH inhibition. Lesion size variance was also shown to be limited in a sub-acute paradigm as opposed to an acute paradigm (Borlongan et al., 1995, Borlongan et al., 1997c).

In mice, both *in vitro* and *in vivo* studies have indicated a clear sex difference in the response to 3-NP. Male animals are predominantly vulnerable and females resistant. The sex difference is hormonally mediated, since in culture, cells treated with estrogen are protected and those treated with testosterone incur greater injury following NP exposure, than untreated cells (Nishino et al., 1998). Similarly *in vivo*, ovariectomized females show a loss of protection, wherein resistance is induced in males treated with estrogen (Nishino et al., 1998, Mogami et al., 2008, Nishino et al., 1997). Such findings imply that estrogen is protective and testosterone deleterious in cases of 3-NP poisoning.

The use of older sexually segregated animals should minimize estrogen-mediated differences between male and female animals (Mogami et al., 2008). A prolonged sub-acute dosing paradigm, such as that described below, should minimize variation in striatal lesion, thus focusing experimental results on genotypic difference not hormonal or chemical. Thus, a pilot study was conducted on male and female animals from the C57Bl/6 inbred mouse, the background from which IL-1R1 null animals are created, to evaluate the effectiveness of the paradigm as well as to determine any sex differences.

2.2. Methodology

Animal Husbandry

Experimental animals were purchased from the Jackson laboratory directly (JAX stock: 000664) or bred from JAX stock in the Syracuse University animal facility. Mice were provided food and water *ad libitum*, while housed up to five animals per cage in a controlled temperature environment operating on a standard 12 hour light/dark cycle in our AALAC accredited facility. All animal procedures were conducted with IACUC approval and this investigator was blind to animal genotype during experimentation.

3-Nitroproprionic Acid Dosing Protocol

3-NP (Sigma Aldrich, N5636) was dissolved in 0.9% saline to a concentration of 25 mg/ml, adjusted to pH 7.4 with 5M NaOH, and filter sterilized (0.2µm Nalgene). 3-NP dosing stock was kept at 4°C for no more than seven days. After five days of acclimatization handling, mice were administered 3-NP via intraperitoneal (IP) injection twice daily with an interval of 8-12 hours using our 11 day protocol as follows: 20 mg/kg – two days, 30 mg/kg – two days, 40

mg/kg – two days, 50 mg/kg – two days, 60 mg/kg three days for a total cumulative dose of 920 mg/kg, or the 12 day protocol as follows: 20 mg/kg – two days, 30 mg/kg – three days, 40 mg/kg – three days, 50 mg/kg – three days, 60 mg/kg one day for a total cumulative dose of 920 mg/kg. After completion of 3-NP dosing, animals were sacrificed by cervical dislocation under isoflurane anaesthesia. Brains were snap frozen in O.C.T. compound (Sakura Finetek USA) for histological analysis. Three separate experiments were performed over two months.

Behavioral Scoring

Behavioral analysis was adapted from Fernagut and colleagues (Fernagut et al., 2002) and conducted before each injection. Hindlimb clasping, general locomotor activity, hindlimb dystonia, truncal dystonia and postural adjustment reflexes were assessed twice per day just prior to each injection by an observer blinded to genotype. The following categories were assessed, abnormal general behaviour, hindlimb clasping, kyphosis, hindlimb dystonia and a postural challenge was administered. Three scales were assigned corresponding to no abnormality (0), moderate (1,3) or severe deficits (2,5). Any mouse attaining a cumulative behavioral score ≥ 9 or sustaining a weight loss ≥ 20% was immediately sacrificed (He et al., 2017).

Inverted Grip

To assess grip strength, the mouse was placed on a 1 cm square wire mesh, which was then inverted 180^{o} and held 40 -50 cm over a padded surface. The time to fall was recorded using a stopwatch. Each animal received up to three trials, with the longest latency to fall of the three trials recorded. The animal was removed from the mesh when a criterion time of 60 s was achieved. (Deacon, 2013).

Histological analysis

Frozen brain sections (40μm) were collected serially from the rostro-caudal extent of each brain (+1.54 to -0.18 relative to bregma) and stained with 0.5% thionin by submersion in multiple wash solutions (70% EtoH, 50% EtoH, ddH2O, thionin, ddH2O, ddH2O, 70% EtoH, 95% EtoH, 100% EtoH, 100% EtoH, 100% Xylenes, 100% Xylenes) as previously described (He et al., 2017). Images were captured by scanning (Epson Perfection 3170) at 2400 dpi. The lesion area, identified by absence of thionin staining, was quantified using NIH Image J at seven levels from bregma (+1.22, +1.02, +0.72, +0.52, +0.22, +0.02, and -0.18) by three individuals blind to genotype and experimental identification. For each level, the percent striatal damage (D) was calculated as a percentage of the total striatum area (T) as (D/Tx100). Area measurements were converted to volume using Cavalieri's principle (volume = $(s_1d_1) + (s_2d_2) + (s_3d_3) + (s_4d_4) + (s_5d_5) + (s_6d_6) + (s_7d_7)$), where s = lesion surface area and d = distance between two sections, as published (Shih et al., 2005). Data are expressed for lesion area as a percentage of striatum at all seven levels, and the mean lesion volume + SEM of all seven levels derived from the mean calculated from all three individuals.

Statistical Analysis

Statistical analysis was performed using GraphPad Prism, Version 7.03. Percent data was transformed by the arcsin square root function (Y=arcsin[sqrt(Y/1000)], while behavioral score data transformed by the log10 function [Y = log (Y + 1)], prior to analysis. Comparisons of mass, lesion size, behavior score and grip strength were made using repeated measures two way analysis of variance (RM 2-way ANOVA) evaluating the main effects (Time x Sex), followed post-hoc by Sidak's multiple comparison test. Lesion and morbidity incidence comparisons were

evaluated by Fisher's exact test. The Kaplan–Meier survival curves, depicting the rate at which animals were removed, were compared by Mantel-Cox log-rank test.

2.3. Pilot Study Results

Animal mass was measured the morning of each day of injection. The average mass, for each day, shown in figure 1, was analyzed by RM 2-way ANOVA. Male and female animals differed significantly in mass (p=0.0001) and the mass of each significantly decreased over time of treatment with 3-NP (p=<0.0001). Both male and female mice demonstrated sequential mass loss from day seven on. Both sexes lost a similar amount of mass over the injection period (≈10-15%). No animal from either group was removed for excessive weight loss.

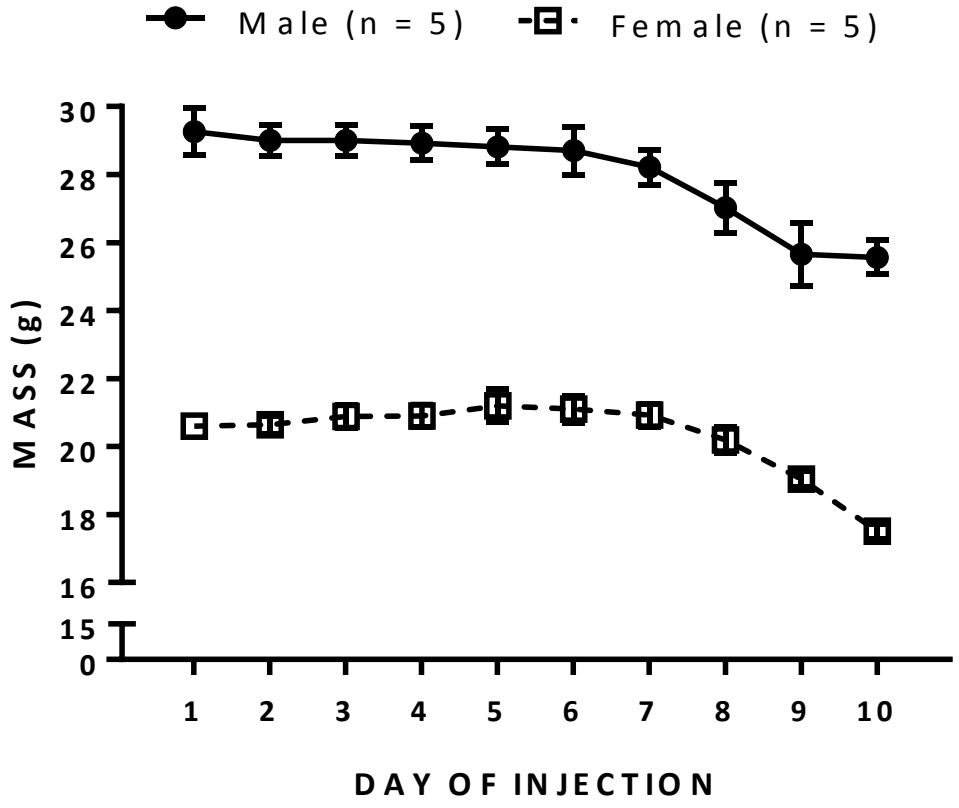

FIGURE 1: Comparison of 3-NP-mediated mass loss in C57Bl/6J mice. Mass of male mice (n = 5) and females (n = 5) were assessed and recorded just prior to each 3-NP injection. Mass was plotted as mean ± SEM. There was both a significant time-effect (p = <0.0001) and sex-effect (p = 0.0001), as determined by repeated measures two-way ANOVA.

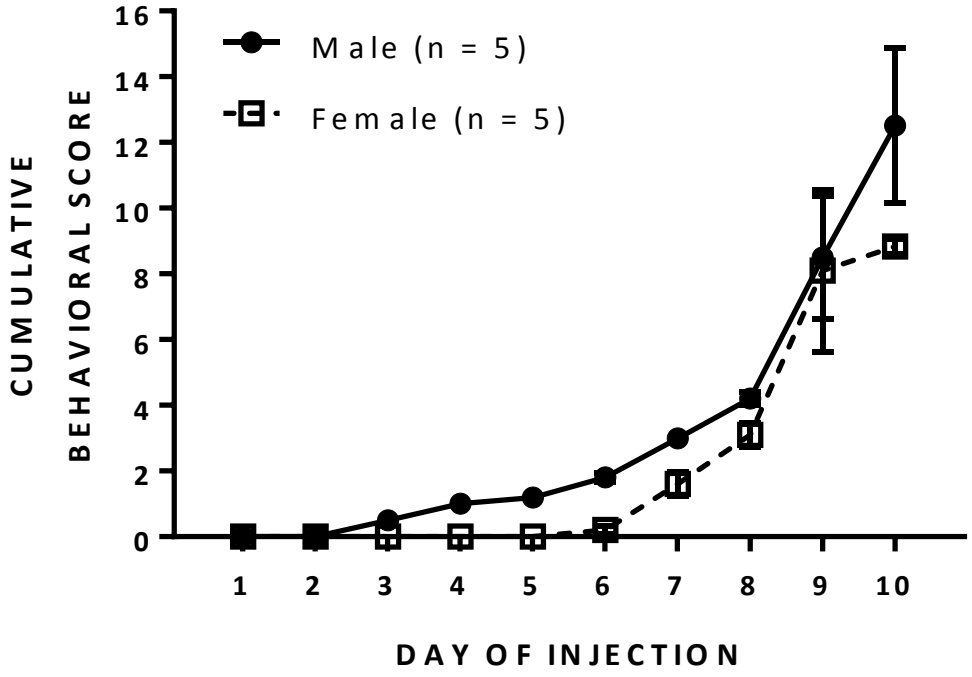

FIGURE 2: Comparison of 3-NP-mediated motor deficit in C57Bl/6J mice. Gross motor behavior of male mice (n = 5) and female (n = 5) were assessed and recorded just prior to each 3-NP injection. The average score for the day was plotted as mean ± SEM. There was a significant time-effect (p = <0.0001) and sex-effect (p = 0.0087), as determined by repeated measures two-way ANOVA, after [Y = log (Y + 1)] transformation.

Additionally, gross motor deficits, measured by twice-daily observation, were scored as detailed in methodology, and are shown in figure 2. Score data was transformed [Y = log (Y+1)] before analyzing by RM 2-way ANOVA. Both males and females development of motor deficits significantly over the days 3-NP was administered (p=0.0001). The right shift observed of female scores demonstrated a delay in the development of motor deficit. Male animals developed observable motor deficits from day three while females only did so from day six. The delay between the groups resulted in a significant difference (p=0.0087).

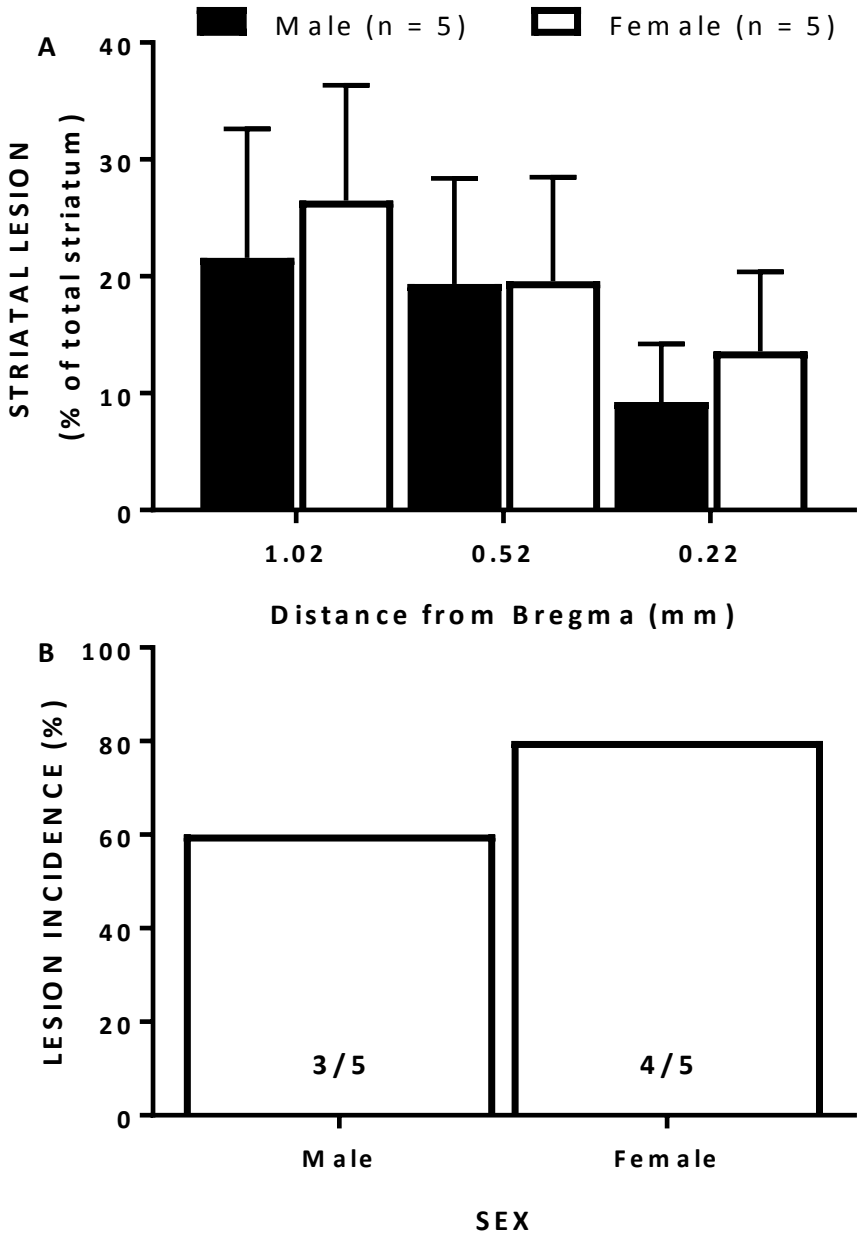

FIGURE 3: Comparison of lesion size and incidence between male and female C57BL/6J mice. Male (n = 5) and female (n = 5) were injected twice daily with 3-NP as described in methods. **(A)** Comparison of lesion area between male and female mice expressed as a percentage of total striatal area. No significant difference between sexes occurs at any level of bregma as determined by repeated measures two-way ANOVA (p = 0.8059). **(B)** Comparison of lesion incidence between male and female mice. The graph depicts the percent of mice of each sex with any size lesion determined by dividing the number with lesion by the total number of mice analyzed. Exact numbers contained within the bars. There was no significant difference in the lesion incidence as determined by Fisher's exact test (p = >0.9999).

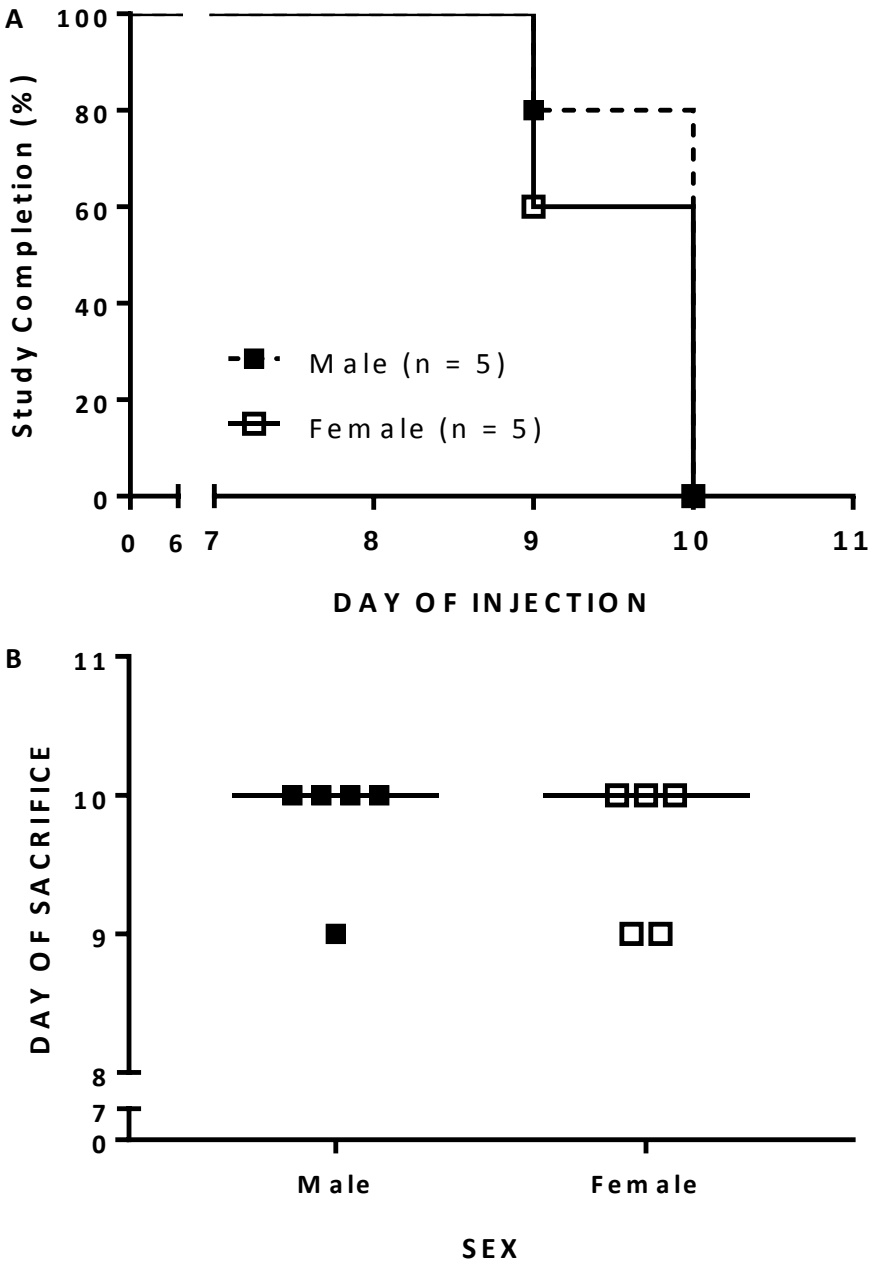

FIGURE 4: Comparison of the amount and rate of removal of male and female C57Bl/6J mice from pilot study. Mice receiving 3-NP were removed from injection series if their behavioral score exceeded nine (9) or if they lost >20% of their body mass. **(A)** A Kaplan–Meier survival curve depicts the rate at which the mice were removed from study. No sex differences in rate of removal was determined by Mantel-Cox log-rank test ($p = 0.3173$). **(B)** The day male and female animals were removed for sacrifice is demonstrated with each individual mouse represented by a data point and a line representing the median day of sacrifice. No sex differences were found when compared by a Mann and Whitney similarity test ($p = >0.9999$).

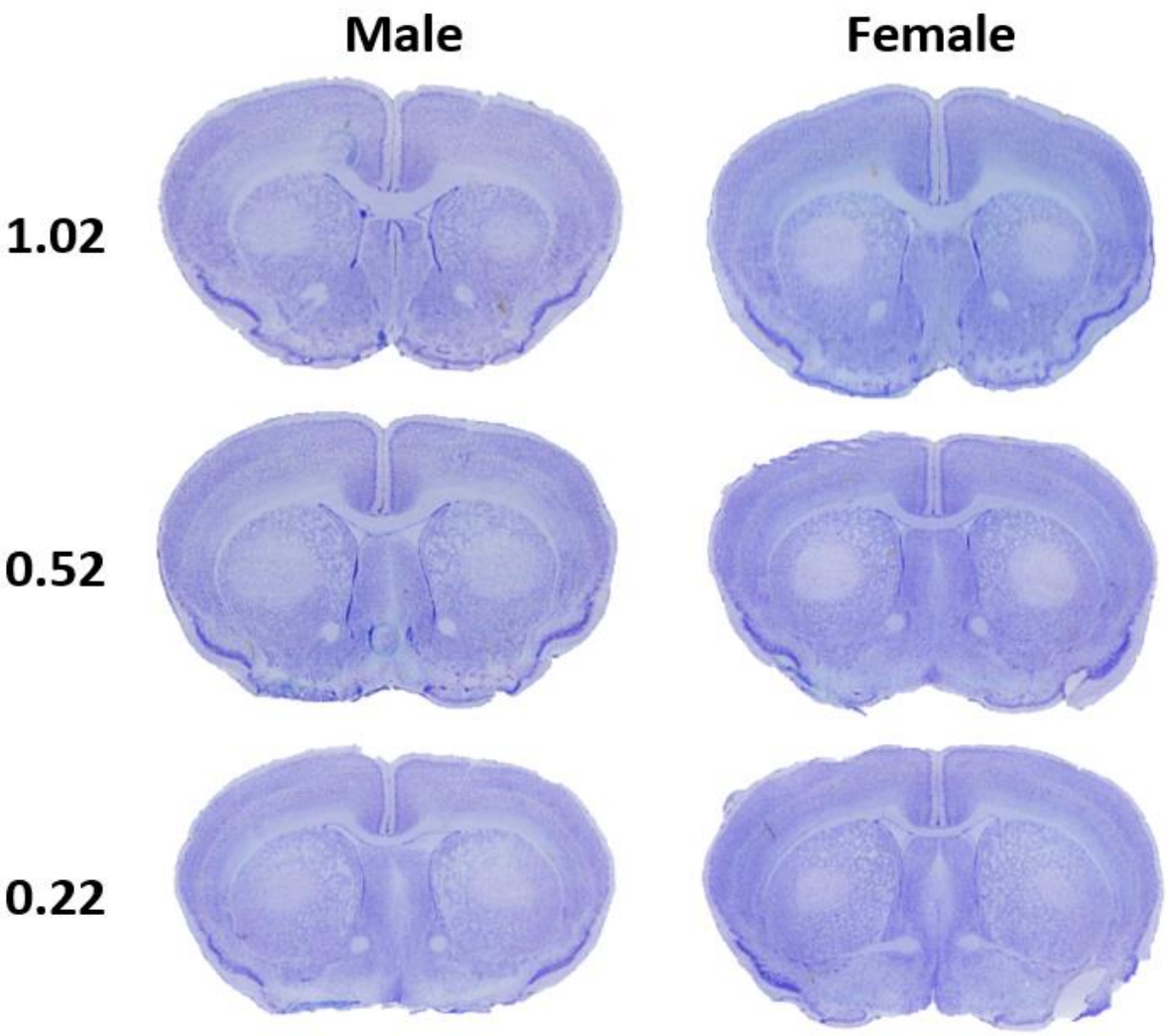

FIGURE 5: Representative images of C57Bl/6J male and female mice. Male (n = 5) and female (n = 5) mice were injected twice daily with 3-NP as described in methods. Photomicrographs depict striatal injury in male (left) and female mice (right) at +1.02 to +0.22 from bregma at day 13 following 3-NP exposure. Lesion identified by absence of stain within striatal area.

Quantitative analysis of the histological striatal lesion, shown in figure 3, demonstrates no discernible difference between male and female animals. The striatal lesion, calculated as a percentage of the total striatal area (fig. 3A) was not significantly different between males and females (p=0.8059). The degree of lesion incidence (fig. 3B) was compared by Fisher's exact test which found no significant difference between the sexes (p=>0.9999). The area of lesioned

tissue was approximately 20% in both males and females but decreased to 10% at 0.22mm from bregma. Completion of the injection paradigm is not expected for all mice (figure 4). All participants had to be removed from the paradigm before study completion due to severe motor deficit. The rate of decline was not significantly different between males and females [fig 4A; log rank Mantel-Cox, analysis (p=0.5127)]. The median day of animal sacrifice was day 10 for both groups (fig. 4B). A single male and two females was removed earlier on day 9. A Mann and Whitney test indicated no significant difference (p=>0.9999) in median ranks between males and females.

Representative images of the coronal sections analyzed for lesion area are shown in figure 5. Clear circular sections of the striata are seen to be absent of stain, indicating the absence of cellular matter. The edges of the circles are clearly defined and of approximately equal size in males and females. There is no sign of blood present in the lesioned area of either group.

A second cohort of three male and three female mice were treated with saline vehicle. Sham animals received a score of one for the assessment of motor deficit for lack of activity towards the end of the injection paradigm, but the animals did not appear to be adversely affected. All completed the full injection series, and no saline treated animal developed a lesion. The female animals demonstrated no significant loss of mass whereas the males lost mass after day 6 of the paradigm. Further investigation identified a clearly different profile for loss of mass in response to 3-NP compared to saline in males. See supplemental data in appendix A.

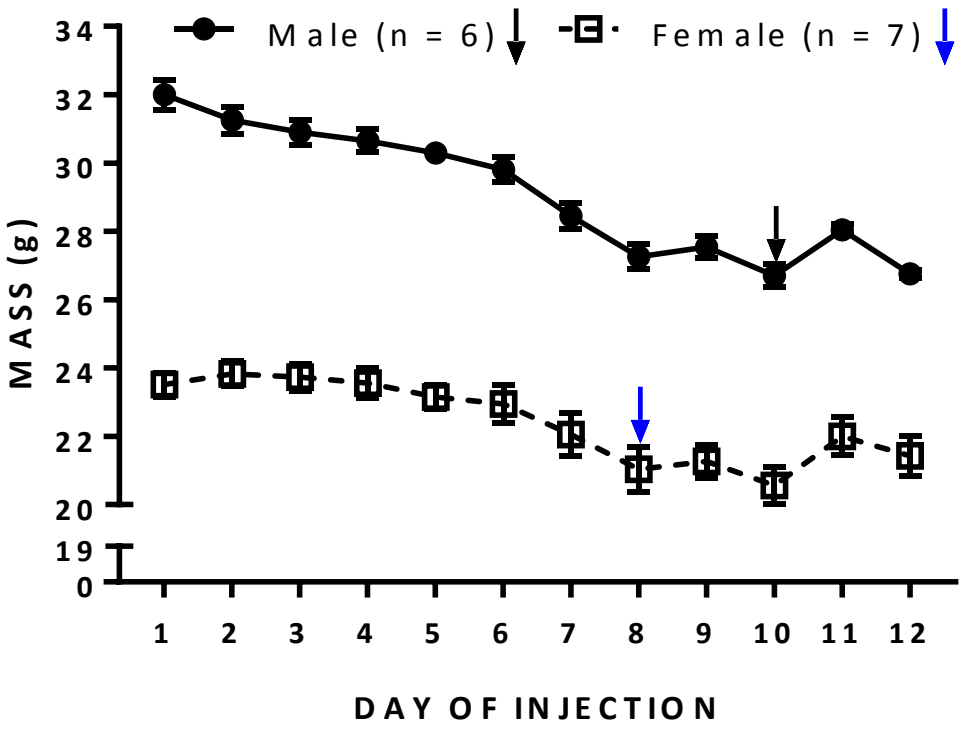

FIGURE 6: Comparison of 3-NP-mediated mass loss in C57Bl/6J mice treated with 12 day protocol. Mass of male (n = 6) and female (n = 7) mice were assessed and recorded just prior to each 3-NP injection. Mass was plotted as mean ± SEM. There was both a significant time-effect ($p = <0.0001$) and sex-effect ($p = <0.0001$), as determined by repeated measures two-way ANOVA. Black arrows indicate the day at which a male mouse was removed from the study, whereas blue arrows indicate the removal of a female mouse.

Pilot Study Results – 12 Day Paradigm

When utilizing the 11-day paradigm no animal was able to complete the full 11 days (figure 4). To determine if this could be improved on, and a higher rate of study completion achieved a second study was conducted to assess wild type response to the 12 day paradigm. Daily mass measurements in male and female mice demonstrated a clear difference in mass ($p=<0.0001$) and both groups lost mass significantly over time ($p=<0.0001$) when analyzed by

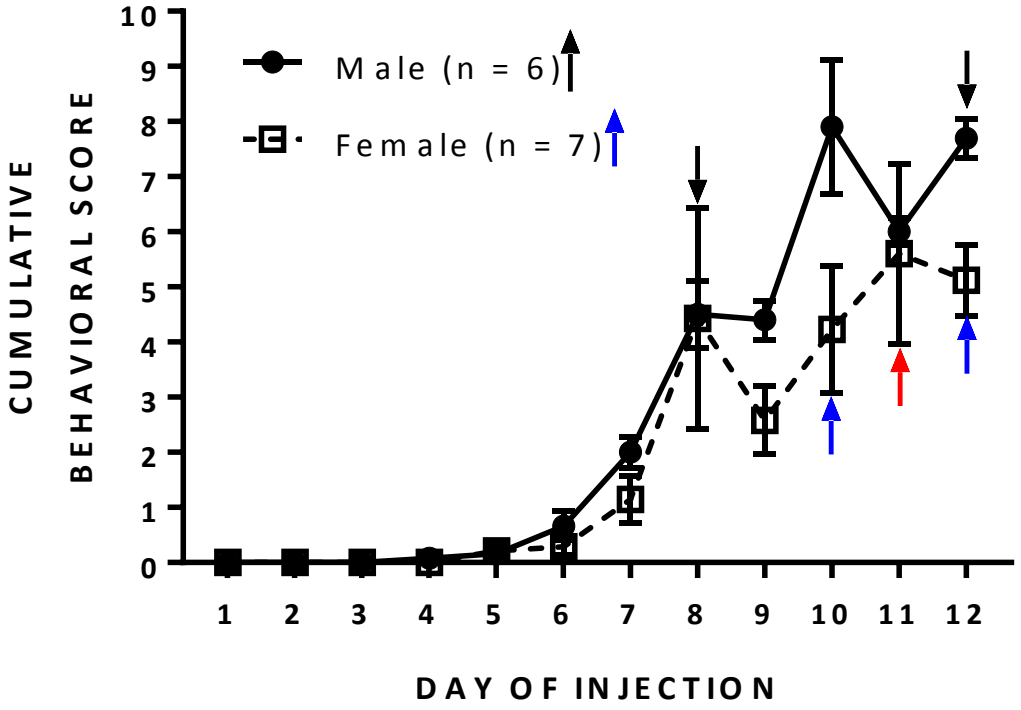

FIGURE 7: Comparison of 3-NP-mediated motor deficit in C57Bl/6J mice treated with 12 day protocol. Gross motor behavior of male (n = 6) and female (n = 7) mice were assessed and recorded just prior to each 3-NP injection. The average score for the day was plotted as mean ± SEM. There was a significant time-effect ($p = <0.0001$) and there was a statistically significant difference between sexes ($p = 0.0138$), as determined by repeated measures two-way ANOVA, after [Y = log (Y + 1)] transformation. Black arrows indicate the day at which a male mouse was removed from the study, whereas blue arrows indicate the removal of a female mouse, the red arrow indicates the day the female mouse was found dead.

RM 2-way ANOVA (figure 6). The males and females lost mass in a more consistent manner than the animals previously tested, (figure 1). Loss of mass was observed to not occur differently between males and females. One male (day 10) and one female (day 8) were removed from the paradigm early due to losing more than 20% of starting body mass. Assessment of gross motor deficit during the 12 day protocol (figure 7) demonstrated the same

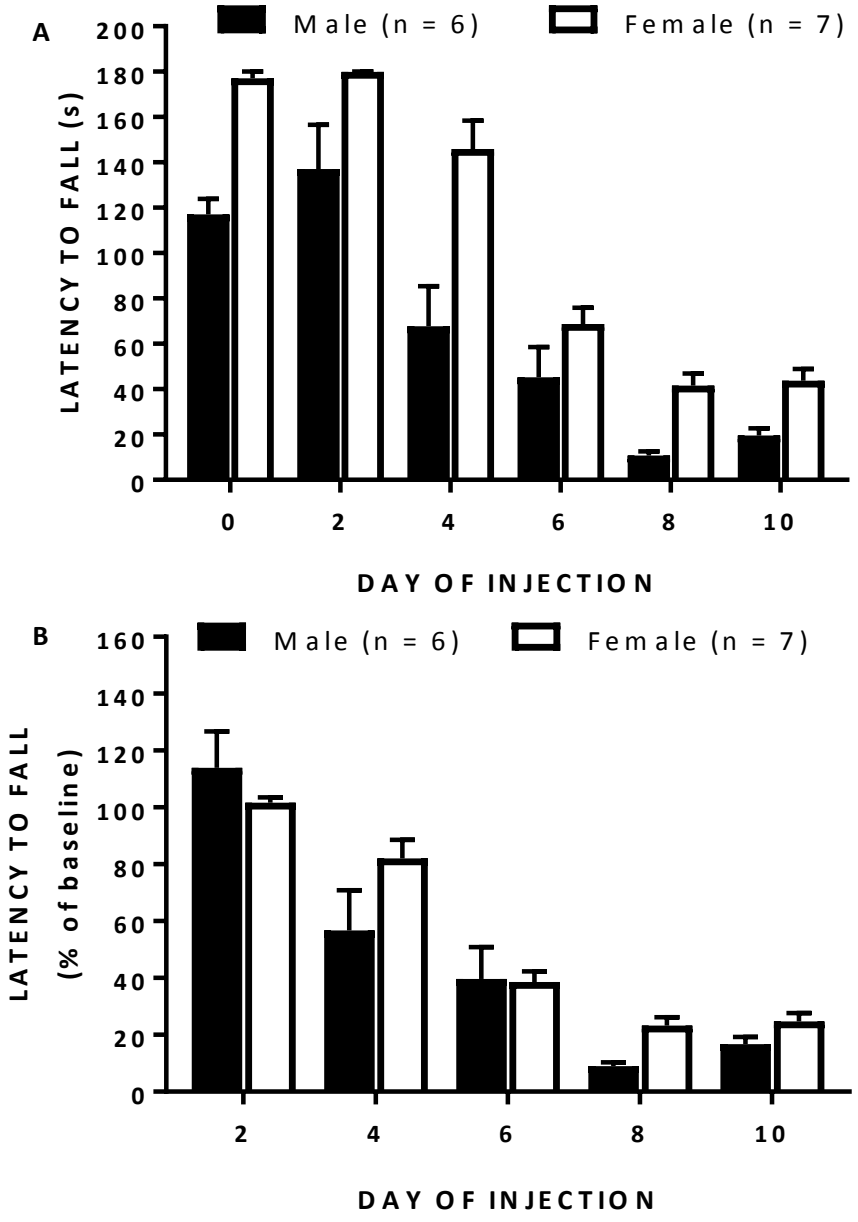

FIGURE 8: Comparison of fine motor deficits between male and female C57Bl/6J mice treated with 12 day protocol. (A) Inverted Grip: Motor strength and coordination was compared between male (n = 6) and female (n = 7) mice just prior to injection of 3-NP. Mice were placed on a wire mesh that was subsequently inverted for a maximum of 180 seconds. Each animal received three trials, with the longest latency to fall of the trials for each sex graphed as the mean ± SEM. There was a between group difference, as determined by repeated measures two-way ANOVA ($p = 0.0006$) **(B) Normalized Inverted Grip:** Latency to fall data was normalized as percentage of day 0 baseline measurements, and each sex graphed as the mean ± SEM. Data was transformed by $Y=\arcsin[\sqrt{Y/1000}]$. There was a between group difference as determined by repeated measures two-way ANOVA ($p = 0.0456$), with statistical differences found at days 4 ($p = 0.0343$) and 8 ($p = 0.0337$), following post-hoc analysis.

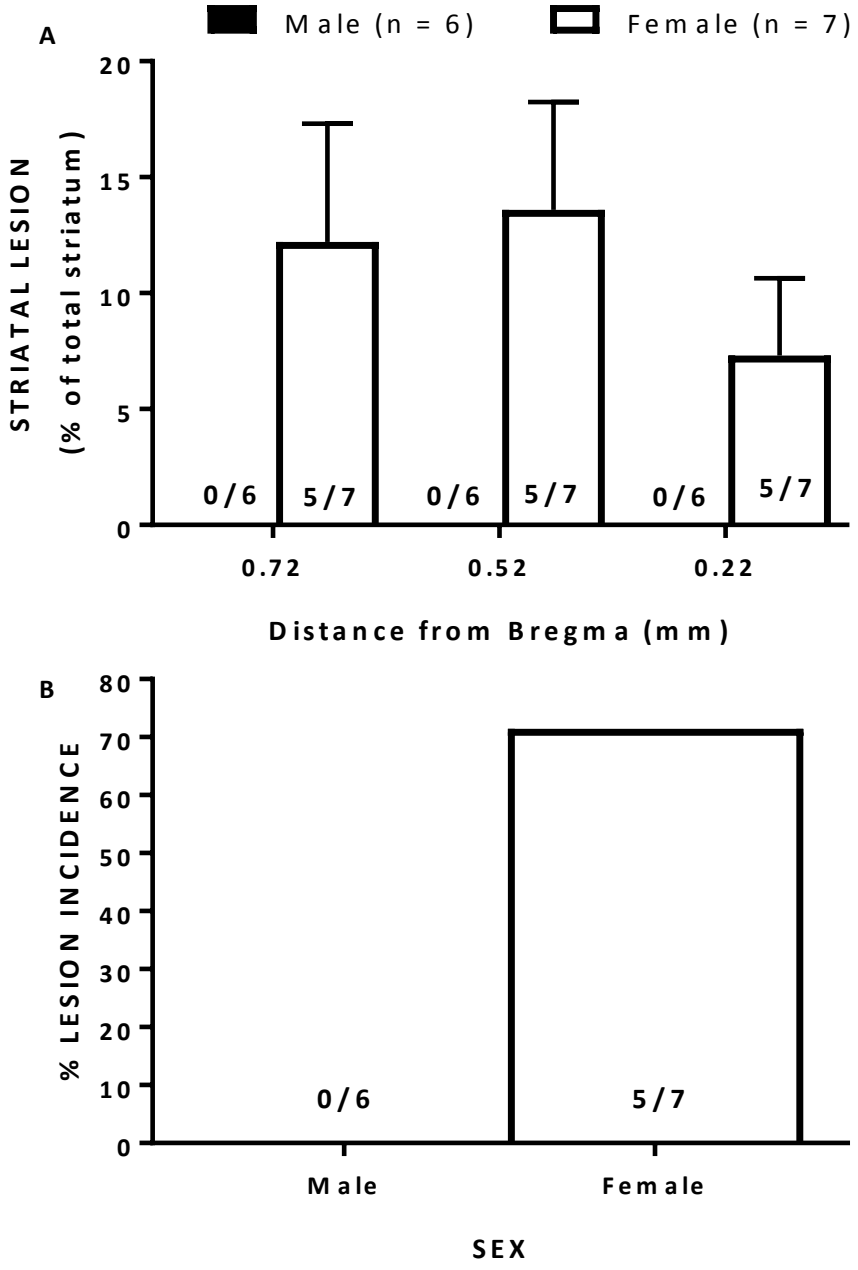

FIGURE 9: Comparison of lesion size and incidence between male and female C57BL/6J mice treated with 12 day protocol. Male (n = 6) and female (n = 7) were injected twice daily with 3-NP as described in methods. **(A)** Comparison of lesion area between male and female mice expressed as a percentage of total striatal area. Significant differences between sex occurs at the three levels of bregma shown, as determined by repeated measures two-way ANOVA ($p = 0.0154$), followed by Sidak's post-hoc t-tests for multiple comparisons ($p = <0.001$ at all shown levels). **(B)** Comparison of lesion incidence between male and female mice. The graph depicts the percent of mice of each sex with any size lesion determined by dividing the number with lesion by the total number of mice analyzed. Exact numbers contained within the bars. There was a significant difference in the lesion incidence as determined by Fisher's exact test ($p = 0.021$).

right shift seen in the original pilot study for female mice. The difference between male and female appears less severe in the 12 day paradigm (fig 7) as compared to the 11 day (fig 2). The set difference remains significant (p=0.0138). Behavior scores began to increase from day five and the female scores shifted to the right from the male scores after day eight. Greater variation is seen between individual animals, as demonstrated by the larger error bars (figure 7, figure 2). Two male animals and two female animals were removed for cumulative behavioral score, while one female was also found dead. The female was found within an hour of death and included in the histological analysis.

Determination of fine motor deficit was examined by measuring skeletal muscle strength through timing latency to fall when a mouse is hanging upside down from a wire mesh. Baseline measurements taken before the start of the injection series are shown as day 0 (figure 8A). Subsequent measurements made on days 2,4,6,8, and 10 demonstrated an overall significant difference between males and females. The distinct difference seen in baseline measurement was removed by normalizing experimental measurements to baseline measurements (figure 8B). Percentage data was transformed and tested by RM 2-way ANOVA, finding the significant difference between the groups remained (p=0.0456), post-hoc analysis demonstrated this difference was only present on days four and eight. In contrast to the behavioral results shown in figures seven to eight, in which females suffered less motor deficit, the histological analysis (figure 9) demonstrates that females developed larger striatal lesion than males (p=0.0154). Females developed lesions covering ten to fifteen percent of the striatum on average at 0.72mm and 0.52mm from bregma. Lesion size decreased to between five and ten percent of the striatum at 0.22mm from bregma.

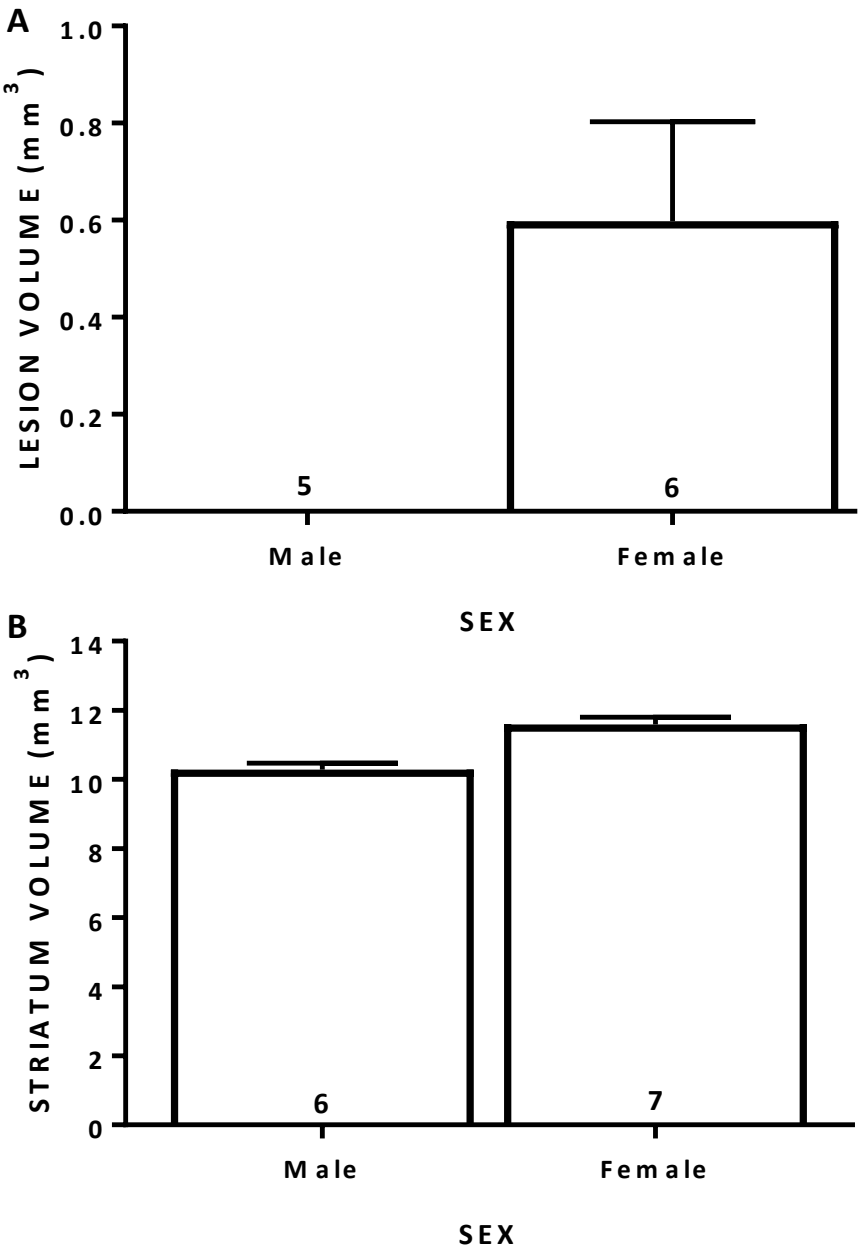

FIGURE 10: **Assessment of C57Bl/6J lesion volume treated with 12 day protocol.** Male (n = 6) and female (n = 7) mice were injected twice daily with 3-NP as described in methods. Lesion **(A)** and striatal **(B)** volume was quantified using the Cavalieri's method and graphed as the mean mm^3 ± SEM). A one-tailed t-test with Welch's correction revealed a significant difference between sexes (p = 0.0167). A significant difference was observed in striatum volume utilizing a two tailed test (p = 0.0007). Sample sizes differ between A and B because of removal of a statistically significant outlier from lesion measurements (Grub's outlier test).

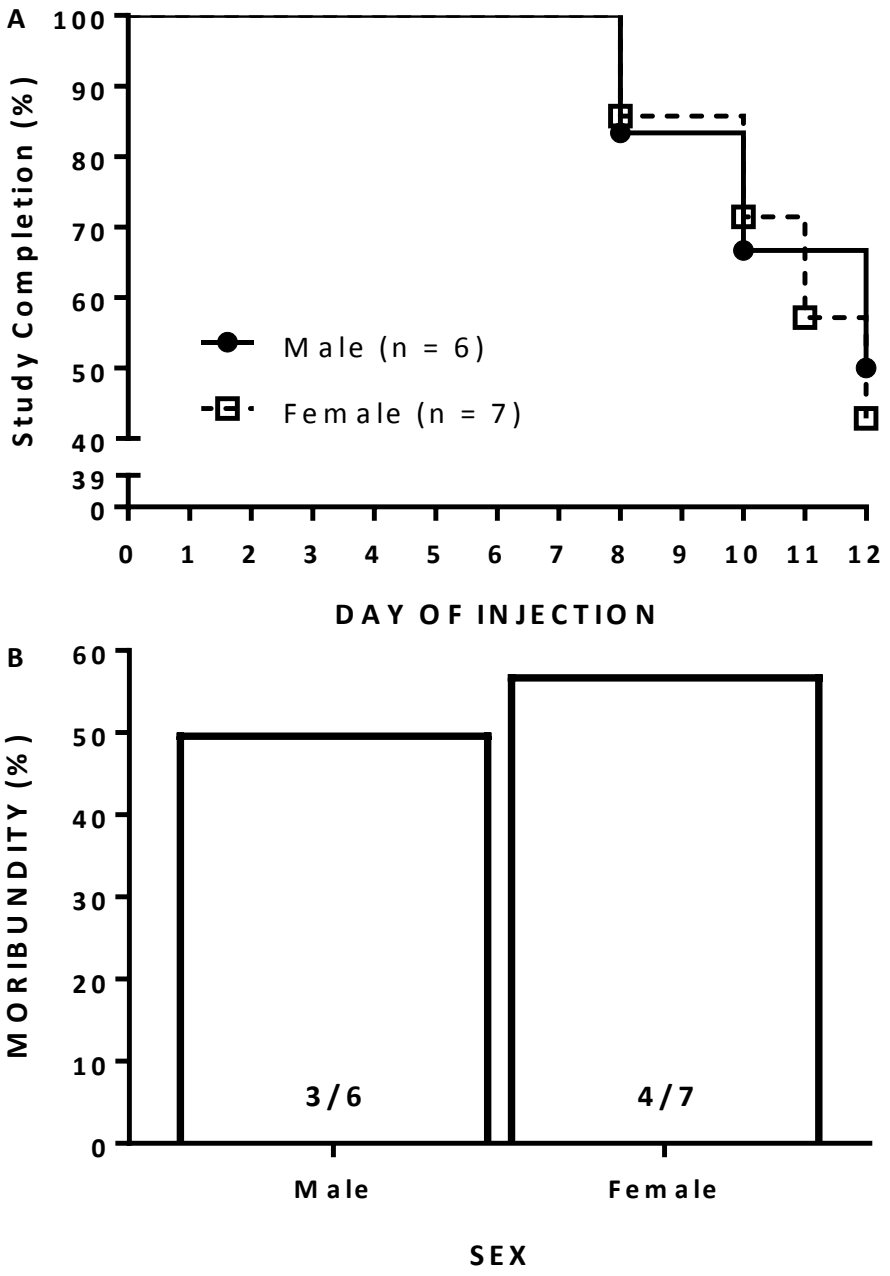

FIGURE 11: Comparison of the amount and rate of removal of male and female C57Bl/6J mice from the 12 day pilot study. Mice receiving 3-NP were removed from injection series if their behavioral score exceeded nine (9) or if they lost >20% of their body mass. **(A)** A Kaplan–Meier survival curve depicts the rate at which the mice were removed from study. No sex differences in rate of removal was determined by Mantel-Cox log-rank test (p = 0.8257). **(B)** The number of male and female mice, determined to be moribund are expressed as the percent of the total number of mice subjected to the systemic injection paradigm (fraction within bars). No sex differences were found when compared by Fisher's exact test (p = > 0.9999).

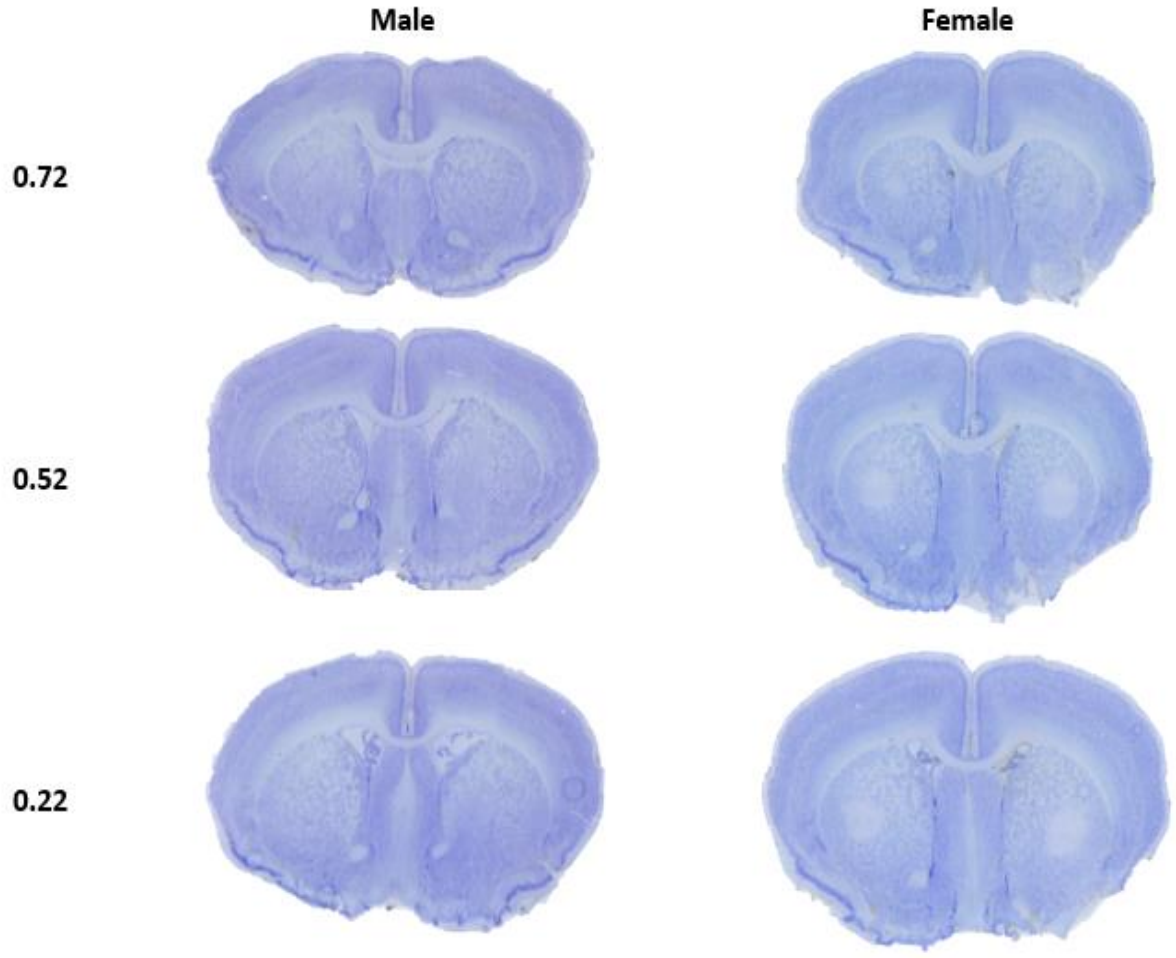

FIGURE 12: Representative images of C57Bl/6J male and female mice treated with 12 day protocol. Male (n = 5) and female (n = 5) mice were injected twice daily with 3-NP as described in methods. Photomicrographs of thionin stained sections depict striatal injury in female (right), but not male mice (left) at +1.02 to +0.22 from bregma at day 13 following 3-NP exposure.

In this paradigm, the males developed no distinct lesion from treatment with 3-NP. A single lesion was seen at one position measured of one male animal, this measurement was removed as an outlier, following analysis with Grubbs outlier test. Overall lesion size was smaller in females treated in the twelve day protocol rather than the eleven day. In the eleven day protocol male animal results were not significantly different from females. In the 12 day

protocol males, in fact, demonstrated no lesion (figure 9). Despite both paradigms administering the same cumulative dose, the rate of administration affects males significantly.

Lesion incidence (figure 9B) was significantly different between males and females with five of seven female animals developing lesion and no male animals developing lesion ($p=0.021$). Striatal volume and lesion volume (figure 10) demonstrated that females had larger striatal volume than the males ($p=0.0007$), although the female lesion was very small ($0.6mm^3$). Female lesion volume was significantly larger than male lesion volume ($p=0.0337$).

The intent of changing the dosing paradigm was to improve viability of experimental animals. In the eleven day paradigm no animals from either group completed the program. Animal removal from the twelve day paradigm (figure 11) demonstrates study completion is improved with 50% of male animals and 45% of female animals over the injection series completing the study. A Kaplan-Meier survival curve (figure 11A) rate of removal, began to decrease from day eight and there was no significant difference between the rate of male and female survival ($p=0.8257$).

Considering the incidence of animal removal (figure 11B), the two groups were not significantly different ($p=>0.9999$). Coronal sections of the male and female brains (figure 12) demonstrate the observed lesion in the female mice but no lesion is present in the males. The lesioned area has a distinct border and is void of stain or blemishes.

2.4. Pilot Study Discussion

To investigate the role of IL-1β signaling in a chemical HD model, 3-NP was administered twice daily in incremental doses. The effect of the total cumulative dose and the rate at which

the dose was increased on the experimental animal was unknown. It was necessary to determine the response to the designed dosing paradigm in the background strain of the IL-1R1 null model before further experimentation was conducted. Sex differences in the response to 3-NP have been reported in previous studies. It was important to investigate any possible effect the sex of the animal may have on the experiment. The use of animals between the age of 16 and 18 weeks was designed to minimize any hormone mediated sex differences (Nishino et al., 1997).

Previous studies indicated that estrogen is the factor responsible for observed resistance to 3-NP in female mice (Nishino et al., 1998). In our first pilot study, using animals aged 16-18 weeks, both male and female animals developed lesions of a similar size and both groups had a similar degree of lesion incidence when treated with 3-NP in the manner detailed in the methodology. The histological similarity of lesion in male and female brain tissue indicates that any sex-mediated differences were not observable with the analysis conducted for this study. Previous findings had indicated that estrogen upregulates Anexin A1, leading to greater integrity of the blood brain barrier (BBB) (Maggioli et al., 2016). If BBB integrity was preserved in females, no effect on lesion size was seen in the results of this study. Gross behavioral deficit, as monitored through daily scoring, did demonstrate a delay in effect for female animals. Histological analysis demonstrated no significant difference in lesion size. The findings from this pilot study indicated that animal sex did not influence striatal lesion size in this dosing paradigm. Although no difference in histology was seen, a delay in effect may be present in female animals. This could be due to differences in metabolism or other undetermined factors.

In the first pilot study no animal completed the injection paradigm. Whereas, the study 40-50% animal moribundity was expected. The need to remove all participating animals presented the problem of the animals receiving less than the intended total dose. In the first pilot study both groups of animals were removed on the same day, therefore, in this case all animals received approximately the same dose. Pilot study findings indicated two areas requiring adjustment. Ideally, striatal lesion size would be approximately 50% to facilitate the visualization of the benefit or detriment of removing IL-1β signalling. Secondly, study completion needed to be increased wherein the majority of animals could receive the full dose.

In order to ensure relative comparability of animals with respect to total dose received, the injection paradigm was adjusted. Increasing striatal lesion in wild type animals to 50% is statistically ideal, however such severe cellular loss in the animal striatum may directly conflict with the priority of having sufficient animal survival. To achieve a decrease in moribundity rate, the increase in dose administered was changed to a more gradual escalating dose regimen. As 3-NP irreversibly inhibits SDH any mitochondria affected would have to be replaced. Should viable mitochondria be able to replicate at a sufficient rate to compensate for the loss of 3-NP affected mitochondria, the host cell would remain viable. Extending the dosing period and minimizing the rate at which the doses increase may prevent the development of a feedback system in which cell death from 3-NP cause's neuronal degradation.

Having repeated the pilot study with the adjusted 12 day dosing paradigm the ability of the animals to complete the study was clearly improved. Further, a clear difference in male female histology became apparent. The intention of adjusting the dosing paradigm was to improve study completion, which was achieved. However, a difference in the histological

results between the two sexes was not expected. In male animals there is no apparent lesion after 12 days of treatment with 3-NP and in females lesions were present but minimal. The difference between the sexes in the development of motor deficit was also maintained in the 12 day paradigm. The change in the development of motor deficit, suggests any peripheral effect on males and females is similar.

The hypothesis to be tested is that the lack of IL-1β signalling will be detrimental and therefore increase the observed lesion area in IL-1R1 null animals. Ideally, the baseline of injury produced by the dosing paradigm would be sufficiently large so that both increase and decrease of lesion size could be observed. However, given my hypothesis, the experimental study continued with the 12 day paradigm as tested, because the hypothesized increase of lesion size would still be testable.

3. CHAPTER THREE

3.1. Rationale of IL-1R1 Study

The generation of ROS and depletion of ATP in HD as previously detailed provides a point of study. It is not currently known if the increase in ROS reported in HD can be attenuated by IL-1R1 signalling or by what mechanism this would occur. Previous research produced by this laboratory has demonstrated that the addition of IL-1β to astrocyte culture can protect against oxidant induced cell death. Further the use of IL-1R1 deficient mice to generate astrocyte culture negates the protection induced from IL-1β pre-treatment (He et al., 2015). These findings suggest that protection against ROS mediated by IL-1β, which would be experimentally demonstrated by an increase in striatal injury when IL-1R1 is absent.

Additional research using murine astrocyte and neuron cultures, demonstrated that the organic peroxide, a ROS, tert-butyl hydroperoxide (t-BOOH) caused astrocytic and neuronal cell death in a concentration-dependent manner. In the presence of IL-1β, death from t-BOOH was attenuated, which was shown to be achieved through the upregulation of glutathione (GSH), the predominant antioxidant in the CNS (Chowdhury, unpublished). These results confirm previous studies which demonstrated IL-1β as a responsible factor for the upregulation of the antiporter system x_c^-, which plays an important role in cystine import (Fogal et al., 2007, Jackman et al., 2010, Shi et al., 2016). Once imported cystine is converted to cysteine the limiting factor in GSH production. Blocking the release of GSH from astrocytes led to loss of protection in neurons (Chowdhury, unpublished).

The implementation of this study was conducted to utilize wild type and IL-1R1$^{-/-}$ animals bred from mice with a heterozygous IL-1R1 genotype in order to examine the result of

IL-1β signalling in the 3-NP model of HD. Building on previous *in vitro* work, examining the effect of 3-NP on the striatal tissue of animals both with and without IL-1R1 signalling will demonstrate if IL-1β is involved and to what extent based on the experimental conditions established in chapter two.

3.2. Methodology

Animal Husbandry

Experimental animals were produced from F1 heterozygous breeding pairs bred from wild type (+/+) C57BL/6J females (JAX stock: 000664) and IL-1R1 null (-/-) males (JAX stock: 003245). Resulting +/+ and -/- littermates from the F2 and F3 generations were used. Genotyping was conducted by standard PCR of tail DNA samples. Primers (Integrated DNA Technologies) 5'-GAG TTA CCC GAG GTC CAG TGG-3' (IL-1RI WT (831)), 5'-CCG AAG AAG CTC ACG TTG TCA AG-3' (IL-1RI All (832)), and 5'-GAA TGG GCT GAC CGC TTC CTC-3' (IL-1RI KO (833)) identify +/+ DNA by a 1150b.p. product and -/- DNA by a 860b.p. product. Mice were provided food and water *ad libitum*, while housed up to five animals per cage in a controlled temperature environment operating on a standard 12 hour light/dark cycle in an AALAC accredited facility. All animal procedures were conducted with IACUC approval and the investigator was blind to animal genotype at time of experimentation.

3-Nitroproprionic Acid Dosing Protocol

3-NP (Sigma Aldrich, N5636) was dissolved in 0.9% saline to a concentration of 25 mg/ml, adjusted to pH 7.4 with 5M NaOH, and filter sterilized (0.2µm Nalgene). 3-NP dosing stock was kept at 4°C for no more than seven days. After five days of acclimatization handling,

mice were administered 3-NP via intraperitoneal (IP) injection twice daily with an interval of 8-12 hours as follows: 20 mg/kg – two days, 30 mg/kg – three days, 40 mg/kg – three days, 50 mg/kg – three days, 60 mg/kg one day for a total cumulative dose of 920 mg/kg. Animals completing the protocol were sacrificed by cervical dislocation under isoflurane anaesthesia. Brains were snap frozen in O.C.T. compound (Sakura Finetek USA) for histological analysis. Three separate experiments were performed over two months.

Behavioral Scoring

Behavioral analysis was adapted from (Fernagut et al., 2002) and conducted before each injection. Hindlimb clasping, general locomotor activity, hindlimb dystonia, truncal dystonia and postural adjustment reflexes were assessed twice per day just prior to each injection by this observer blinded to genotype. Three point scales were assigned corresponding to no abnormality (0), moderate (1,3) or severe deficits (2,5). Any mouse attaining a cumulative behavioral score ≥ 9 or sustaining a weight loss ≥ 20% was immediately sacrificed (He et al., 2017). Three separate experiments were performed over two months.

Rotor-Rod

Motor strength and coordination were evaluated using an automated Rotor-Rod system (Ugo Basile, Model 47650, with a rod diameter of 3 cm). Mice were placed on the silent treadmill for 15 seconds to acclimate and then the rotating treadmill set in motion with increasing speed up to 55 rpm over two 5 min test periods. Each animal received two trials per assessment, with the longest latency to fall (onto a soft surface with automatic timer), a measure of the ability to maintain balance, recorded per trial and then averaged. Clasping the

rod resulted in cessation of the trial. After a minimum of five minutes rest, a new trial was commenced. Two separate experiments were performed over two months.

Inverted Grip

To assess grip strength, the mouse was placed on a 1 cm square wire mesh, which was then inverted 180^{o} and held 40 -50 cm over a padded surface. The time to fall was recorded using a stopwatch. Each animal received up to three trials, with the longest latency to fall of the three trials recorded. The animal was removed from the mesh when a criterion time of 60 s was achieved. (Deacon, 2013). Two separate experiments were performed over two months

Histological analysis

Frozen brain sections (40μm) collected serially from the rostro-caudal extent of each brain (+1.54 to -0.18 relative to bregma) and stained with 0.5% thionin by submersion in multiple wash solutions (70% EtoH, 50% EtoH, ddH2O, thionin, ddH2O, ddH2O, 70% EtoH, 95% EtoH, 100% EtoH, 100% EtoH, 100% Xylenes, 100% Xylenes) as previously described (He et al., 2017). Images were captured by scanning (Epson Perfection 3170) at 2400 dpi. The lesion area, identified by absence of thionin staining, was quantified using NIH Image J at seven levels from bregma (+1.22, +1.02, +0.72, +0.52, +0.22, +0.02, and -0.18) by three individuals blind to genotype and experimental identification. For each level, the percent striatal damage (D) was calculated as a percentage of the total striatum area (T) as (D/Tx100). Area measurements were converted to volume using Cavalieri's principle (volume = $(s_1d_1) + (s_2d_2) + (s_3d_3) + (s_4d_4) + (s_5d_5) + (s_6d_6) + (s_7d_7)$), where s = lesion surface area and d = distance between two sections, as published (Shih et al., 2005). Data are expressed as lesion area as a percentage of striatum at all

seven levels, and the mean lesion volume + SEM of all seven levels derived from the mean calculated from all three individuals.

Succinate Dehydrogenase (SDH) Assay

SDH activity was determined in crude brain mitochondrial preparations derived from wild type and IL-1R1 null animals. Two hours following injection with either saline or 150 mg/kg 3-NP, brains were removed from the cranium and striatal tissue dissected and homogenized in an extraction buffer containing 10 mM Tris-HCl (pH 7.4), 0.44M sucrose, 10 mM EDTA and 0.1% BSA. Homogenates were spun (2100g, 4˚C, 5min), the supernatant collected, and re-spun (14,000g, 4˚C for 15min). Following aspiration of the supernatant, the crude mitochondrial pellet was resuspended in extraction buffer (1 ml), respun (7,000g, 4˚C for 15min) and resuspended again (500 µl). Twenty microliters was incubated for 20 min at 37°C in a reaction mixture (final volume = 200 µl) consisting of 0.1M potassium phosphate buffer (pH 7.4), 0.1M succinate, 0.05M sucrose, 1mg/ml p-iodonitrotetrazolium chloride (prepared fresh). The change in absorbance of the formazan product was read at 490 nm in a microtiter plate reader (Molecular Devices) (Pennington, 1961) Twenty microliters of the same crude mitochondrial prep was used for protein concentration measurement via the BCA assay (Thermo Scientific, Kalamazoo, MI). Data was normalized to the SDH activity of the saline treated animals for each genotype.

Statistical Analysis

Statistical analysis was performed using GraphPad Prism, Version 7.03. Percent data was transformed by the arcsin square root function (Y=arcsin[sqrt(Y/1000)], while behavioral score data transformed by the function [Y = log (Y + 1)], prior to analysis. Comparisons of mass,

lesion size, behavior score and grip strength were made using repeated measures two way analysis of varience followed post-hoc by Sidak's multiple comparison test. Lesion and morbidity incidence comparisons were evaluated by Fisher's exact test. The Kaplan–Meier survival curves, depicting the rate at which animals were removed, were compared by Mantel-Cox log-rank test. Differences in SDH activity was assessed by 2-way ANOVA (Treatment x Genotype) with Bonferroni's multiple comparisons.

3.3. IL-1R1 Results

Male and female results are reported and considered separately due to differences observed in the pilot study. The results are grouped by sex.

IL-1R1 Male Results

Comparison of mass of male IL-1R1 null animals and wild type littermates (figure 13), demonstrated no significant difference over the course of the dosing paradigm (p=0.6635). Both groups differed significantly over time (p=>0.0001). Mass decreased in a steady manner. On average, both groups lost four grams of mass over the injection period. Two wild type, and three IL-1R1 null animals, were removed for losing more than 20% of body mass. The average mass for both groups increased on day twelve. Individual animal mass would fluctuate on a day to day basis with an overall downward trend. Animal removal on day eleven combined with small increases of mass in surviving animals could result in the increase seen in plotted averages.

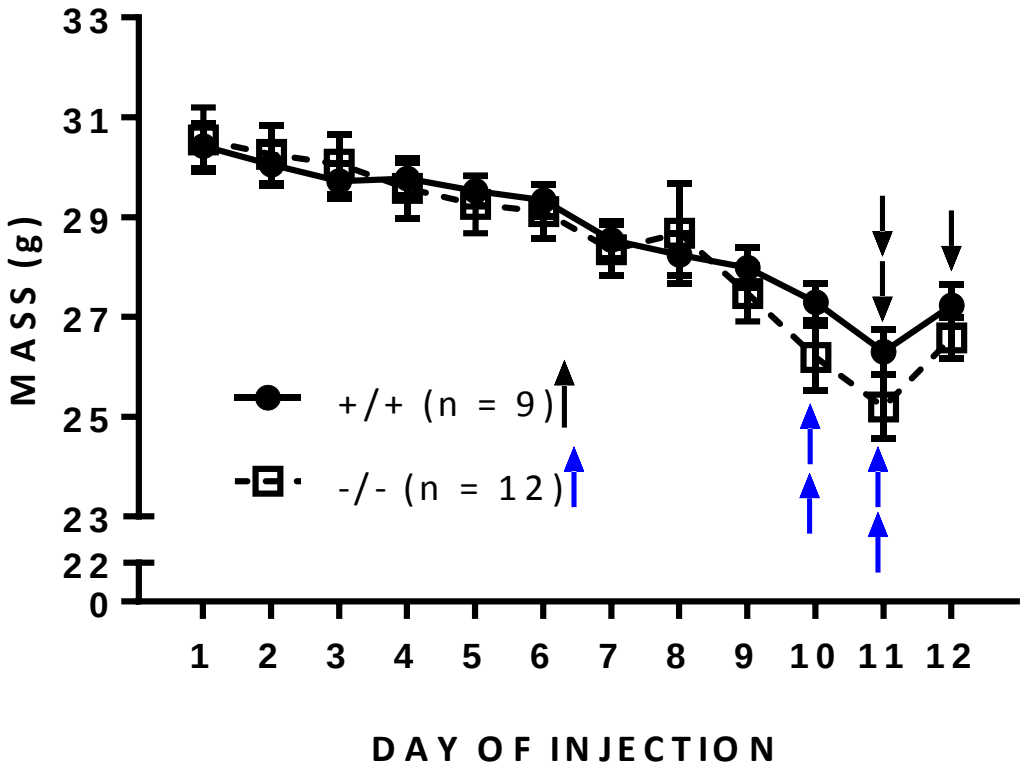

FIGURE 13: Comparison of 3-NP-mediated mass loss in male mice. Mass of IL-1R1 null mutant mice (−/−, n = 12) and their wild-type littermates (+/+, n = 9) were assessed and recorded just prior to each 3-NP injection. Mass was plotted as mean ± SEM. Although there was a significant effect over time (p = <0.0001) for both genotypes, there was no statistically significant difference between genotypes (p = 0.6635), as determined by repeated measures two-way ANOVA. Black arrows indicate the day at which a wild type animal was removed from the study, whereas blue arrows indicate the removal of an IL-1R1 null mutant mouse for score.

Gross motor deficit (figure 14) as scored from twice daily observation demonstrated no significant difference between genotypes (p=0.6506). Removal for incurred motor deficit based on score was more common than removal for loss of mass. Five wild type and two null animals were removed over the injection period. In both groups motor deficit began to become observable from day five. Fine motor deficit (figure 15) was measured through rotor-rod testing for motor function and inverted grip testing for muscle strength. Wild type and IL-1R1 null

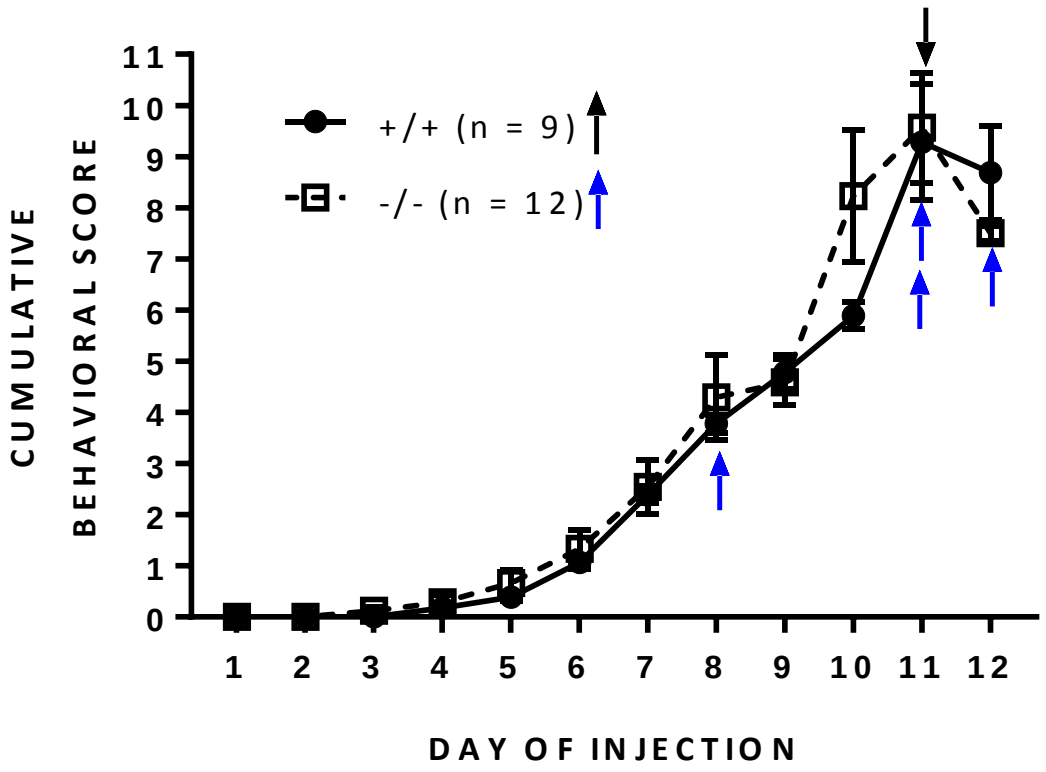

FIGURE 14: Comparison of 3-NP-mediated motor deficit in male mice. Gross motor behavior of IL-1R1 null mutant mice (−/−, n = 12) and their wild-type littermates (+/+, n = 9) were assessed and recorded just prior to each 3-NP injection. The average score for the day was plotted as mean ± SEM. There was a time dependent increase in behavioral deficits ($p = <0.0001$) that did not differ between genotypes ($p = 0.6506$) as determined by repeated measures two-way ANOVA, after [Y = log (Y + 1)] transformation. The black arrow indicates the day at which a wild type animal was removed from the study, whereas blue arrows indicate the removal of an IL-1R1 null mutant mouse.

animals from two cohorts over two months demonstrated no significant difference in motor function as assessed by rotor-rod ($p=0.9757$). Animals from both groups demonstrated an increase in latency to fall from the baseline measurement until day four (figure 15A) of the injection paradigm, followed by a rapid decline in latency to fall by day eight. Inverted grip strength comparison (figure 15B) exhibited no significant difference ($p=0.8986$). No decrease in

latency to fall from the baseline measurement was observed until day four, after which both groups latency to fall continually declined.

Unlike behavioral testing, histological analysis of IL-1R1 null and wild type littermate control animals demonstrated a significant difference (figure 16). Lesion area, as a percentage of striatal area (figure 16A) was significantly larger in IL-1R1 null animals ($p=0.0163$). The region from 1.02mm to 0.22mm relative to bregma contained the largest lesion. Wild type animals presented lesions from 0.72mm relative to bregma as opposed to IL-1R1 null animals which showed lesion at all measured positions. Lesion incidence (figure 16B) was more prevalent in IL-1R1 null animals with 75% displaying lesion, compared to 37.5% of wild types, although the difference was not statistically significant according to a Fisher's exact test ($p=0.1675$) shown in figure 16.

Lesion volume was calculated from area measurements (figure 17) to examine actual size. Measured striatal volume was not significantly different between genotypes (Fig. 17B; $p=0.0674$). A statistically significant difference in male lesion volume, fig. 17A ($p=0.01$) was observed. Published measurements of striatal volume are shown and the relation to this study is discussed in Appendix A. Animal removal (figure 18) displayed the completion of the injection paradigm to be comparable to that shown in figure 11. The study completion of wild type and IL-1R1 null animals was not significantly different ($p=0.2049$). The incidence of animal removal was not significantly different between the tested groups ($p=0.3964$). Representative images of the lesions of male wild type and IL-1R1 null animals (figure 19) demonstrates a large lesion with blood present in the lesion of null animals and a small clear lesion for wild type. Blood was common in animals with larger lesions, and could indicate endothelial damage.

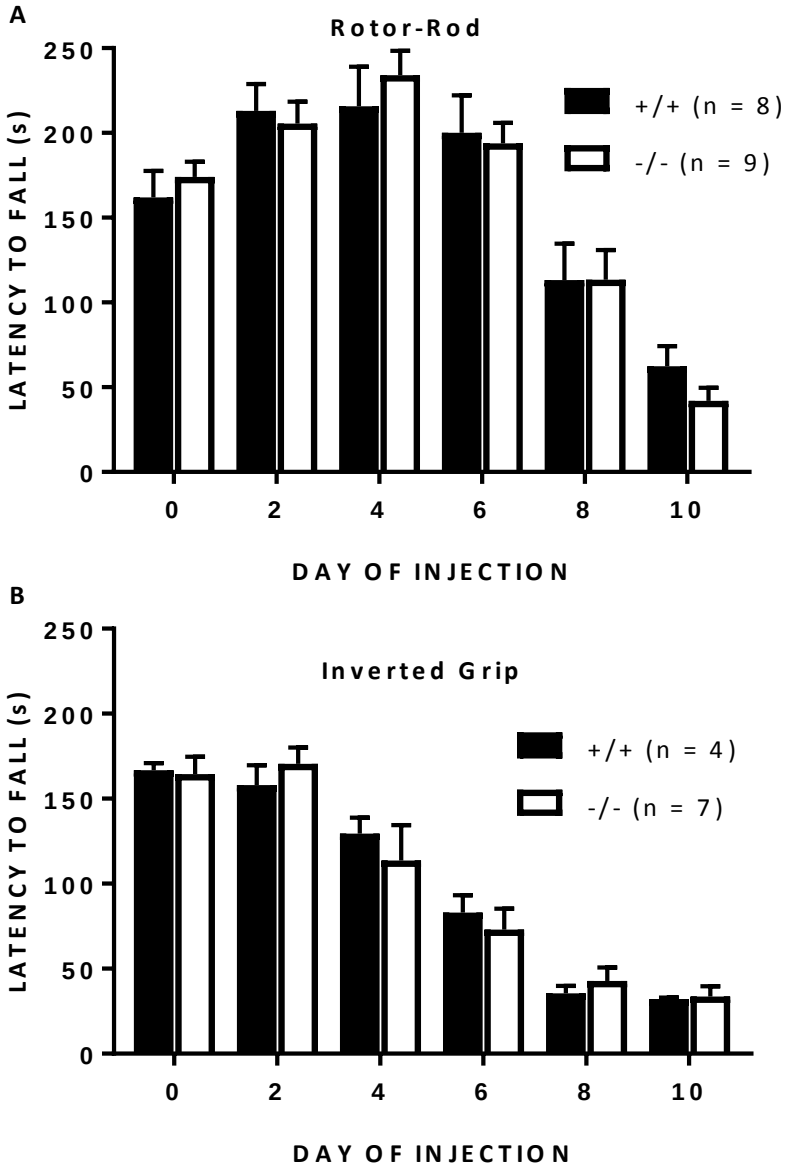

FIGURE 15: Comparison of fine motor deficits between wild type and IL-1R1 deficient male mice. (A) Rotor-rod: Motor strength and coordination was compared between male wild type (+/+, n = 8) and IL-1R1 null (-/-, n = 9) mice just prior to injection of 3-NP using an accelerated rotor-rod paradigm (300 sec; 5-55RPM) on the days indicated on the x axis. A record of the latency to fall from two independent trails was made and the data graphed as the mean ± SEM. There was no significant difference in time to fall between genotypes as determined by repeated measures two-way ANOVA ($p = 0.9757$). A significant time-effect was observed ($p = < 0.0001$). **(B) Inverted Grip:** Male wild type (+/+, n = 4) and IL-1R1 null (-/-, n = 7) were placed on a wire mesh that was subsequently inverted for a maximum of 180 seconds. Each animal received three trials, with the longest latency to fall of the trials for each genotype graphed as the mean ± SEM. There were no between-group differences as determined by repeated measures two-way ANOVA ($p = 0.8986$). A significant time-effect was observed ($p = < 0.0001$). Sample sizes differ from Figure 13 because not all cohorts received the same behavioral tests.

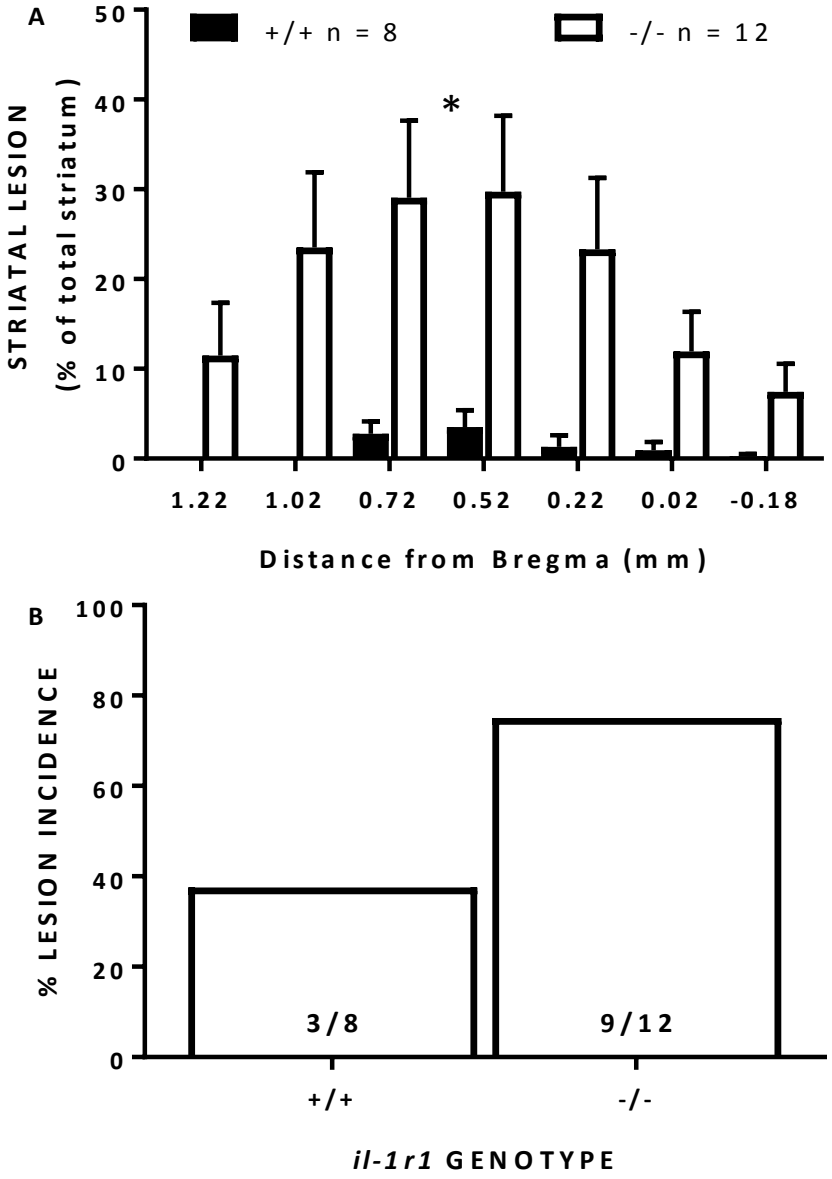

FIGURE 16: Comparison of lesion size and incidence between male wild type and IL-1R1 deficient mice. Male IL-1R1 null mutant mice (-/-, n = 12) and their wild-type littermates (+/+, n = 8) were injected twice daily with 3-NP as described in methods. **(A)** Comparison of lesion area between IL-1R1$^{+/+}$ and IL-1R1$^{-/-}$ mice expressed as a percentage of total striatal area. A significant difference between genotypes occurs at every level of bregma as determined by repeated measures two-way ANOVA (p = 0.0163), followed by Sidaks post-hoc t-tests for multiple comparisons (p = <0.0001 at all levels). **(B)** Comparison of lesion incidence between IL-1R1$^{+/+}$ and IL1R1$^{-/-}$ mice. The graph depicts the percent of mice from each genotype with any size lesion determined by dividing the number with lesion by the total number of mice analyzed. Exact numbers contained within the bars. There was no significant difference in the lesion incidence as determined by Fisher's exact test (p = 0.1675).

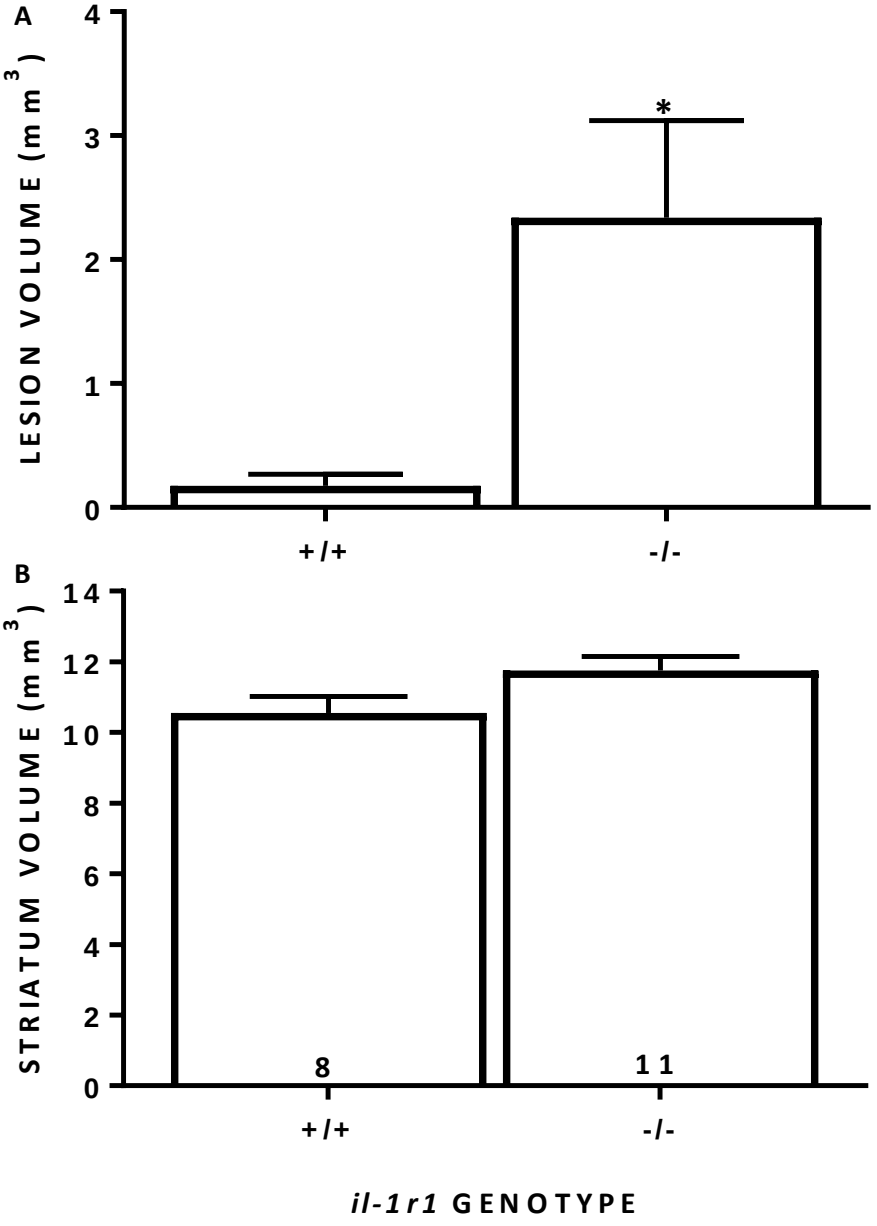

FIGURE 17: Assessment of male lesion volume. Male IL-1R1 null mutant mice (-/-, n = 11) and their wild-type littermates (+/+, n = 8) were injected twice daily with 3-NP as described in methods. Lesion **(A)** and striatal **(B)** volume was quantified using the Cavalieri's method and graphed as the mean mm^3 ± SEM. A one-tailed t-test with Welch's correction revealed a significant difference between genotypes (p = 0.01). No significant difference was observed in striatum volume utilizing a two tailed t-test (p = 0.0674). Sample sizes differ from Figure 16 because of removal of a statistically significant outlier from the null group (Grub's outlier test).

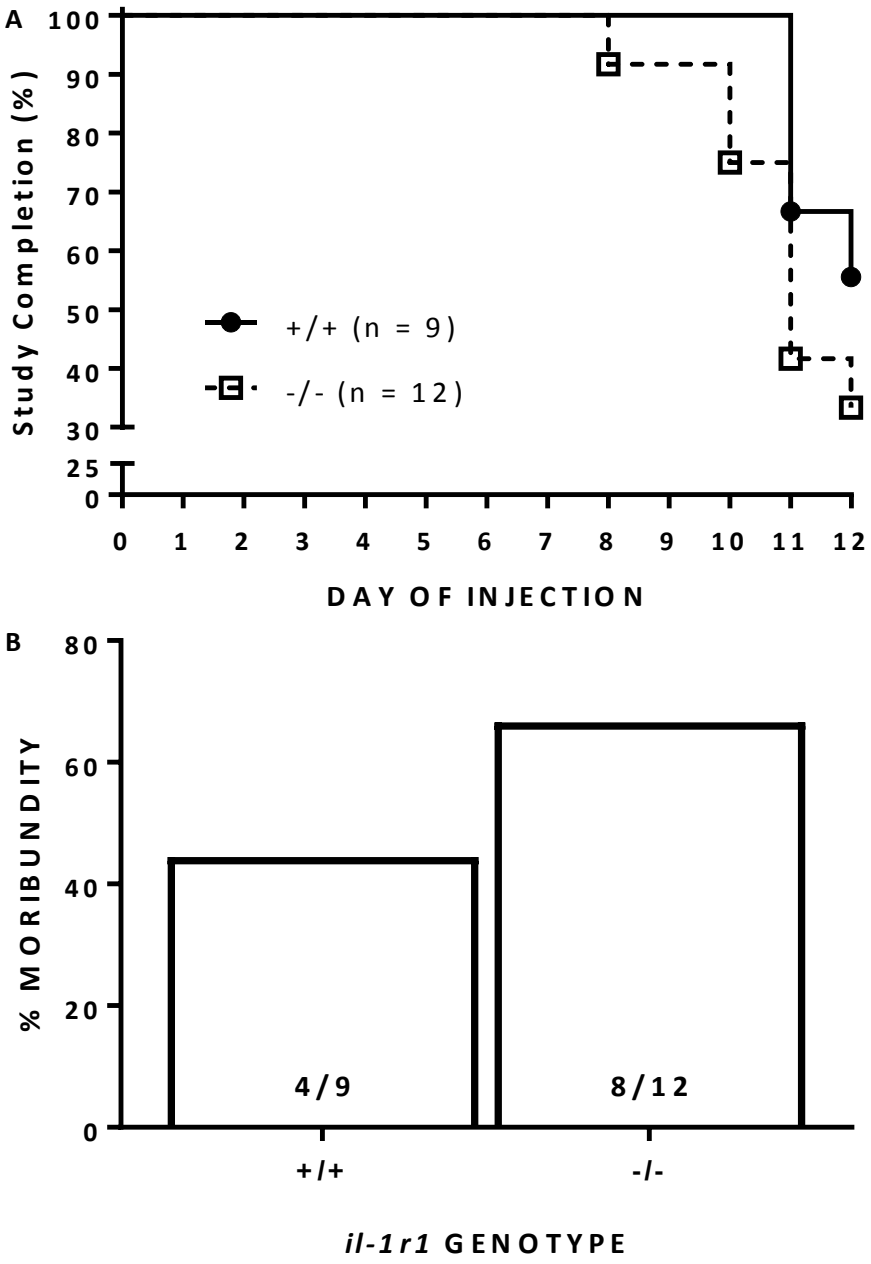

FIGURE 18: Comparison of the amount and rate of removal of wild-type (+/+) and IL-1R1 null (-/-) male mice from 3-NP study. Mice receiving 3-NP were removed from injection series if their behavioral score exceeded nine (9) or if they lost >20% of their body mass. **(A)** A Kaplan–Meier survival curve depicts the rate at which the mice were removed from study. No genotypic differences in rate of removal was determined by Mantel-Cox log-rank test (p = 0.2049). **(B)** The number of IL-1R1$^{+/+}$ and IL-1R1 $^{-/-}$ mice determined to be moribund are expressed as the percent of the total number of mice subjected to the systemic injection paradigm (fraction within bars). No genotypic differences were found when compared by Fisher's exact test (p = 0.3964).

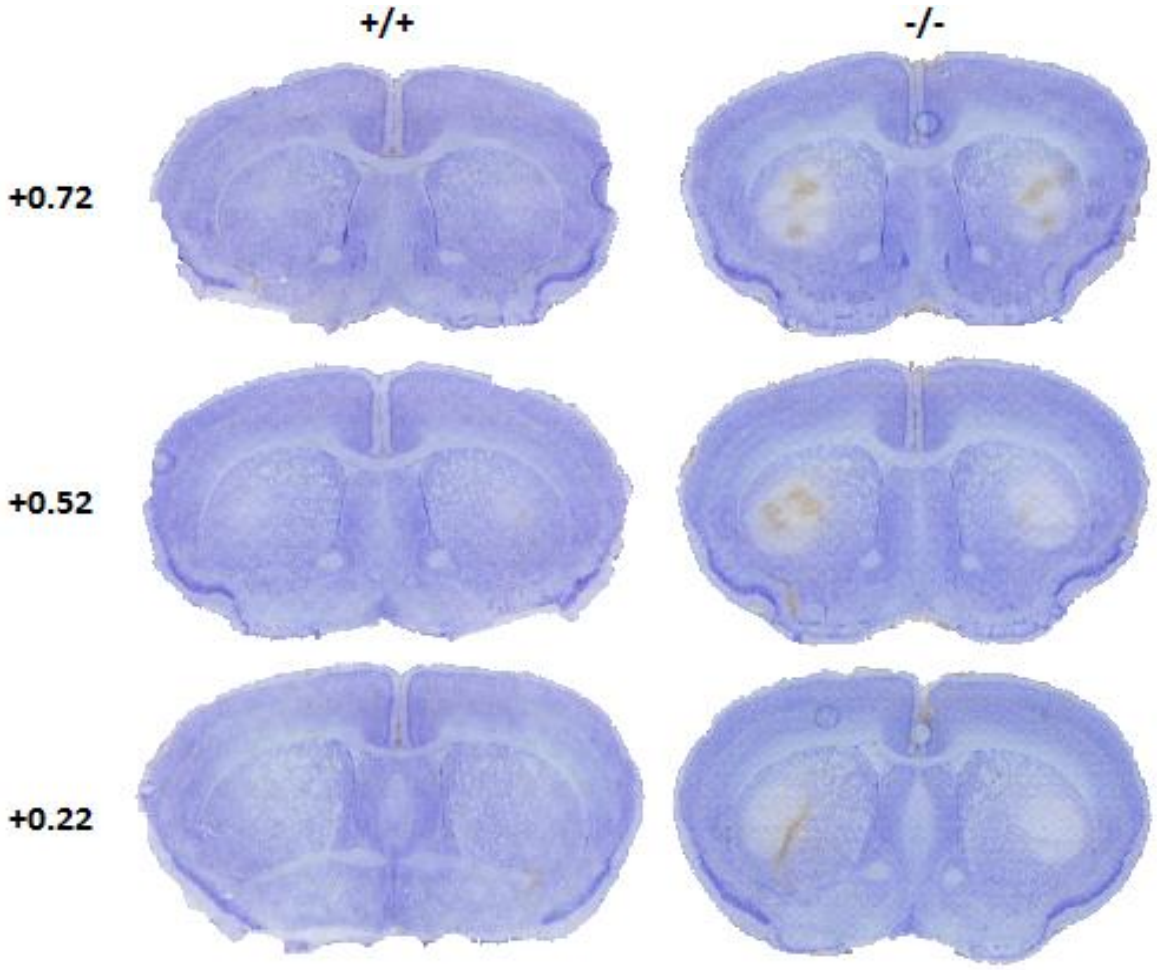

FIGURE 19: Representative images of male wild type and IL-1R1 deficient mice. Male IL-1R1 null mutant mice (-/-, n = 12) and their wild-type littermates (+/+, n = 8) were injected twice daily with 3-NP as described in methods. Photomicrographs of thionin stained sections for determination of striatal injury in IL-1R1$^{+/+}$ (left) and IL-1R1$^{-/-}$ mice (right) at +0.72 to +0.22 from bregma at day 13 following 3-NP exposure are depicted.

IL-1R1 Females

Like males, female animals (figure 20) demonstrat a steady continual loss of mass over the injection period. No significant difference between IL-1R1 null and wild type female mice was evident (p=0.6222). There was a significant change in mass that occurred independent of genotype (p=<0.0001). As demonstrated in males, mass did increase on day twelve. The

increase in average mass was likely due to the removal of animals that were most affected, and increases in individual animal mass.

The gross behavior score in females (figure 21) demonstrated a significant change in score over time ($p=<0.0001$). Observable motor deficit occurred from day five, in both genotypes. The wild type animal score shifted to the right, indicating a delay in incurred motor deficit, until after day seven, but this was not statistically significant ($p=0.1314$). Removal of animals for reaching the maximum behavioral score was more prevalent in IL-1R1 null animals, three of which were removed. Two wild types were removed for behavioral score. Fine motor deficit (figure 22) was assessed by rotor-rod and inverted grip testing. No significant difference between genotypes was seen in rotor-rod testing over the injection series ($p=0.8665$). Additionally, significant between group difference in the latency to fall during the inverted grip test was seen ($p=0.2813$). During rotor- rod testing (figure 22A), animals demonstrated an increase in latency to fall from the baseline measurements up to day four of the injection series with loss of motor function occurring from day six to ten.

Mice demonstrated a decrease in the latency to fall from day six to ten. Histological analysis of lesion area in female mice (figure 23) did not demonstrate any significant difference between the genotypes. Lesion area as a percentage of striatal area (figure 23A) demonstrated a wider spread of lesion along the striatum in female mice, but any difference was not statistically significant ($p=0.5592$). Lesion area covered 20% of striatal area in both groups, at the most severely lesioned positions. Lesion area in female IL-1R1 null animals was smaller than that of

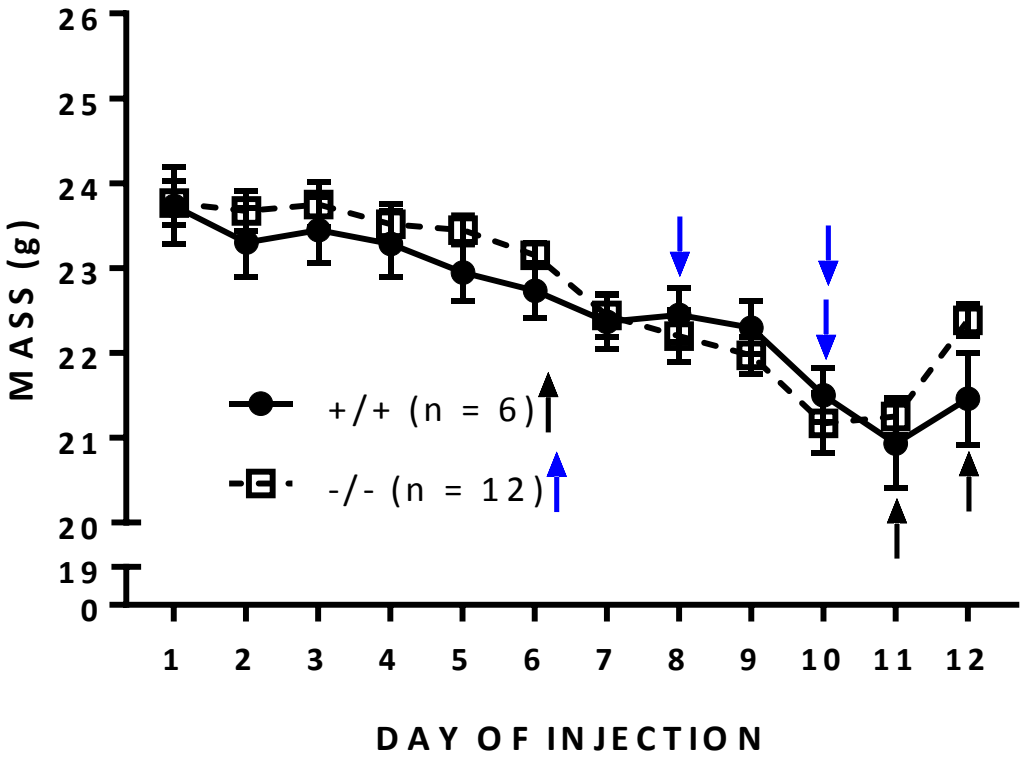

FIGURE 20: Comparison of 3-NP-mediated mass loss in female mice. Mass of IL-1R1 null mutant mice (−/−, n = 12) and their wild-type littermates (+/+, n = 6) were assessed and recorded just prior to each 3-NP injection. Mass was plotted as mean ± SEM. There was a significant time-effect (p = <0.0001). There was no statistically significant difference between genotypes (p = 0.6222). Determined by repeated measures two-way ANOVA. Black arrows indicate the day at which a wild type animal was removed from the study, whereas blue arrows indicate the removal of an IL-1R1 null mutant mouse.

female IL-1R1 null animals. Lesion incidence (figure 23B) was greater in wildtype animals but not statistically significant (p=0.6418). Female striatal volume was not significantly different between genotypes (p=0.3195). Lesion volume was not significantly different (p=0.3884). Wild type striatum and lesion volume are both smaller than the corresponding volume in IL-1R1 null animals. The lesion volume varied between 1.5 and 2.5mm^3.

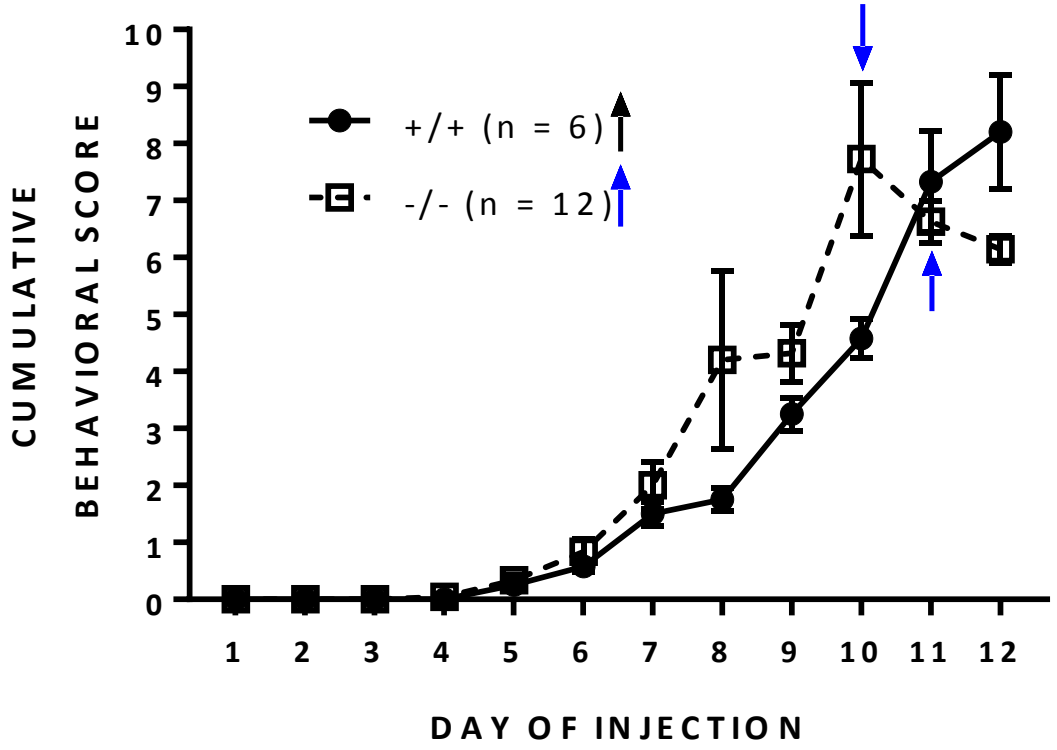

FIGURE 21: **Comparison of 3-NP-mediated motor deficit in female mice.** Gross motor behavior of IL-1R1 null mutant mice (−/−, n = 12) and their wild-type littermates (+/+, n = 6) were assessed and recorded just prior to each 3-NP injection. The average score for the day was plotted as mean ± SEM. There was a significant time-effect (p = <0.0001), but there was no statistically significant difference between genotypes (p = 0.1314). Determined by repeated measures two-way ANOVA, after [Y = log (Y + 1)] transformation. Blue arrows indicate the removal of an IL-1R1 null mutant mouse.

The survival of female animals through the injection series (figure 25) were categorized as when animals completed the full injection series and "moribund" when animals met one or both removal conditions. The rate of study completion (figure 25A) was not significantly different between genotypes (p=0.5887) in females. The incidence of moribundity (figure 25B) was not significantly different (p=>0.9999). Representative images from female IL-1R1 null and

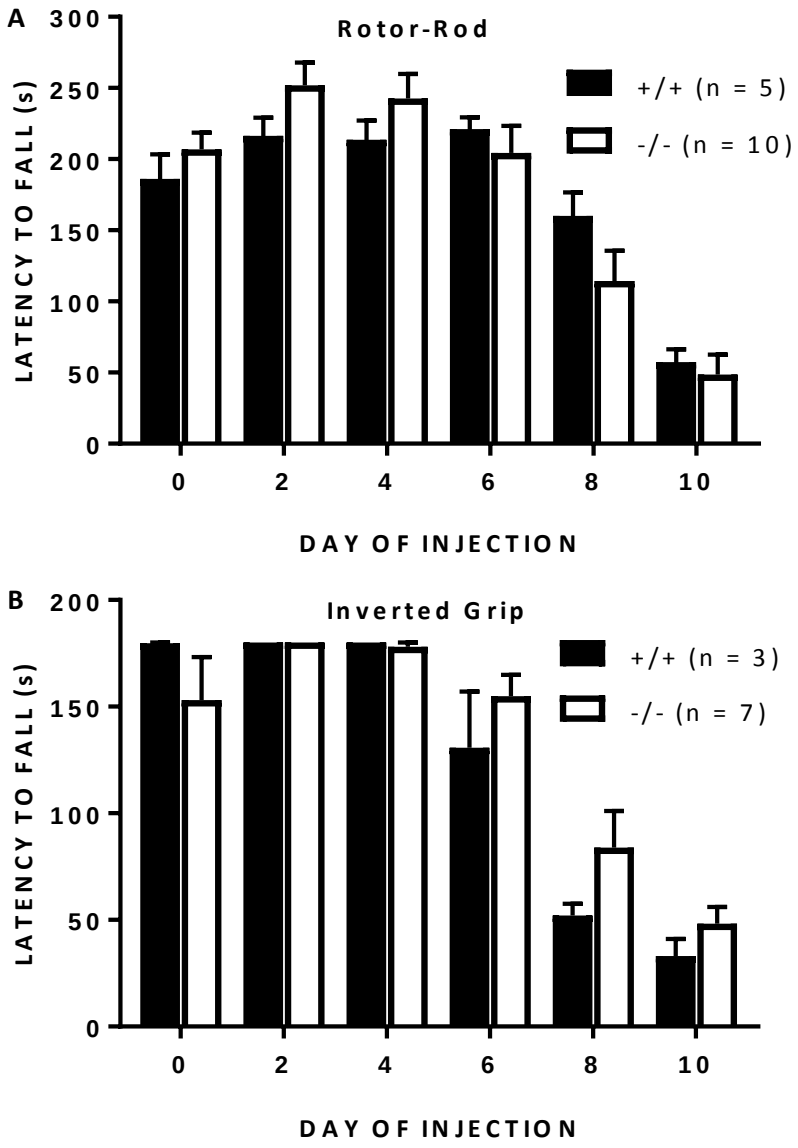

FIGURE 22: Comparison of fine motor deficits between wild type and IL-1R1 deficient female mice. (A) Rotor-rod: Motor strength and coordination was compared between female wild type (+/+, n = 5) and IL-1R1 null (-/-, n = 10) mice just prior to injection of 3-NP using an accelerated Rotor-rod paradigm (300 sec; 5-55RPM) on the days indicated on the x axis. A record of the latency to fall from two independent trials was made and the data graphed as the mean ± SEM. There was no significant difference in time to fall between genotypes as determined by repeated measures two-way ANOVA (p = 0.8665). A significant time-effect was observed (p = < 0.0001) **(B) Inverted Grip**: Female wild type (+/+, n = 3) and IL-1R1 null (-/-, n = 7) were placed on a wire mesh that was subsequently inverted for a maximum of 180 seconds. Each animal received three trials, with the longest latency to fall of the trials for each genotype graphed as the mean ± SEM. There were no between-group differences as determined by repeated measures two-way ANOVA (p = 0.2813) A significant time-effect was observed (p = < 0.0001). Sample sizes differ from Figure 21 because not all cohorts received the same behavioral tests.

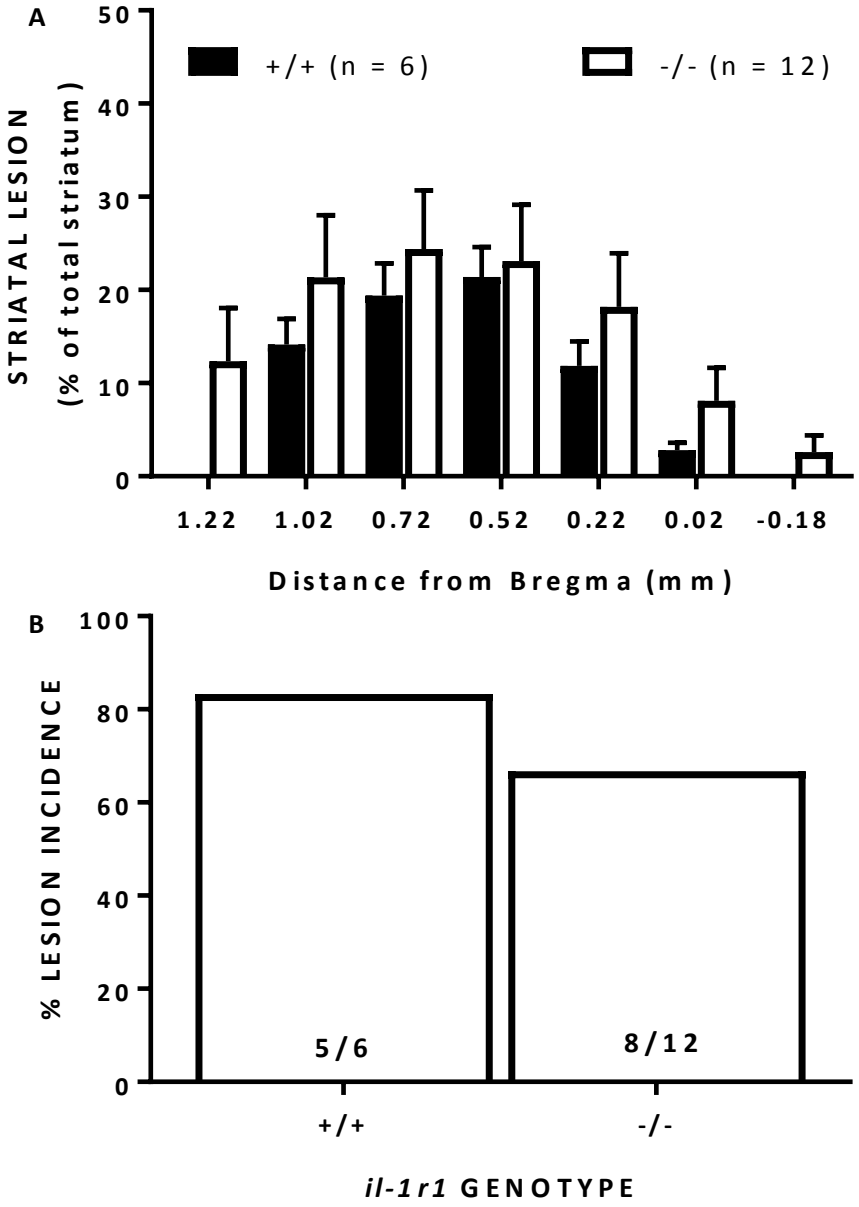

FIGURE 23: Comparison of lesion size and incidence between female wild type and IL-1R1 deficient mice. Female IL-1R1 null mutant mice (-/-, n = 12) and their wild-type littermates (+/+, n = 6) were injected twice daily with 3-NP as described in methods. **(A)** Comparison of lesion area between IL-1R1$^{+/+}$ and IL1R1$^{-/-}$ mice expressed as a percentage of total striatal area. No significant difference between genotypes occurs determined by repeated measures two-way ANOVA after Y=arcsin[sqrt(Y/1000)] transformation (p = 0.5592). **(B)** Comparison of lesion incidence between IL-1R1$^{+/+}$ and IL-1R1$^{-/-}$ mice. The graph depicts the percent of mice from each genotype with any size lesion determined by dividing the number with lesion by the total number of mice analyzed. Exact numbers contained within the bars. There was no significant difference in the lesion incidence as determined by Fisher's exact test (p = 0.6148).

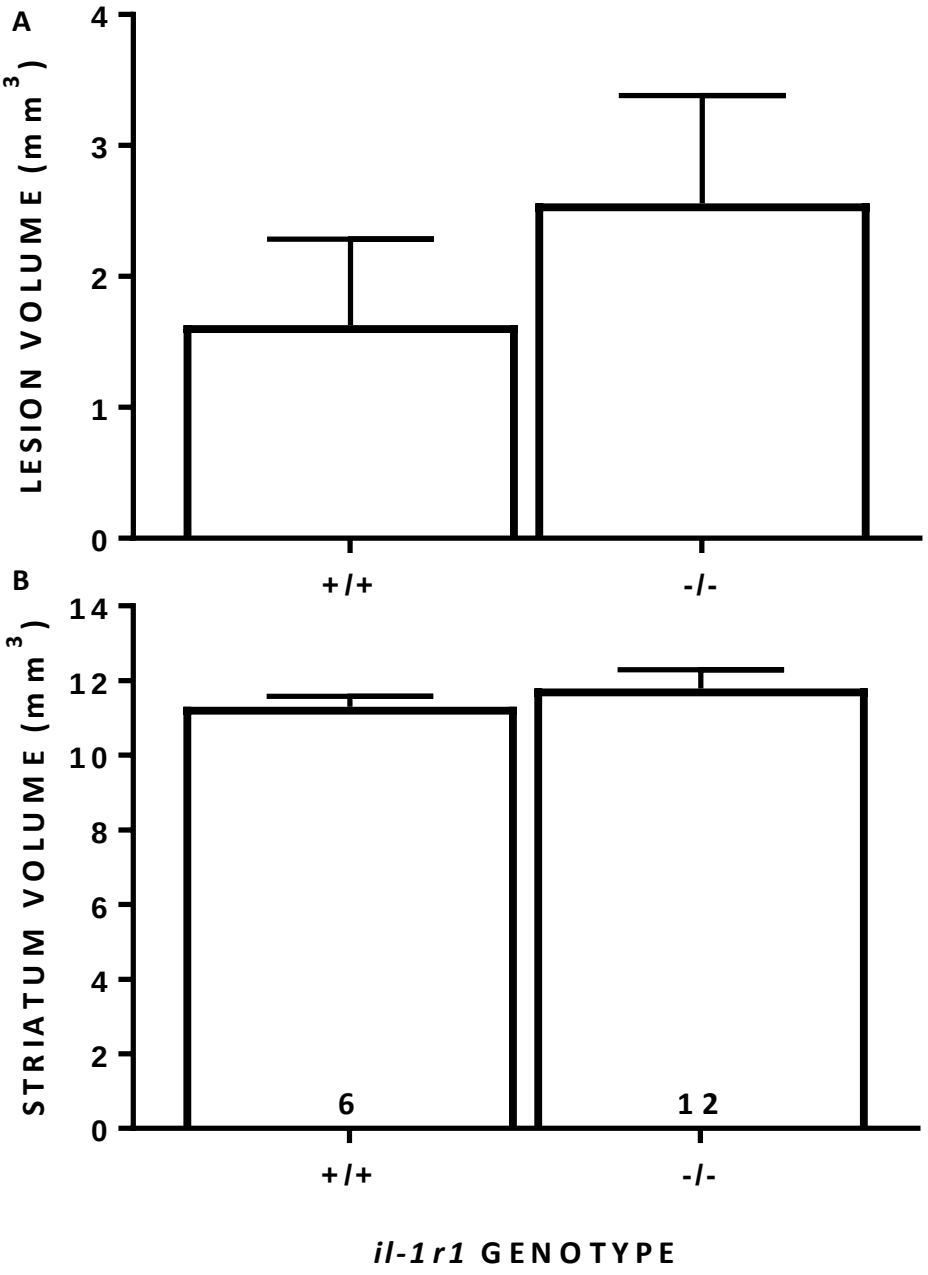

FIGURE 24: Assessment of female lesion volume. Female IL-1R1 null mutant mice (-/-, n = 12) and their wild-type littermates (+/+, n = 6) were injected twice daily with 3-NP as described in methods. Lesion **(A)** and striatal **(B)** volume was quantified using the Cavalieri's method and graphed as the mean mm^3 ± SEM. A one-tailed t-test with Welch's correction revealed no significant difference between genotypes (p = 0.1942). No significant difference was observed in striatum volume, utilizing a two tailed test (p = 0.3951).

wild type animals (figure 26) treated with 3-NP demonstrate similar lesion size in both genotypes. A tendency for larger lesion size in IL-1R1 null animals was present but this was not statistically significant.

SDH Measurements

Animals treated with a 150mg/kg dose of 3-NP, demonstrated a loss of SDH activity in the striatum, cortex and hippocampus. Of interest to this study is the effect on the striatum. Male, female, wild type and IL-1R1 null animal's lost SDH activity equally in the striatum (figure 27). Male animals demonstrated a significant loss in SDH activity when treated with 3-NP, normalized to saline injection, regardless of genotype (+/+ $p = 0.0266$, -/- $p = 0.0171$). No significant difference was seen in the loss of SDH activity between genotypes ($p = >0.9999$) shown in figure 27A. Female animals demonstrated a significant loss in SDH activity when treated with 3-NP, normalized to saline injection, regardless of genotype (+/+ $p = 0.0473$, -/- $p = 0.0023$). No significant difference was seen in the loss of SDH activity between genotypes ($p = 0.3486$) shown in figure 27B.

In the cortex and hippocampus loss of SDH activity was also observed (figure 28). Male animals demonstrated a significant loss in SDH activity when treated with 3-NP, normalized to saline injection, regardless of genotype in cortex (+/+ $p = 0.0005$, -/- $p = 0.0016$), figure 28A and hippocampus (+/+ $p = 0.0010$, -/- $p = 0.0017$), figure 28B. No significant difference was seen in the loss of SDH activity between genotypes in cortex ($p = >0.9999$) or in hippocampus ($p = >0.9999$). Female animals demonstrated a significant loss in SDH activity when treated with

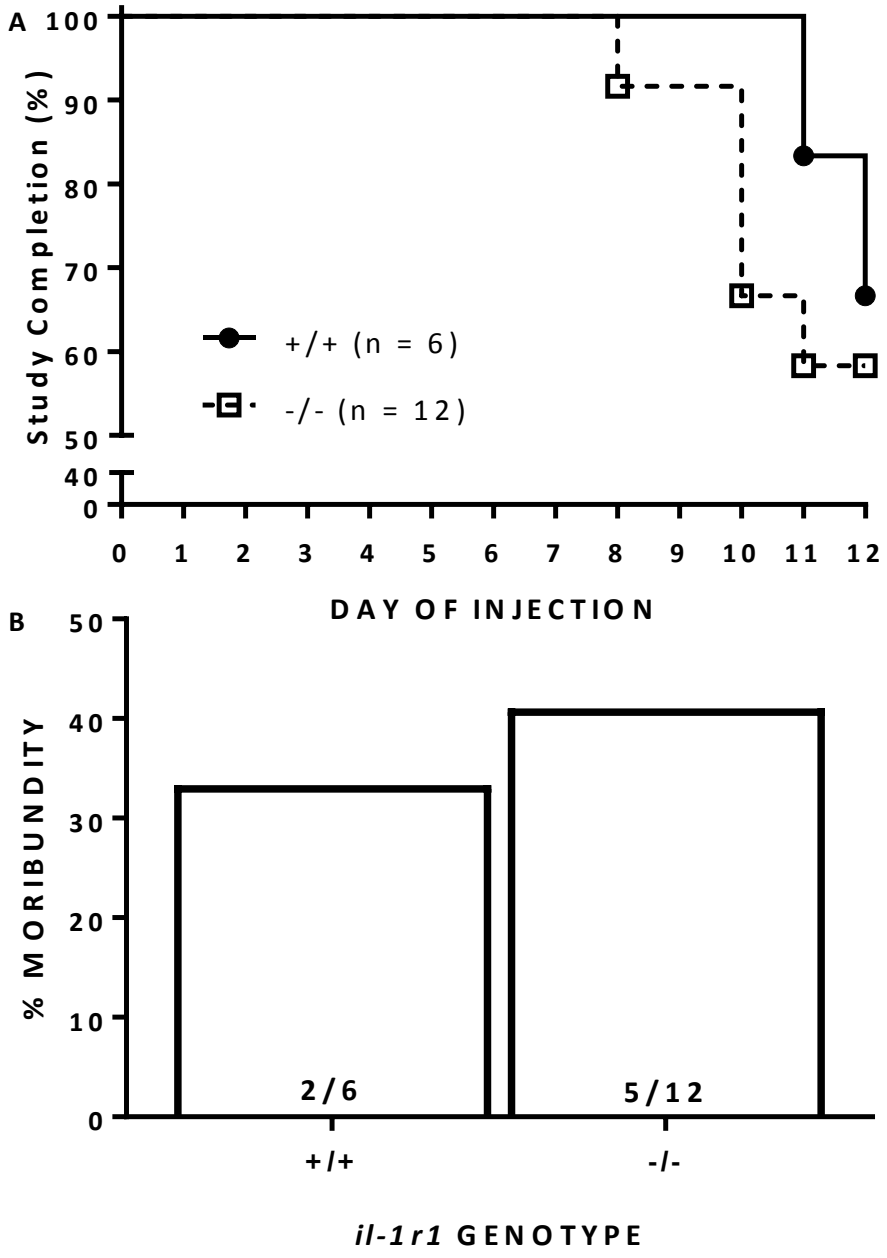

FIGURE 25: Comparison of the amount and rate of removal of wild-type (+/+) and IL-1R1 null (-/-) female mice from 3-NP study. Mice receiving 3-NP were removed from injection series if their behavioral score exceeded nine (9) or if they lost >20% of their body mass. **(A)** A Kaplan–Meier survival curve depicts the rate at which the mice were removed from study. No genotypic differences in rate of removal was determined by Mantel-Cox log-rank test (p = 0.5887). **(B)** The number of IL-1R1$^{+/+}$ and IL-1R1 $^{-/-}$ mice determined to be moribund are expressed as the percent of the total number of mice subjected to the systemic injection paradigm (fraction within bars). No genotypic differences were found when compared by Fisher's exact test (p = >0.9999).

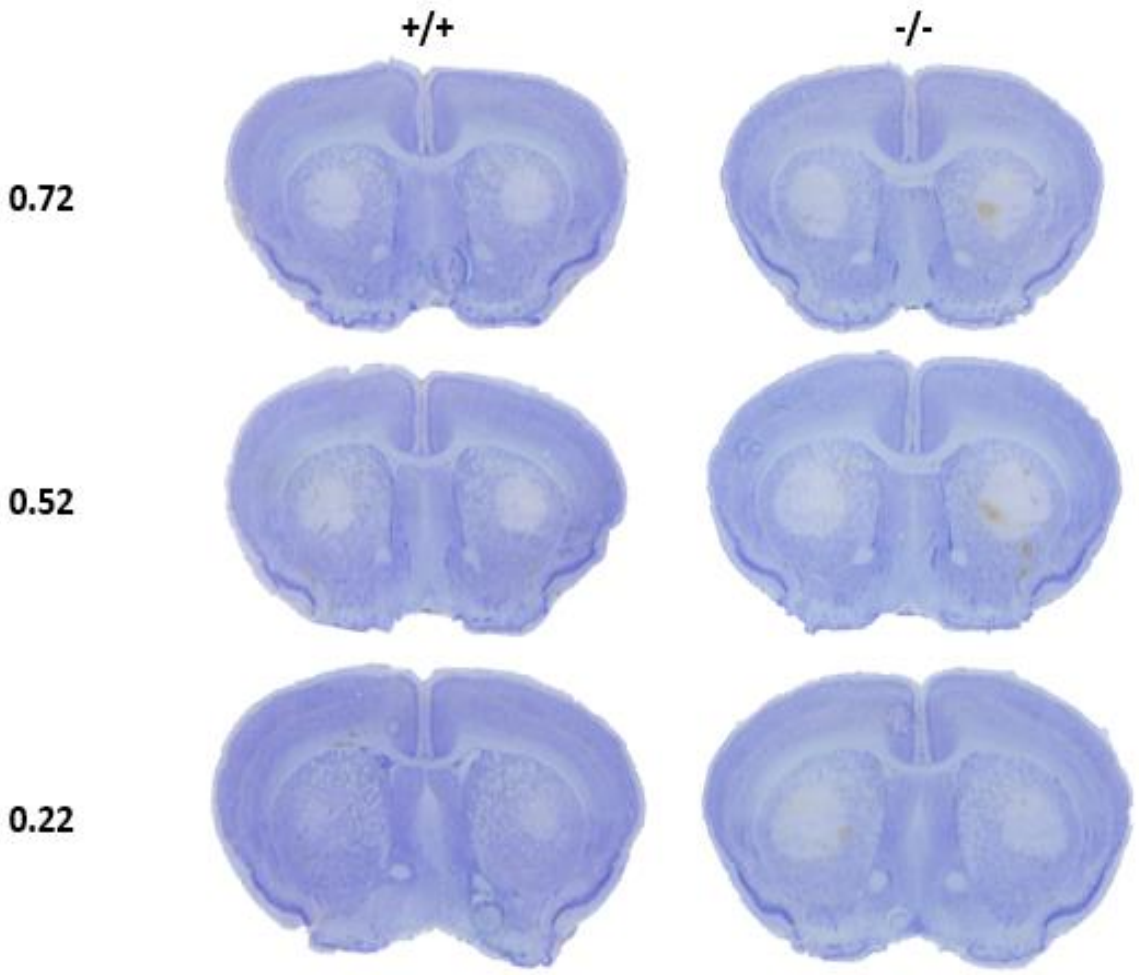

FIGURE 26: Representative images of female wild type and IL-1R1 deficient mice. Female IL-1R1 null mutant mice (-/-, n = 12) and their wild-type littermates (+/+, n = 6) were injected twice daily with 3-NP as described in methods. Photomicrographs depicting striatal injury in IL-1R1$^{+/+}$ (left) and IL-1R1$^{-/-}$ mice (right) at +0.72 to +0.22 from bregma at day 13 following 3-NP exposure.

3-NP, normalized to saline injection, regardless of genotype in cortex (+/+ p = 0.0245, -/- p = 0.0026) figure 28C and hippocampus (+/+ p = 0.015, -/- p = 0.0171) figure 28D. No significant difference was seen in the loss of SDH activity between genotypes in cortex (p = >0.9999) or in hippocampus (p = >0.9999).

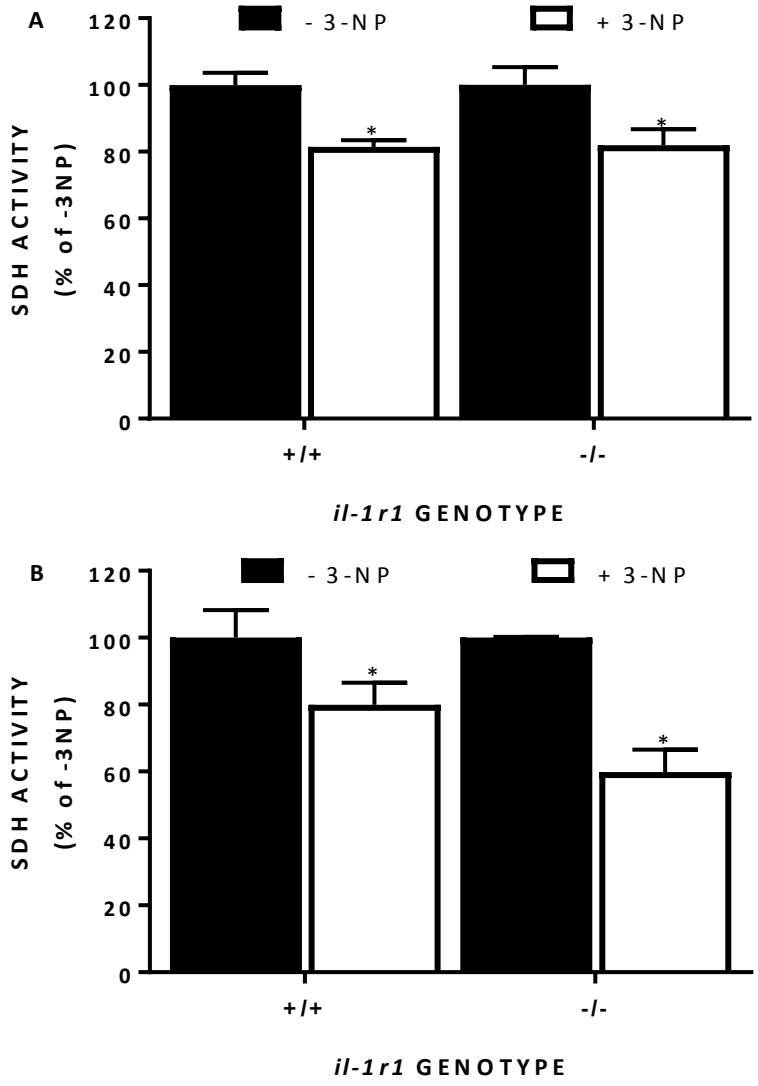

FIGURE 27: Striatal SDH Activity after acute 3-NP injection. IL-1R1 null mutant mice and wildtype littermates were injected with 150 mg/kg 3-NP or saline. Two hours after injection, SDH activities were measured from crude brain mitochondrial extract as described in methods. Data were normalized to each genotype control group (- 3NP) and expressed as mean + SEM. **A.** Male wild type (-3-NP n=5, +3-NP n=4) and IL-1R1 null (-3-NP n=5, +3-NP n=6) demonstrated significant between-group differences (*; 3-NP treatment; (+/+ p = 0.0266, -/- p = 0.0171)), but no within-group (i.e., genotype) differences (p = >0.9999) found by two-way ANOVA followed by Bonferonni's test for multiple comparisons. **B.** Female wild type (-3-NP n=5, +3-NP n=4) and IL-1R1 null (-3-NP n=4, +3-NP n=4) demonstrated significant between-group differences (*; 3-NP treatment; (+/+ p = 0.0473, -/- p = 0.0023)), but no within-group (i.e., genotype) differences (p = 0.3486) found by two-way ANOVA followed by Bonferonni's test for multiple comparisons.

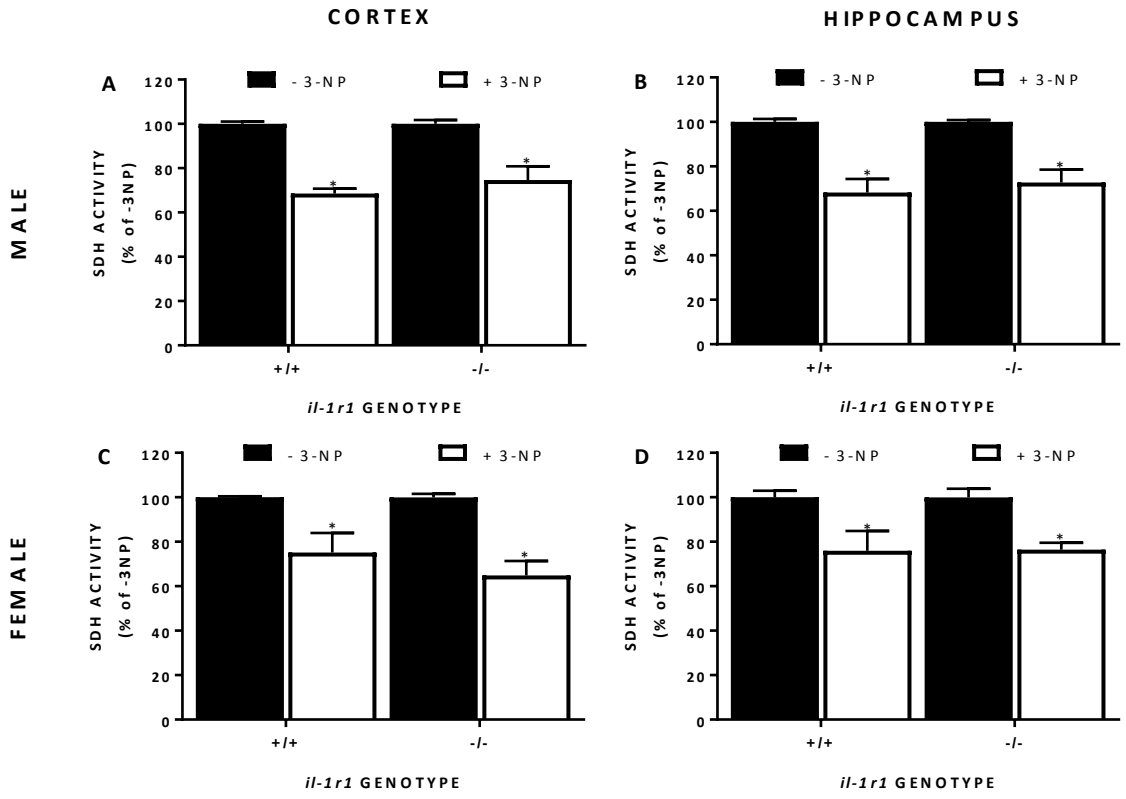

FIGURE 28: Cortical and Hippocampal SDH Activity after acute 3-NP injection. IL-1R1 null mutant mice and wildtype littermates were injected with 150 mg/kg 3-NP or saline. Two hours after injection, SDH activities were measured from crude brain mitochondrial extract as described in methods. Data were normalized to each genotype control group (- 3NP) and expressed as mean + SEM. **A.** Cortex of male wild type (-3-NP n=5, +3-NP n=4) and IL-1R1 null (-3-NP n=5, +3-NP n=6) demonstrated significant between-group differences (*; 3-NP treatment; (+/+ p = 0.0005, -/- p = 0.0016)), but no within-group (i.e., genotype) differences (p = >0.9999) found by two-way ANOVA followed by Bonferonni's test for multiple comparisons. **B.** Hippocampus of male wild type (-3-NP n=5, +3-NP n=4) and IL-1R1 null (-3-NP n=5, +3-NP n=6) demonstrated significant between-group differences (*; 3-NP treatment; (+/+ p = 0.0010, -/- p = 0.0017)), but no within-group (i.e., genotype) differences (p = >0.9999) found by two-way ANOVA followed by Bonferonni's test for multiple comparisons. **C.** Cortex of female wild type (-3-NP n=5, +3-NP n=4) and IL-1R1 null (-3-NP n=4, +3-NP n=4) demonstrated significant between-group differences (*; 3-NP treatment; (+/+ p = 0.0245, -/- p = 0.0026)), but no within-group (i.e., genotype) differences (p = >0.9999) found by two-way ANOVA followed by Bonferonni's test for multiple comparisons. **D.** Hippocampus of female wild type (-3-NP n=4, +3-NP n=4) and IL-1R1 null (-3-NP n=4, +3-NP n=4) demonstrated significant between-group differences (*; 3-NP treatment; (+/+ p = 0.015, -/- p = 0.0171)), but no within-group (i.e., genotype) differences (p = >0.9999) found by two-way ANOVA followed by Bonferonni's test for multiple comparisons.

3.4. IL-1R1 Discussion

In the model of neurodegeneration implemented in this study several observations can be made. Male mice lacking IL-1R1 and their wildtype littermates both lose mass in a similar manner when treated with 3-NP. The genotype having no observable influence on mass implies that the systemic effects of intoxication with a mitochondrial toxin are acting equally on both groups of mice. Furthermore, the gross behavioral scoring conducted throughout the dosing paradigm indicates no difference in the development of the observable motor deficit between the genotypes. When motor deficit is examined in detail, no difference is observed between wild type and IL-1R1 null littermates. Further examination of fine behaviour was conducted with a rotor-rod test to examine motor control and the inverted grip test to examine grip strength. Utilizing the fine behavioral tests a more objective analysis of the development of motor deficit could be made. Considering male mice of both genotypes demonstrate no statistical difference in loss of mass, increase in gross motor deficit score or decreased latency to fall the both tests of fine motor behaviour, it is possible to conclude that male mice with and without IL-1R1 respond in the same manner to exposure to 3-NP. However, the histology points to a slightly different conclusion.

The histology of male mouse brain tissue was conducted after the mice either completed the study or were sacrificed before completion due to loss of mass greater than 20% or incurred behavioral score of 9 or more. Examination of male mouse brain tissue indicated a distinct difference between wild type and null animals. Both lesion area as a percentage of the striatal area (per section) and lesion volume converted from lesion area measurements were considered. It was observed that animals in which IL-1R1 is absent have considerably larger

lesion than those in which it is present. It is possible to conclude from these findings that in male mice IL-1R1 provides protection from the striatal injury incurred by, the sub-acute escalating dosing paradigm administered.

The histological difference in male mice is distinct, however no behavioral differences are evident between the genotypes. If male wild type mouse brain tissue does not contain visible lesion but the physical condition of the mice deteriorates in the same manner as the IL-1R1 null animals, then two possibilities are apparent for this difference. Firstly the observation of lesion is dependent on the development of clear cell loss within the striatum. The wild type mice may be suffering from cellular damage that is not observable through the staining method implemented. Secondly the wildtype mice may not be incurring damage to the striatal tissue but are presenting behavioral deficit because of the systemic effects of 3-NP exposure. Further experimentation would be needed to determine the reason for difference between male histology and behavioral findings.

To determine if the effect seen in male mice was mediated by the change in IL-1R1 signalling or a difference in the action of 3-NP between the genotypes an assay of SDH activity was conducted. After an acute dose of 3-NP both IL-1R1 null and their wildtype littermates demonstrated a similar degree of loss of SDH activity. The assay utilised an assessment of SDH activity in crude mitochondrial extract, normalized to total protein content. Using a crude extract from tissue samples wherein the mitochondria may be damaged or stressed, could have been problematic as if the mitochondria had become enlarged as a result of toxic insult the centrifugation used to separate the extract may have erroneously excluded the damaged mitochondria isolating only the healthy. However, results from the assays were internally

consistent indicating that this was not the case while an acute model is not directly comparable to the sub-acute dose. The similar response indicates that 3-NP is not acting differently in either genotype.

In female mice, like in males no statistical difference was seen in the recorded decrease in mass or performance in the tests of fine motor behavior. This difference was not statistically significant and power analysis of the female gross behaviour score using graphpad statmate 2 software indicates that at the determined experimental power of the completed experiment an n of 8 would be required to detect a significant difference between the two groups. Considering the sample size for the wild type genotype was 6 it may be possible that this difference would become significant if the sample size was increased. Histological analysis of female mouse brain tissue indicated no significant difference between genotypes.

Findings in this study relate to those of HD through the generation of ROS. Administration of 3-NP has been demonstrated to increase ROS in a dose dependent manner (Fontaine et al., 2000, Liot et al., 2009) and an increase in ROS is evident in HD (Milakovic and Johnson, 2005). In cases of HD the source of injury is the accumulation off HTT protein, and disease progression has been associated with increased accumulation (Becher et al., 1998, Arrasate and Finkbeiner, 2012). A previous study has demonstrated that loss of IL-1R1 increases HTT aggregation in a HD mouse model (Wang et al., 2010). However, in this study 3-NP has been used and therefore no HTT aggregation is present and cannot be responsible for the observed injury. The protection observed in this study in male, but not female, mice may be due to amelioration of ROS damage. Previous work conducted in this laboratory has demonstrated that in an *in vitro* culture of astrocytes, IL-1β pre-treatment is protective against

an organic peroxide via a GSH dependent mechanism and signalling through IL-1R1 is required for this protection to be evident (He et al., 2015). Further, IL-1β has been demonstrated to increase the expression of xCT a component of system x_c^-, an antiporter which imports the rate limiting component required for GSH synthesis (Shi et al., 2016, Fogal et al., 2007, Jackman et al., 2010). This study demonstrates when a chemical known to increase ROS is administered, the presence of IL-1R1 is protective. Such findings are consistent with previous work indicating IL-1β can result in in increased GSH production *in vitro*. More research is needed to demonstrate a direct association in the model implemented in this study.

The protection observed in males is not present in the female mice tested. This study presents no evidence to explain this difference. If the protection is associated with the upregulation of xCT there is some evidence in published literature to suggest an involvement of estrogen in xCT regulation which indicating a possible reason for the difference. In studies employing breast cancer cells, the estrogen receptor has been shown to be involved in xCT expression with an estrogen response element being computationally identified in the xCT promoter region (Linher-Melville et al., 2015). To further tie estrogen to xCT, Pit-1 sites, which have been long associated with estrogen signalling, have been identified in the non-coding 5' region of xCT (Nowakowski and Maurer, 1994, Linher-Melville et al., 2015). What effect, if any, estrogen has on xCT regulation is not yet fully understood, but if estrogen were upregulating xCT the action of IL-1R1 signalling may not be able to further upregulate xCT. If the upregulation of xCT is able to redress the redox imbalance created by the increased generation of ROS an inability to increase xCT expression would result in females being unable to compensate for ROS generated by 3-NP dosing. If this were true a higher basal expression of xCT in females may

explain why in previous studies females where resistant to 3-NP dosing. Although, wild type females in this study did not display such innate resistance.

The limitations of this study suggest caution in drawing sweeping conclusions. The use of only one stain to examine histology resulted in only one gross assessment of injury. Including a specific neuronal stain would have allowed an accurate quantification of neuronal cell loss in addition to the assessment of lesion size. Such an extension of this study would have allowed a more detailed analysis of histological sections which did not show lesion damage. Further, in this analysis had a mitotracker stain or the examination of other markers of oxidative phosphorylation been used an assessment of mitochondrial function as well as oxidant mediated cell death could have been made. The purpose of this study was to examine the effect of 3-NP on mice with and without IL-1R1. The most evident limitation of this study is the lack of analysis of the mechanism behind the effect. With no evidence directly examining the mechanism behind the observed protection in males, it is not possible to make any direct assertions to what mediates the protective effect of IL-1R1 signalling in males in this study. Possibilities for further study into the effect seen in this thesis will be discussed in detail in chapter four.

4. CHAPTER FOUR

4.1. Does IL-1β signalling have a protective effect?

IL-1β signalling is heavily dependent on environmental conditions. IL-1 signalling has been shown to be detrimental in a number of models, particularly those modelling ischemic stroke (Fogal et al., 2007, Yang et al., 1998). Free radical accumulation and energy deprivation is associated with stroke but also with the administration of 3-NP. The findings of this study, that IL-1β signalling in male (but not female) mice protects against 3-NP induced striatal injury, indicates that the pleiotropic effects of IL-1β signalling, influence physiological outcomes. The findings of this study are supported by studies which demonstrated a protective effect of IL-1β against oxidative stress in astrocytes (He et al., 2015) and astrocyte neuron co-culture (Choudhury, unpublished). Support from previous studies and the demonstrated reproducibility indicate the result seen in this study represents a real effect that needs further study to elucidate the mechanism underlying the protection seen in this model.

4.2. Future Directions

To definitively rule out any genotypic difference in the ability of 3-NP to inhibit SDH, the SDH assay could be next performed at set time points throughout the sub-acute dosing paradigm. The data shows loss of SDH activity in the cortex and in the hippocampus. By conducting the experiment during the sub-acute paradigm, it would be possible demonstrate the rate of SDH inhibition and show the effect on other brain regions when receiving multiple sub-acute doses. To address the issue limited histological analysis, IL-1R1 animals and wild type

littermates should be utilized to label different types of cell by immunofluorescence. To examine comparable sections throughout the lesioned area and determining the effects on different cell types. Such an investigation will provide insight into the observed cell loss and which cell type if any is more severely affected. By labelling different cell types it would be possible to observe the differing response primarily if neurons experience more cell loss depending on genotype or if astrocytes are effected to a different extent. Examining microglia would also enable a measure of microglial activation. Conducting additional cohorts in which animals are removed for immunofluorescent analysis at set time points over the injection time course would demonstrate the development of cell loss in regards to cell type. By examining the development it will be possible to see which cell types are affected first.

To determine if the protection observed is due to the upregulation of xCT, a sub cohort of the animals should be utilized to examine changes in xCT mRNA expression. Such an experiment could be achieved by dividing the hemispheres of the animals used for a time course of SDH activity and extracting RNA from the hemisphere not used for mitochondrial extraction. IL-1β enhances the synthesis and export of GSH (He et al., 2015). Although, this has been demonstrated *in vitro* it would be beneficial to conduct this experiment *in vivo* to elucidate if the same effect is occurring in the model utilized in this study which would provide *in vivo* support for *in vitro* findings. To determine whether our findings are mechanistically linked to system x_c^-, an *in vitro* approach could be taken.

In a separate cohort of animals, biological markers of oxidative stress would be measured and compared between wild-type and IL-1R1 null mice. At the cessation of the dosing protocol, the ratio of reduced and oxidized glutathione (GSH/GSSG) can be quantified in

cerebro-spinal fluid and in brain tissue, to assess the extra and intracellular activity of glutathione respectively. The quantity of 8-OHG, an oxidative stress marker of RNA damage, and 4-HNE, a marker of lipid peroxidation can be measured via ELISA. Examining oxidative stress markers in different regions of the brain will enable a determination of the type of damage occurring during the injection paradigm.

Finally, an *in vitro* approach that represents the in vivo situation could be used to elucidate mechanism. Organotypic slice cultures (400µm coronal sections), derived from P7 pups from wild-type or *sut/sut* littermates, could be treated with vehicle or IL-1β, after which 3-NP could be added. The extent of SDH inhibition, striatal cell viability, and oxidative stress, could be measured for comparison. Additionally, cell viability of the cultures could be quantified via measurement of lactate dehydrogenase released into the cell culture medium. The presence of oxidative stress markers could be quantified and compared. ROS could be measured via dihydroethidium fluorescence imaging.

Investigating the cell types effected in the dosing paradigm would better characterize the effects of the experimental model. While important it is necessary to associate the observed protection with an underlying mechanism. It is hypothesised in this thesis that the underlying cause is an upregulation of xCT resulting in the increased generation of GSH. The examination of secreted GSH shuttled into the CSF and the intracellular GSH present in tissue samples would demonstrate if the more GSH is produced and expressed following 3-NP treatment. The assessment of markers of oxidative stress will demonstrate that the administration of 3-NP is resulting in cellular damage from ROS. In measurements of both GSH and oxidative stress markers the use of IL-1R1$^{+/+}$ and IL-1R1$^{-/-}$ littermates should demonstrate

greater oxidative stress markers in IL-1R1 null animals but greater GSH in wild type. Finally, to tie IL-1R1 activity to xCT *in vivo* the use of *sut*/*sut* animals could replicate IL-1R1 null findings.

Appendix A

Pilot Study Sham Mass

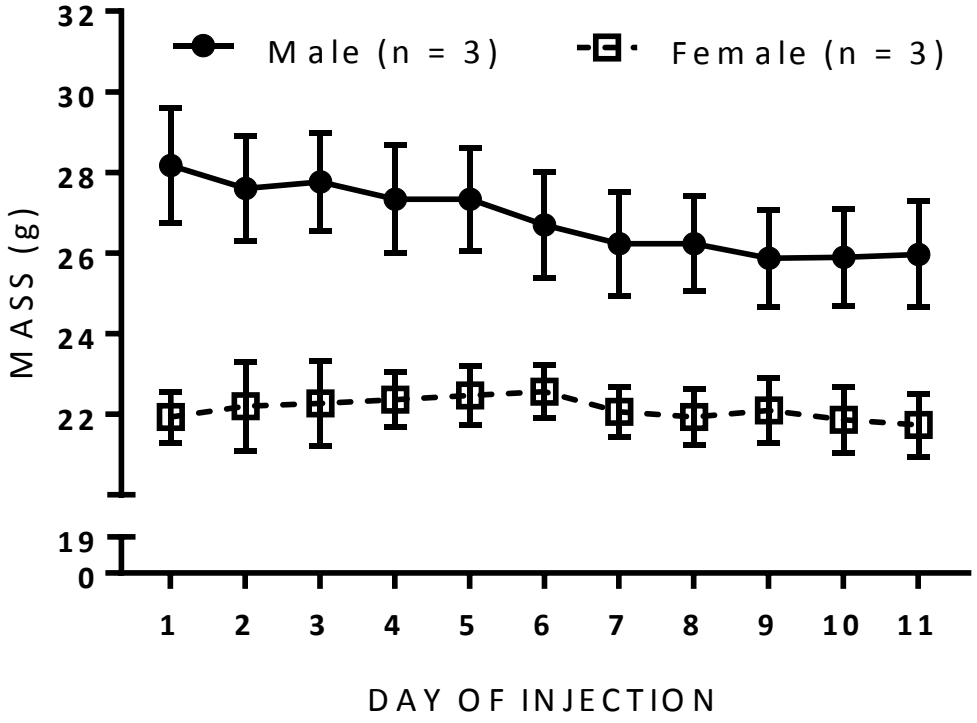

FIGURE S1: Comparison of saline-mediated mass loss in C57Bl/6J mice. Mass of male (n = 3) and female (n = 3) mice, were assessed and recorded just prior to each sham 3-NP injection. Mass was plotted as mean ± SEM. There was a significant time-effect after day five at p = <0.0004) for male mice only. There was no statistically significant difference between sexes (p = 0.1098), as determined by repeated measures two-way ANOVA with Sidak's multiple comparisons.

A study has demonstrated that male and female C57Bl/6J mice have statistically significant difference in body mass (Reed et al., 2007). The average mass of males was significantly different in comparison to day one after day five indicating significant loss of mass. Loss of mass in males could indicate a differing response to stress caused from repeated injection.

Pilot Study Sham Behavioral Score

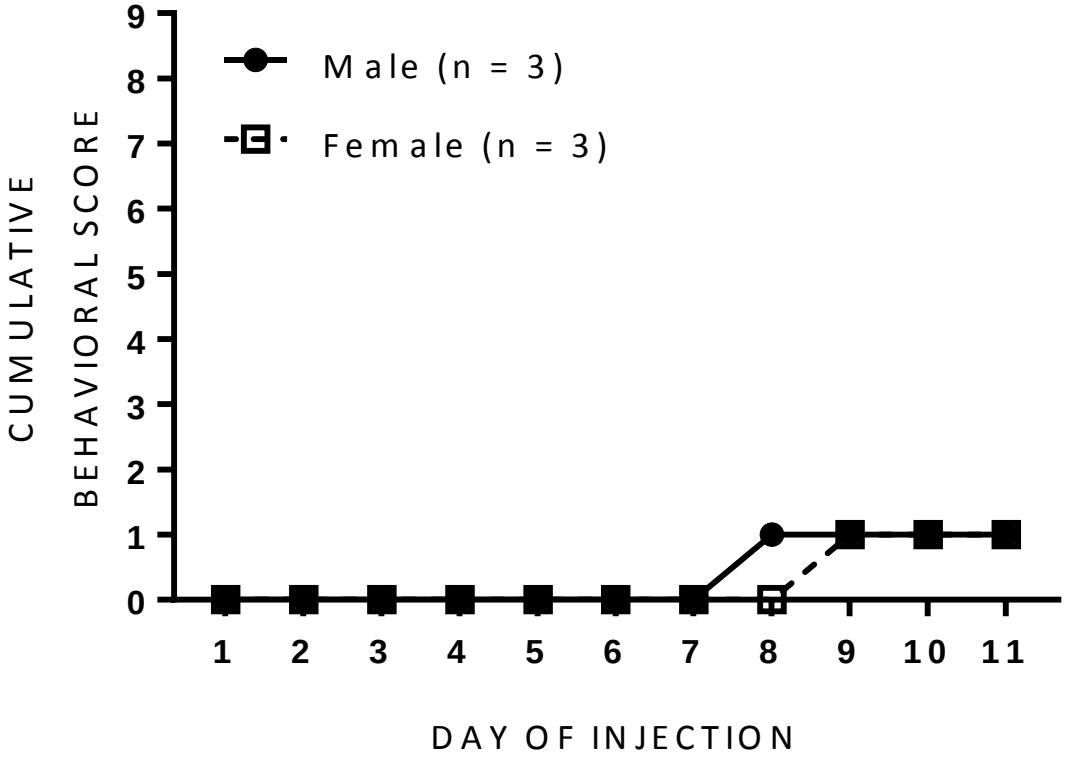

FIGURE S2: Comparison of saline-mediated motor deficit in C57Bl/6J mice. Gross motor behavior of male mice (n = 5) and female (n = 5) were assessed and recorded just prior to each 3-NP injection. The average score for the day was plotted as mean ± SEM. A significant difference over time was seen in both sexes ($p = <0.0001$). There was a statistically significant difference between sex at day 8 only ($p = <0.0001$), as determined by two-way ANOVA, with Sidak's multiple comparisons, after [Y = log (Y + 1)] transformation.

Animal score was incurred by both sexes in the later stages of injection, driven by the fact that mice became less active, although mice appeared to be in good health and demonstrated no sign of motor deficit. Score never exceeded one and demonstrated no sign of distress throughout the protocol.

Pilot Study Sham Representative Image

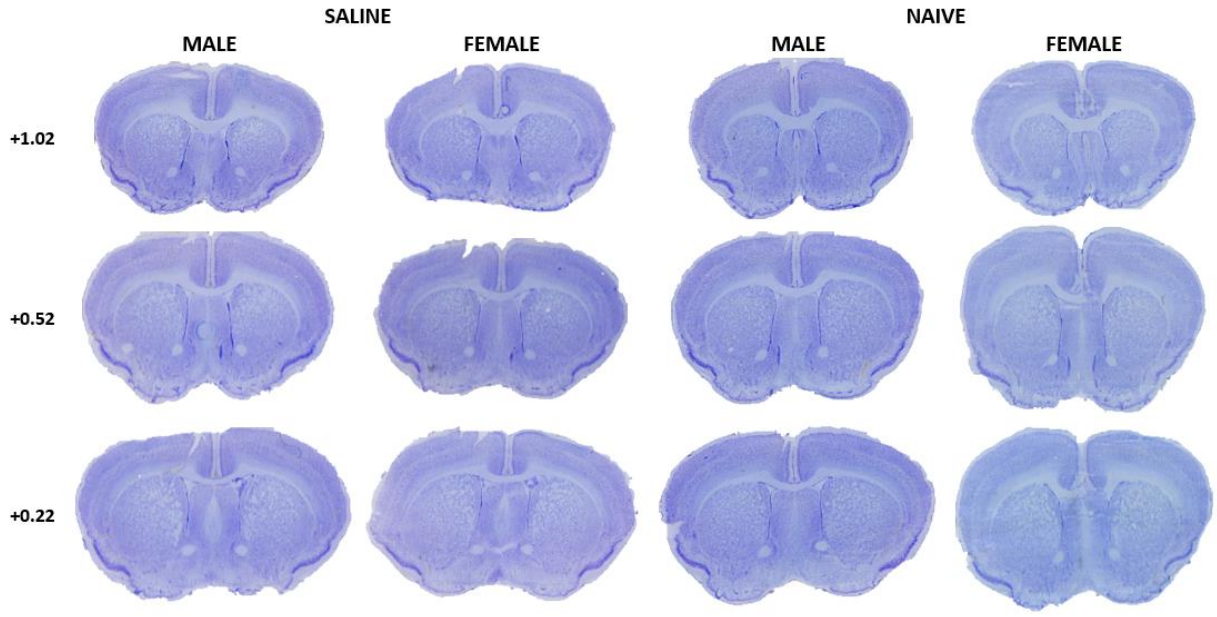

FIGURE S3: Representative images of male and female saline injected and Naïve mice. Photomicrographs depicting thionin stained coronal sections from saline (left) and naïve mice (right) at +1.02 to +0.22 from bregma at day 13 following saline injection as detailed in methods for 3-NP injection, or between from naïve animal sacrificed between the age of 16-18 weeks.

No difference was seen between male or female animals treated with saline or male and female naïve animals. No lesion or abnormality was observed during any stage of histological processing or analysis in any of the four groups detailed in figure S3.

IL-1R1 Sham Mass

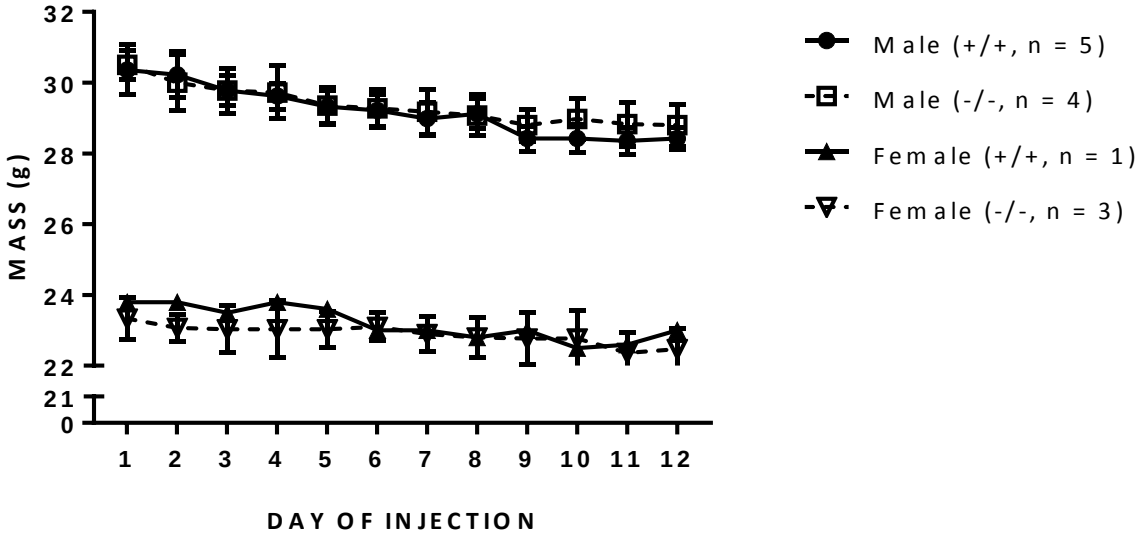

FIGURE S4: Comparison of saline-mediated mass loss in male and female wild type and IL-1R1 null mice. Mass of IL-1R1 null (n = 6) and wild type littermates (n = 7) mice, were assessed and recorded just prior to each saline 3-NP injection. Mass was plotted as mean ± SEM. Females demonstrated no significant difference between genotype or over time (genotype p = 0.3843, time p = 0.9689,). Males demonstrated no difference by genotype but a significant difference over time (genotype p = >0.9999, time p = 0.0045) as determined by two-way ANOVA.

Saline treated animals from IL-1R1 cohorts replicate findings from pilot study saline treated animals. It is unclear what causes the males but not the females to lose mass during sham injection. The number of female wild type animals which received sham treatment was decreased to one because on secondary post mortem genotyping some animals were revealed to be heterozygous at the IL-1R1 allele.

IL-1R1 Sham Behavioral Score

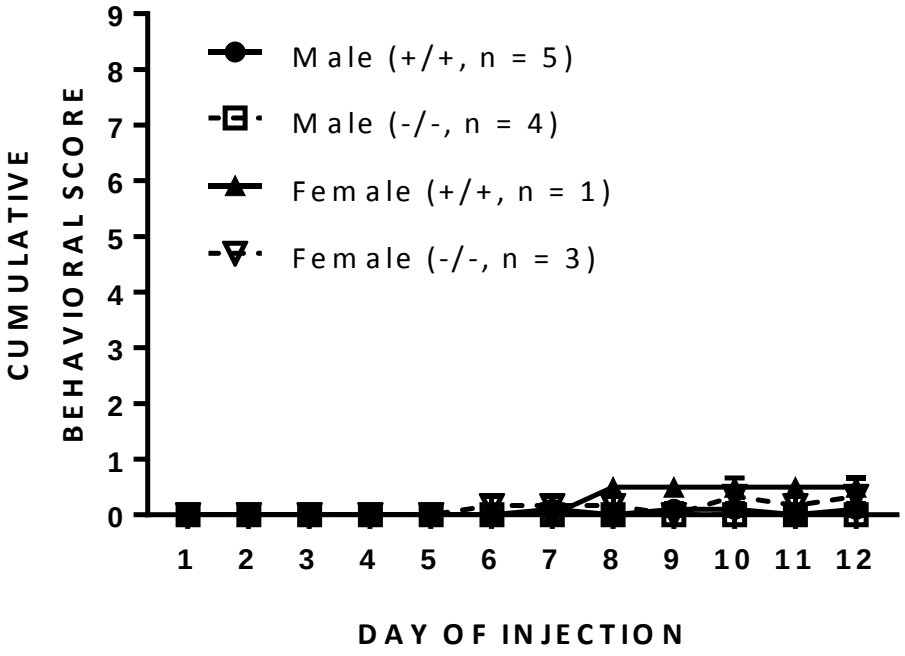

FIGURE S5: Comparison of saline-mediated motor deficit in C57Bl/6J mice. Gross motor behavior of male mice (n = 5) and female (n = 5) were assessed and recorded just prior to each 3-NP injection. The average score for the day was plotted as mean ± SEM. A significant difference over time was seen in both sexes ($p = <0.0001$). There was a statistically significant difference between groups infrequently after day 8 ($p = <0.0245$ at all differing comparisons), as determined by two-way ANOVA, with Sidak's multiple comparisons, after [Y = log (Y + 1)] transformation.

In instances when saline animals received a behavioral score, this was due to occasional intermittent clasping possibly because of irritation at the injection site. No animal appeared in distress throughout saline injection with no gross changes in behaviour was observed regardless of sex or genotype.

IL-1R1 Study Sham Representative Image

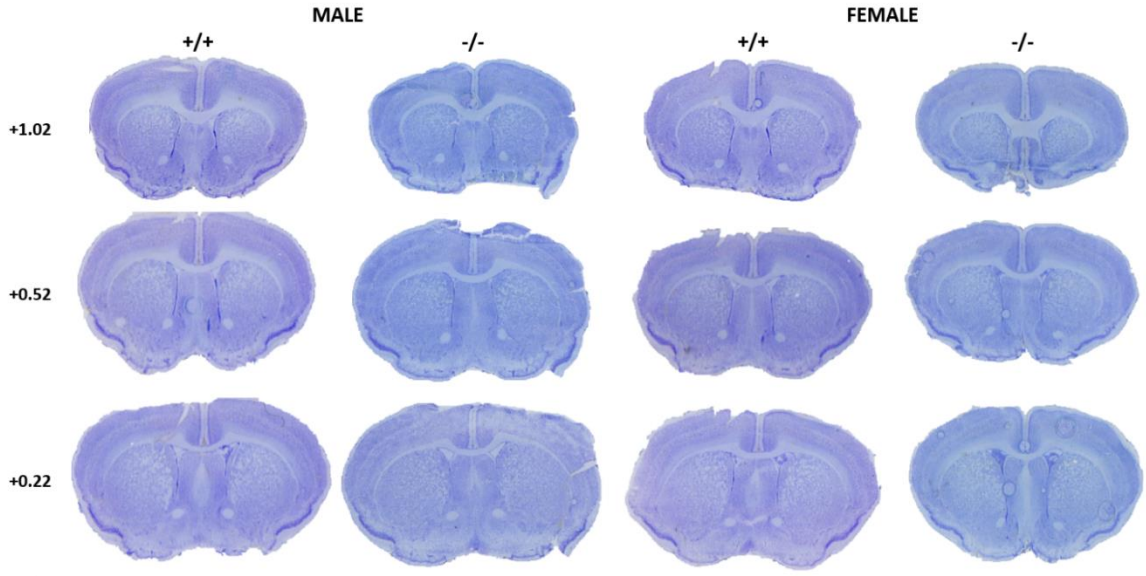

FIGURE S6: Representative images of male and female sham injected of both wild type and IL-1R1 null genotypes. Photomicrographs depicting thionin stained coronal sections from male (left) and female mice (right) at +1.02 to +0.22 from bregma at day 13 following sham injection as detailed in methods for 3-NP injection.

No difference was seen between male or female animals treated with saline of either genotype. No lesion or abnormality was observed during any stage of histological processing or analysis in any of the four groups as representatively demonstrated in figure S6.

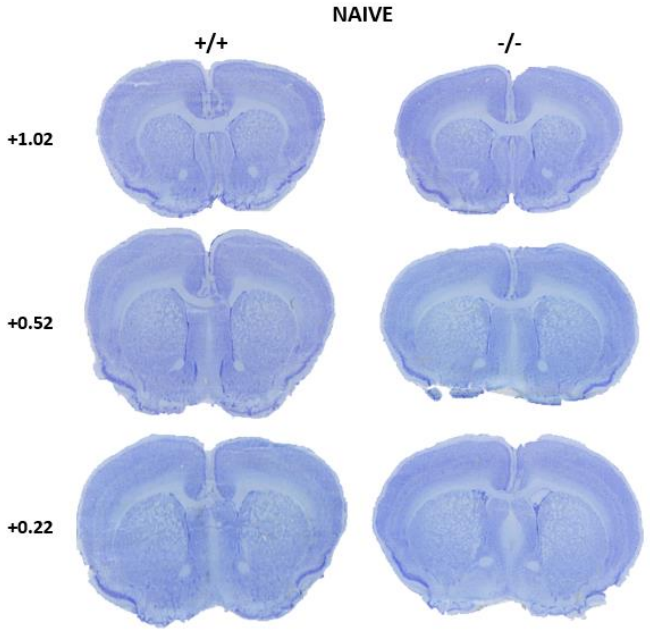

FIGURE S7: **Representative images of wild type and IL-1R1 null naïve animals.** Photomicrographs depicting thionin stained coronal sections from male wild type (left) and IL-1R1 null mice (right) at +1.02 to +0.22 from mice sacrificed between 16 – 18 weeks of age.

No difference was seen between male, female, saline or naïve animals regardless of genotype. No visible lesion was present in any case and no observable abnormalities was noticed between any treated groups.

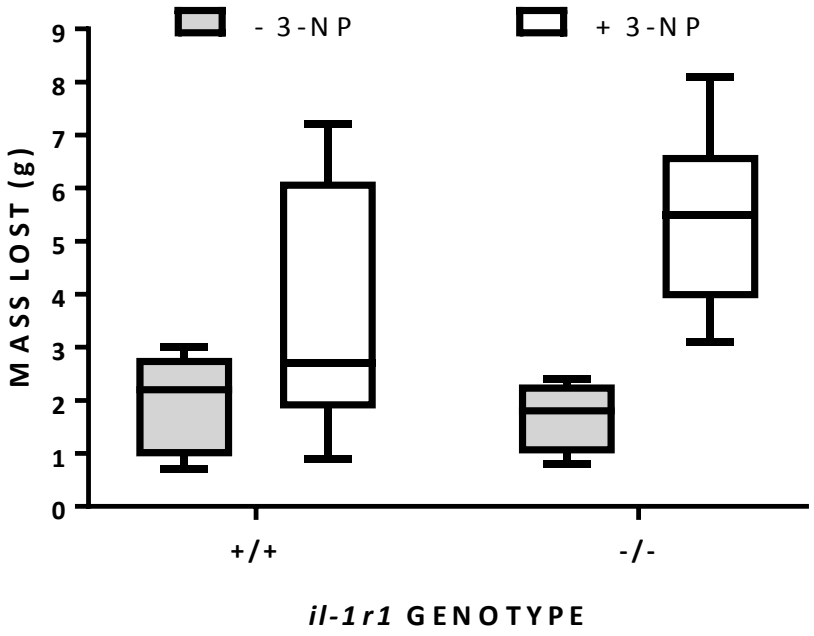

FIGURE S8: Comparison of total mass lost between IL-1R1 null and their wild type littermates in male mice exposed to 3-NP or saline dosing. Mice received twice daily injection of 3-NP (+3-NP) or saline injection (–3-NP) as detailed in methods section. Total mass lost is calculated by subtracting the final animal mass from the starting mass. Group comparisons made by 2x2 two way ANOVA. A significant overall difference is seen between 3-NP treated and saline-treated animals ($p = 0.0005$) and between IL-1R1 null saline and 3-NP-treatment ($p = 0.002$) but not in wild type ($p = 0.1417$). There is no significant difference between wild type and IL-1R1 3-NP treated groups ($p = 0.23$)

Comparing the total mass lost indicates a significant difference between treatments in the IL-1R1 null genotype only. A far greater spread in lost mass is seen in wild type animals treated with 3-NP, however the mean value does not vary greatly from that seen in saline treated.

Summary of saline treated animal and naïve findings

Male mice appear to lose mass when injected with saline, whereas females do not. As a previous study has indicated male and female C57Bl/6J have the same body fat composition (Reed et al., 2007), therefore the loss of mass is less likely to be attributed to excess fat loss in males. The wild type male animals depict a large variation in the amount of mass lost. There remains a clear difference in observable motor deficit and histology compared to saline-treated animals as expected.

Saline vehicle treatment had no observable effect on the animals. Histology demonstrates no visual difference between saline vehicle-treated and naïve animals. Sex or genotype had no effect on the presence of lesion in saline-treated and naïve animals.

C57Bl/6 Striatal Volume Assessment

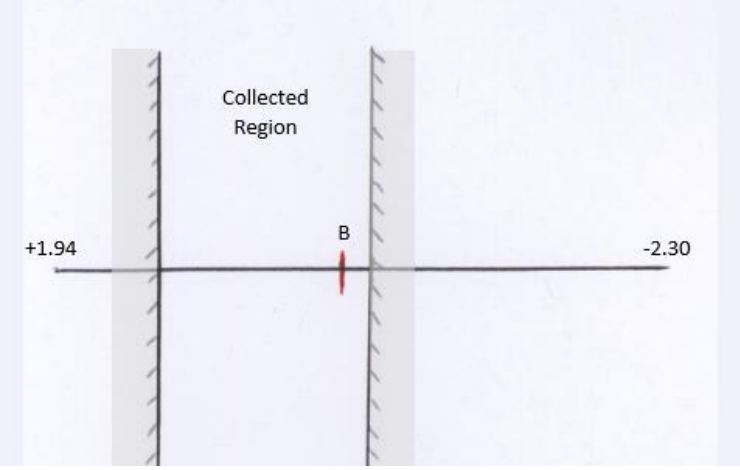

FIGURE S9: Cartoon indicating the region of striatum collected for analysis during this project. Horizontal line denotes length of striatum throughout mouse brain relative to bregma as indicated from Allen Brain Atlas data. Red line marked by 'B' denotes bregma. The region between the two vertical lines was collected in 40µm cryosections as detailed in methodology

Striatal volume calculations made in this work demonstrated an equivalent striatal volume of 12mm^3 (see chapters two and three). Measurement where made from sections taken within the collected region and converted to a volume using Cavailari's principle. While striatal volume was reasonably consistent throughout this study, a

difference is seen between this study, and published whole striatal measurements. Three studies utilizing C57Bl/6 mice reported a total striatal volume of 23mm [see (Harms et al., 2012, Rosen et al., 2009, Rosen and Williams, 2001)]. The determined volume in this work represents half of that reported in literature. Only a short region of the striatum was collected for this study. The striatum spans 4.26mm in length but collections were only made over a 1.4mm span. When the striatum is visualised in a 2D format by charting striatal span and striatal width at multiple points the collections were made in the largest region of the striatum. It is plausible to assume the volume measurements made in this work represents half of the total striatum and is consistent with the reported measurements.

5. REFERENCES

ALBIN, R. L. & GREENAMYRE, J. T. 1992. Alternative excitotoxic hypotheses. *Neurology,* 42**,** 733-8.

ALSTON, T. A., MELA, L. & BRIGHT, H. J. 1977. 3-Nitropropionate, the toxic substance of Indigofera, is a suicide inactivator of succinate dehydrogenase. *Proc Natl Acad Sci U S A,* 74**,** 3767-71.

ARRASATE, M. & FINKBEINER, S. 2012. Protein aggregates in Huntington's disease. *Experimental Neurology,* 238**,** 1-11.

AURON, P. E., WEBB, A. C., ROSENWASSER, L. J., MUCCI, S. F., RICH, A., WOLFF, S. M. & DINARELLO, C. A. 1984. Nucleotide sequence of human monocyte interleukin 1 precursor cDNA. *Proc Natl Acad Sci U S A,* 81**,** 7907-11.

AVSHALUMOV, M. V., CHEN, B. T., MARSHALL, S. P., PENA, D. M. & RICE, M. E. 2003. Glutamate-dependent inhibition of dopamine release in striatum is mediated by a new diffusible messenger, H2O2. *J Neurosci,* 23**,** 2744-50.

BANNAI, S. & TATEISHI, N. 1986. Role of membrane transport in metabolism and function of glutathione in mammals. *J Membr Biol,* 89**,** 1-8.

BASU, A., LAZOVIC, J., KRADY, J. K., MAUGER, D. T., ROTHSTEIN, R. P., SMITH, M. B. & LEVISON, S. W. 2005. Interleukin-1 and the interleukin-1 type 1 receptor are essential for the progressive neurodegeneration that ensues subsequent to a mild hypoxic/ischemic injury. *J Cereb Blood Flow Metab,* 25**,** 17-29.

BATES, G. P., DORSEY, R., GUSELLA, J. F., HAYDEN, M. R., KAY, C., LEAVITT, B. R., NANCE, M., ROSS, C. A., SCAHILL, R. I., WETZEL, R., WILD, E. J. & TABRIZI, S. J. 2015. Huntington disease. *Nat Rev Dis Primers,* 1**,** 15005.

BEAL, M. F. 1994. Neurochemistry and toxin models in Huntington's disease. *Curr Opin Neurol,* 7**,** 542-7.

BEAL, M. F., BROUILLET, E., JENKINS, B. G., FERRANTE, R. J., KOWALL, N. W., MILLER, J. M., STOREY, E., SRIVASTAVA, R., ROSEN, B. R. & HYMAN, B. T. 1993. Neurochemical and histologic characterization of striatal excitotoxic lesions produced by the mitochondrial toxin 3-nitropropionic acid. *J Neurosci,* 13**,** 4181-92.

BECHER, M. W., KOTZUK, J. A., SHARP, A. H., DAVIES, S. W., BATES, G. P., PRICE, D. L. & ROSS, C. A. 1998. Intranuclear Neuronal Inclusions in Huntington's Disease and Dentatorubral and Pallidoluysian Atrophy: Correlation between the Density of Inclusions andIT15CAG Triplet Repeat Length. *Neurobiology of Disease,* 4**,** 387-397.

BERMAN, S. B. & HASTINGS, T. G. 1997. Inhibition of glutamate transport in synaptosomes by dopamine oxidation and reactive oxygen species. *J Neurochem,* 69**,** 1185-95.

BLACK, R. A., KRONHEIM, S. R. & SLEATH, P. R. 1989. Activation of interleukin- 1β by a co-induced protease. *FEBS Letters,* 247**,** 386-390.

BORLONGAN, C. V., KOUTOUZIS, T. K., FREEMAN, T. B., CAHILL, D. W. & SANBERG, P. R. 1995. Behavioral pathology induced by repeated systemic injections of 3-nitropropionic acid mimics the motoric symptoms of Huntington's disease. *Brain Res,* 697**,** 254-7.

BORLONGAN, C. V., KOUTOUZIS, T. K., FREEMAN, T. B., HAUSER, R. A., CAHILL, D. W. & SANBERG, P. R. 1997a. Hyperactivity and hypoactivity in a rat model of Huntington's disease: the systemic 3-nitropropionic acid model. *Brain Res Brain Res Protoc,* 1**,** 253-7.

BORLONGAN, C. V., KOUTOUZIS, T. K. & SANBERG, P. R. 1997b. 3-Nitropropionic acid animal model and Huntington's disease. *Neurosci Biobehav Rev,* 21**,** 289-93.

BORLONGAN, C. V., NISHINO, H. & SANBERG, P. R. 1997c. Systemic, but not intraparenchymal, administration of 3-nitropropionic acid mimics the neuropathology of Huntington's disease: a speculative explanation. *Neurosci Res,* 28**,** 185-9.

BRABERS, N. A. & NOTTET, H. S. 2006. Role of the pro-inflammatory cytokines TNF-alpha and IL-1beta in HIV-associated dementia. *Eur J Clin Invest,* 36**,** 447-58.

BROWNE, S. E., FERRANTE, R. J. & BEAL, M. F. 1999. Oxidative stress in Huntington's disease. *Brain Pathol,* 9**,** 147-63.

CABISCOL, E., TAMARIT, J. & ROS, J. 2000. Oxidative stress in bacteria and protein damage by reactive oxygen species. *Int Microbiol,* 3**,** 3-8.

CASADIO, R., FRIGIMELICA, E., BOSSU, P., NEUMANN, D., MARTIN, M. U., TAGLIABUE, A. & BORASCHI, D. 2001. Model of interaction of the IL-1 receptor accessory protein IL-1RAcP with the IL-1beta/IL-1R(I) complex. *FEBS Lett,* 499**,** 65-8.

CERRETTI, D. P., KOZLOSKY, C. J., MOSLEY, B., NELSON, N., VAN NESS, K., GREENSTREET, T. A., MARCH, C. J., KRONHEIM, S. R., DRUCK, T., CANNIZZARO, L. A. & ET AL. 1992. Molecular cloning of the interleukin-1 beta converting enzyme. *Science,* 256**,** 97-100.

CHANG, D. T., RINTOUL, G. L., PANDIPATI, S. & REYNOLDS, I. J. 2006. Mutant huntingtin aggregates impair mitochondrial movement and trafficking in cortical neurons. *Neurobiol Dis,* 22**,** 388-400.

CHEVALIER-LARSEN, E. & HOLZBAUR, E. L. 2006. Axonal transport and neurodegenerative disease. *Biochim Biophys Acta,* 1762**,** 1094-108.

CHOO, Y. S., JOHNSON, G. V., MACDONALD, M., DETLOFF, P. J. & LESORT, M. 2004. Mutant huntingtin directly increases susceptibility of mitochondria to the calcium-induced permeability transition and cytochrome c release. *Hum Mol Genet,* 13**,** 1407-20.

CLÉMENT, M.-V., PONTON, A. & PERVAIZ, S. 1998. Apoptosis induced by hydrogen peroxide is mediated by decreased superoxide anion concentration and reduction of intracellular milieu. *FEBS Letters,* 440**,** 13-18.

COGSWELL, J. P., GODLEVSKI, M. M., WISELY, G. B., CLAY, W. C., LEESNITZER, L. M., WAYS, J. P. & GRAY, J. G. 1994. NF-kappa B regulates IL-1 beta transcription through a consensus NF-kappa B binding site and a nonconsensus CRE-like site. *J Immunol,* 153**,** 712-23.

COLES, C. J., EDMONDSON, D. E. & SINGER, T. P. 1979. Inactivation of succinate dehydrogenase by 3-nitropropionate. *J Biol Chem,* 254**,** 5161-7.

DEACON, R. M. J. 2013. Measuring Motor Coordination in Mice. *Journal of Visualized Experiments : JoVE*, 2609.

DESCHEPPER, M., HOOGENDOORN, B., BROOKS, S., DUNNETT, S. B. & JONES, L. 2012. Proteomic changes in the brains of Huntington's disease mouse models reflect pathology and implicate mitochondrial changes. *Brain Res Bull,* 88**,** 210-22.

DINARELLO, C. A. 1984. Interleukin-1. *Rev Infect Dis,* 6**,** 51-95.

DINARELLO, C. A. 1988. Biology of interleukin 1. *Faseb j,* 2**,** 108-15.

DINARELLO, C. A. 1994. The interleukin-1 family: 10 years of discovery. *Faseb j,* 8**,** 1314-25.

DINARELLO, C. A., RENFER, L. & WOLFF, S. M. 1977. Human leukocytic pyrogen: purification and development of a radioimmunoassay. *Proc Natl Acad Sci U S A,* 74**,** 4624-7.

DRUILHE, A., SRINIVASULA, S. M., RAZMARA, M., AHMAD, M. & ALNEMRI, E. S. 2001. Regulation of IL-1beta generation by Pseudo-ICE and ICEBERG, two dominant negative caspase recruitment domain proteins. *Cell Death Differ,* 8**,** 649-57.

DUYAO, M., AMBROSE, C., MYERS, R., NOVELLETTO, A., PERSICHETTI, F., FRONTALI, M., FOLSTEIN, S., ROSS, C., FRANZ, M., ABBOTT, M. & ET AL. 1993. Trinucleotide repeat length instability and age of onset in Huntington's disease. *Nat Genet,* 4**,** 387-92.

EMERIT, J., EDEAS, M. & BRICAIRE, F. 2004. Neurodegenerative diseases and oxidative stress. *Biomed Pharmacother,* 58**,** 39-46.

EMSLEY, H. C., SMITH, C. J., GEORGIOU, R. F., VAIL, A., HOPKINS, S. J., ROTHWELL, N. J. & TYRRELL, P. J. 2005. A randomised phase II study of interleukin-1 receptor antagonist in acute stroke patients. *J Neurol Neurosurg Psychiatry,* 76**,** 1366-72.

ESPINOSA, L., MARGALEF, P. & BIGAS, A. 2015. Non-conventional functions for NF-kappaB members: the dark side of NF-kappaB. *Oncogene,* 34**,** 2279-87.

FERNAGUT, P. O., DIGUET, E., STEFANOVA, N., BIRAN, M., WENNING, G. K., CANIONI, P., BIOULAC, B. & TISON, F. 2002. Subacute systemic 3-nitropropionic acid intoxication induces a distinct motor disorder in adult C57Bl/6 mice: behavioural and histopathological characterisation. *Neuroscience,* 114**,** 1005-1017.

FOGAL, B., LI, J., LOBNER, D., MCCULLOUGH, L. D. & HEWETT, S. J. 2007. System x(c)- activity and astrocytes are necessary for interleukin-1 beta-mediated hypoxic neuronal injury. *J Neurosci,* 27**,** 10094-105.

FONTAINE, M. A., GEDDES, J. W., BANKS, A. & BUTTERFIELD, D. A. 2000. Effect of exogenous and endogenous antioxidants on 3-nitropionic acid-induced in vivo oxidative stress and striatal lesions: insights into Huntington's disease. *J Neurochem,* 75**,** 1709-15.

FRANCIS, K., SMITHERMAN, C., NISHINO, S. F., SPAIN, J. C. & GADDA, G. 2013. The biochemistry of the metabolic poison propionate 3-nitronate and its conjugate acid, 3-nitropropionate. *IUBMB Life,* 65**,** 759-68.

FRENCH, R. A., VANHOY, R. W., CHIZZONITE, R., ZACHARY, J. F., DANTZER, R., PARNET, P., BLUTHÉ, R.-M. & KELLEY, K. W. 1999. Expression and localization of p80 and p68 interleukin-1 receptor proteins in the brain of adult mice. *Journal of Neuroimmunology,* 93**,** 194-202.

GARLANDA, C., DINARELLO, C. A. & MANTOVANI, A. 2013. The interleukin-1 family: back to the future. *Immunity,* 39**,** 1003-18.

GAYLE, D., ILYIN, S. E. & PLATA-SALAMAN, C. R. 1997. Central nervous system IL-1 beta system and neuropeptide Y mRNAs during IL-1 beta-induced anorexia in rats. *Brain Res Bull,* 44**,** 311-7.

GILMORE, T. D. 2006. Introduction to NF-kappaB: players, pathways, perspectives. *Oncogene,* 25**,** 6680-4.

GUYOT, M. C., HANTRAYE, P., DOLAN, R., PALFI, S., MAZIERE, M. & BROUILLET, E. 1997. Quantifiable bradykinesia, gait abnormalities and Huntington's disease-like striatal lesions in rats chronically treated with 3-nitropropionic acid. *Neuroscience,* 79**,** 45-56.

HARMS, L. R., COWIN, G., EYLES, D. W., KURNIAWAN, N. D., MCGRATH, J. J. & BURNE, T. H. 2012. Neuroanatomy and psychomimetic-induced locomotion in C57BL/6J and

129/X1SvJ mice exposed to developmental vitamin D deficiency. *Behav Brain Res,* 230**,** 125-31.
HASSEL, B. & SONNEWALD, U. 1995. Selective inhibition of the tricarboxylic acid cycle of GABAergic neurons with 3-nitropropionic acid in vivo. *J Neurochem,* 65**,** 1184-91.
HAYDEN, M. S. & GHOSH, S. 2004. Signaling to NF-kappaB. *Genes Dev,* 18**,** 2195-224.
HE, F., ZHANG, S., QIAN, F. & ZHANG, C. 1995. Delayed dystonia with striatal CT lucencies induced by a mycotoxin (3-nitropropionic acid). *Neurology,* 45**,** 2178-83.
HE, Y., AKUMUO, R. C., YANG, Y. & HEWETT, S. J. 2017. Mice deficient in L-12/15 lipoxygenase show increased vulnerability to 3-nitropropionic acid neurotoxicity. *Neurosci Lett,* 643**,** 65-69.
HE, Y., JACKMAN, N. A., THORN, T. L., VOUGHT, V. E. & HEWETT, S. J. 2015. Interleukin-1beta protects astrocytes against oxidant-induced injury via an NF-kappaB-dependent upregulation of glutathione synthesis. *Glia,* 63**,** 1568-80.
HEWETT, S. J., JACKMAN, N. A. & CLAYCOMB, R. J. 2012. Interleukin-1beta in Central Nervous System Injury and Repair. *Eur J Neurodegener Dis,* 1**,** 195-211.
HISCOTT, J., MAROIS, J., GAROUFALIS, J., D'ADDARIO, M., ROULSTON, A., KWAN, I., PEPIN, N., LACOSTE, J., NGUYEN, H., BENSI, G. & ET AL. 1993. Characterization of a functional NF-kappa B site in the human interleukin 1 beta promoter: evidence for a positive autoregulatory loop. *Mol Cell Biol,* 13**,** 6231-40.
HUNTINGTON, G. 1872. On Chorea. *The Medical and Surgical Reporter,* 26**,** 317-321.
JACKMAN, N. A., ULIASZ, T. F., HEWETT, J. A. & HEWETT, S. J. 2010. Regulation of system x(c)(-)activity and expression in astrocytes by interleukin-1beta: implications for hypoxic neuronal injury. *Glia,* 58**,** 1806-15.
KASUKAWA, T., MASUMOTO, K. H., NIKAIDO, I., NAGANO, M., UNO, K. D., TSUJINO, K., HANASHIMA, C., SHIGEYOSHI, Y. & UEDA, H. R. 2011. Quantitative expression profile of distinct functional regions in the adult mouse brain. *PLoS One,* 6**,** e23228.
KAUR, C., SIVAKUMAR, V., ZOU, Z. & LING, E. A. 2014. Microglia-derived proinflammatory cytokines tumor necrosis factor-alpha and interleukin-1beta induce Purkinje neuronal apoptosis via their receptors in hypoxic neonatal rat brain. *Brain Struct Funct,* 219**,** 151-70.
KIM, H. J., JEONG, M.-Y., NA, U. & WINGE, D. R. 2012. Flavinylation and Assembly of Succinate Dehydrogenase Are Dependent on the C-terminal Tail of the Flavoprotein Subunit. *The Journal of Biological Chemistry,* 287**,** 40670-40679.
KÖTTER, R. 1994. Postsynaptic integration of glutamatergic and dopaminergic signals in the striatum. *Progress in Neurobiology,* 44**,** 163-196.
LABRIOLA-TOMPKINS, E., CHANDRAN, C., KAFFKA, K. L., BIONDI, D., GRAVES, B. J., HATADA, M., MADISON, V. S., KARAS, J., KILIAN, P. L. & JU, G. 1991. Identification of the discontinuous binding site in human interleukin 1 beta for the type I interleukin 1 receptor. *Proc Natl Acad Sci U S A,* 88**,** 11182-6.
LAKHAN, S. E., KIRCHGESSNER, A. & HOFER, M. 2009. Inflammatory mechanisms in ischemic stroke: therapeutic approaches. *J Transl Med,* 7**,** 97.
LECHAN, R. M., TONI, R., CLARK, B. D., CANNON, J. G., SHAW, A. R., DINARELLO, C. A. & REICHLIN, S. 1990. Immunoreactive interleukin-1β localization in the rat forebrain. *Brain Research,* 514**,** 135-140.

LEE, W. C., YOSHIHARA, M. & LITTLETON, J. T. 2004. Cytoplasmic aggregates trap polyglutamine-containing proteins and block axonal transport in a Drosophila model of Huntington's disease. *Proc Natl Acad Sci U S A,* 101**,** 3224-9.

LI, P., ALLEN, H., BANERJEE, S., FRANKLIN, S., HERZOG, L., JOHNSTON, C., MCDOWELL, J., PASKIND, M., RODMAN, L., SALFELD, J. & ET AL. 1995. Mice deficient in IL-1 beta-converting enzyme are defective in production of mature IL-1 beta and resistant to endotoxic shock. *Cell,* 80**,** 401-11.

LI, X., FANG, P., MAI, J., CHOI, E. T., WANG, H. & YANG, X. F. 2013. Targeting mitochondrial reactive oxygen species as novel therapy for inflammatory diseases and cancers. *J Hematol Oncol,* 6**,** 19.

LIN, M. T. & BEAL, M. F. 2006. Mitochondrial dysfunction and oxidative stress in neurodegenerative diseases. *Nature,* 443**,** 787-95.

LINHER-MELVILLE, K., HAFTCHENARY, S., GUNNING, P. & SINGH, G. 2015. Signal transducer and activator of transcription 3 and 5 regulate system Xc- and redox balance in human breast cancer cells. *Mol Cell Biochem,* 405**,** 205-21.

LIOT, G., BOSSY, B., LUBITZ, S., KUSHNAREVA, Y., SEJBUK, N. & BOSSY-WETZEL, E. 2009. Complex II inhibition by 3-NP causes mitochondrial fragmentation and neuronal cell death via an NMDA- and ROS-dependent pathway. *Cell death and differentiation,* 16**,** 899-909.

LOMEDICO, P. T., GUBLER, U., HELLMANN, C. P., DUKOVICH, M., GIRI, J. G., PAN, Y. C., COLLIER, K., SEMIONOW, R., CHUA, A. O. & MIZEL, S. B. 1984. Cloning and expression of murine interleukin-1 cDNA in Escherichia coli. *Nature,* 312**,** 458-62.

LUDOLPH, A. C., HE, F., SPENCER, P. S., HAMMERSTAD, J. & SABRI, M. 1991. 3-Nitropropionic acid-exogenous animal neurotoxin and possible human striatal toxin. *Can J Neurol Sci,* 18**,** 492-8.

LUDOLPH, A. C., SEELIG, M., LUDOLPH, A. G., SABRI, M. I. & SPENCER, P. S. 1992. ATP deficits and neuronal degeneration induced by 3-nitropropionic acid. *Ann N Y Acad Sci,* 648**,** 300-2.

MACDONALD, M. E., AMBROSE, C. M., DUYAO, M. P., MYERS, R. H., LIN, C., SRINIDHI, L., BARNES, G., TAYLOR, S. A., JAMES, M., GROOT, N., MACFARLANE, H., JENKINS, B., ANDERSON, M. A., WEXLER, N. S., GUSELLA, J. F., BATES, G. P., BAXENDALE, S., HUMMERICH, H., KIRBY, S., NORTH, M., YOUNGMAN, S., MOTT, R., ZEHETNER, G., SEDLACEK, Z., POUSTKA, A., FRISCHAUF, A.-M., LEHRACH, H., BUCKLER, A. J., CHURCH, D., DOUCETTE-STAMM, L., O'DONOVAN, M. C., RIBA-RAMIREZ, L., SHAH, M., STANTON, V. P., STROBEL, S. A., DRATHS, K. M., WALES, J. L., DERVAN, P., HOUSMAN, D. E., ALTHERR, M., SHIANG, R., THOMPSON, L., FIELDER, T., WASMUTH, J. J., TAGLE, D., VALDES, J., ELMER, L., ALLARD, M., CASTILLA, L., SWAROOP, M., BLANCHARD, K., COLLINS, F. S., SNELL, R., HOLLOWAY, T., GILLESPIE, K., DATSON, N., SHAW, D. & HARPER, P. S. 1993. A novel gene containing a trinucleotide repeat that is expanded and unstable on Huntington's disease chromosomes. *Cell,* 72**,** 971-983.

MAGGIOLI, E., MCARTHUR, S., MAURO, C., KIESWICH, J., KUSTERS, D. H., REUTELINGSPERGER, C. P., YAQOOB, M. & SOLITO, E. 2016. Estrogen protects the blood-brain barrier from inflammation-induced disruption and increased lymphocyte trafficking. *Brain Behav Immun,* 51**,** 212-22.

MARCH, C. J., MOSLEY, B., LARSEN, A., CERRETTI, D. P., BRAEDT, G., PRICE, V., GILLIS, S., HENNEY, C. S., KRONHEIM, S. R., GRABSTEIN, K. & ET AL. 1985. Cloning, sequence and expression of two distinct human interleukin-1 complementary DNAs. *Nature,* 315**,** 641-7.

MÁRQUEZ-VALADEZ, B., MALDONADO, P. D., GALVÁN-ARZATE, S., MÉNDEZ-CUESTA, L. A., PÉREZ-DE LA CRUZ, V., PEDRAZA-CHAVERRÍ, J., CHÁNEZ-CÁRDENAS, M. E. & SANTAMARÍA, A. 2012. Alpha-mangostin induces changes in glutathione levels associated with glutathione peroxidase activity in rat brain synaptosomes. *Nutritional Neuroscience,* 15**,** 13-19.

MARTINON, F. & TSCHOPP, J. 2007. Inflammatory caspases and inflammasomes: master switches of inflammation. *Cell Death Differ,* 14**,** 10-22.

MAVERAKIS, E., KIM, K., SHIMODA, M., GERSHWIN, M. E., PATEL, F., WILKEN, R., RAYCHAUDHURI, S., RUHAAK, L. R. & LEBRILLA, C. B. 2015. Glycans in the immune system and The Altered Glycan Theory of Autoimmunity: a critical review. *J Autoimmun,* 57**,** 1-13.

MEISER, J., WEINDL, D. & HILLER, K. 2013. Complexity of dopamine metabolism. *Cell Communication and Signaling : CCS,* 11**,** 34-34.

MILAKOVIC, T. & JOHNSON, G. V. 2005. Mitochondrial respiration and ATP production are significantly impaired in striatal cells expressing mutant huntingtin. *J Biol Chem,* 280**,** 30773-82.

MIN, K. J., JOU, I. & JOE, E. 2003. Plasminogen-induced IL-1beta and TNF-alpha production in microglia is regulated by reactive oxygen species. *Biochem Biophys Res Commun,* 312**,** 969-74.

MOGAMI, M., HAYASHI, Y., MASUDA, T., KOHRI, K., NISHINO, H. & HIDA, H. 2008. Altered striatal vulnerability to 3-nitropropionic acid in rats due to sex hormone levels during late phase of brain development. *Neurosci Lett,* 436**,** 321-5.

MORRIS, M. P., PAGAN, C. & WARMKE, H. E. 1954. Hiptagenic Acid, a Toxic Component of Indigofera endecaphylla. *Science,* 119**,** 322-3.

NABEL, G. J. & VERMA, I. M. 1993. Proposed NF-kappa B/I kappa B family nomenclature. *Genes Dev,* 7**,** 2063.

NAGATA, S. 1997. Apoptosis by Death Factor. *Cell,* 88**,** 355-365.

NISHINO, H., HIDA, H., KUMAZAKI, M., SHIMANO, Y., NAKAJIMA, K., SHIMIZU, H., OOIWA, T. & BABA, H. 2000. The striatum is the most vulnerable region in the brain to mitochondrial energy compromise: a hypothesis to explain its specific vulnerability. *J Neurotrauma,* 17**,** 251-60.

NISHINO, H., KUMAZAKI, M., FUKUDA, A., FUJIMOTO, I., SHIMANO, Y., HIDA, H., SAKURAI, T., DESHPANDE, S. B., SHIMIZU, H., MORIKAWA, S. & INUBUSHI, T. 1997. Acute 3-nitropropionic acid intoxication induces striatal astrocytic cell death and dysfunction of the blood-brain barrier: involvement of dopamine toxicity. *Neurosci Res,* 27**,** 343-55.

NISHINO, H., NAKAJIMA, K., KUMAZAKI, M., FUKUDA, A., MURAMATSU, K., DESHPANDE, S. B., INUBUSHI, T., MORIKAWA, S., BORLONGAN, C. V. & SANBERG, P. R. 1998. Estrogen protects against while testosterone exacerbates vulnerability of the lateral striatal artery to chemical hypoxia by 3-nitropropionic acid. *Neurosci Res,* 30**,** 303-12.

NOWAKOWSKI, B. E. & MAURER, R. A. 1994. Multiple Pit-1-binding sites facilitate estrogen responsiveness of the prolactin gene. *Mol Endocrinol,* 8**,** 1742-9.

O'DONNELL, M. A., HASE, H., LEGARDA, D. & TING, A. T. 2012. NEMO inhibits programmed necrosis in an NFkappaB-independent manner by restraining RIP1. *PLoS One,* 7**,** e41238.

OLEJNICZAK, M., URBANEK, M. O. & KRZYZOSIAK, W. J. 2015. The role of the immune system in triplet repeat expansion diseases. *Mediators Inflamm,* 2015**,** 873860.

ONA, V. O., LI, M., VONSATTEL, J. P., ANDREWS, L. J., KHAN, S. Q., CHUNG, W. M., FREY, A. S., MENON, A. S., LI, X. J., STIEG, P. E., YUAN, J., PENNEY, J. B., YOUNG, A. B., CHA, J. H. & FRIEDLANDER, R. M. 1999. Inhibition of caspase-1 slows disease progression in a mouse model of Huntington's disease. *Nature,* 399**,** 263-7.

PALOMO, J., DIETRICH, D., MARTIN, P., PALMER, G. & GABAY, C. 2015. The interleukin (IL)-1 cytokine family--Balance between agonists and antagonists in inflammatory diseases. *Cytokine,* 76**,** 25-37.

PEDRAZA-CHAVERRÍ, J., REYES-FERMÍN, L. M., NOLASCO-AMAYA, E. G., OROZCO-IBARRA, M., MEDINA-CAMPOS, O. N., GONZÁLEZ-CUAHUTENCOS, O., RIVERO-CRUZ, I. & MATA, R. 2009. ROS scavenging capacity and neuroprotective effect of α-mangostin against 3-nitropropionic acid in cerebellar granule neurons. *Experimental and Toxicologic Pathology,* 61**,** 491-501.

PENNINGTON, R. J. 1961. Biochemistry of dystrophic muscle. Mitochondrial succinate-tetrazolium reductase and adenosine triphosphatase. *Biochem J,* 80**,** 649-54.

PEREZ-SEVERIANO, F., SANTAMARIA, A., PEDRAZA-CHAVERRI, J., MEDINA-CAMPOS, O. N., RIOS, C. & SEGOVIA, J. 2004. Increased formation of reactive oxygen species, but no changes in glutathione peroxidase activity, in striata of mice transgenic for the Huntington's disease mutation. *Neurochem Res,* 29**,** 729-33.

PERKINS, N. D. 2006. Post-translational modifications regulating the activity and function of the nuclear factor kappa B pathway. *Oncogene,* 25**,** 6717-30.

PETERS, V. A., JOESTING, J. J. & FREUND, G. G. 2013. IL-1 receptor 2 (IL-1R2) and its role in immune regulation. *Brain, behavior, and immunity,* 32**,** 1-8.

PETRUSKA, J., HARTENSTINE, M. J. & GOODMAN, M. F. 1998. Analysis of strand slippage in DNA polymerase expansions of CAG/CTG triplet repeats associated with neurodegenerative disease. *J Biol Chem,* 273**,** 5204-10.

PRIESTLE, J. P., SCHAR, H. P. & GRUTTER, M. G. 1988. Crystal structure of the cytokine interleukin-1 beta. *Embo j,* 7**,** 339-43.

RAY, P. D., HUANG, B.-W. & TSUJI, Y. 2012. Reactive oxygen species (ROS) homeostasis and redox regulation in cellular signaling. *Cellular Signalling,* 24**,** 981-990.

REED, D. R., BACHMANOV, A. A. & TORDOFF, M. G. 2007. Forty mouse strain survey of body composition. *Physiology & behavior,* 91**,** 593-600.

RELTON, J. K. & ROTHWELL, N. J. 1992. Interleukin-1 receptor antagonist inhibits ischaemic and excitotoxic neuronal damage in the rat. *Brain Res Bull,* 29**,** 243-6.

REN, K. & TORRES, R. 2009. Role of interleukin-1β during pain and inflammation. *Brain research reviews,* 60**,** 57-64.

ROSEN, G. D., PUNG, C. J., OWENS, C. B., CAPLOW, J., KIM, H., MOZHUI, K., LU, L. & WILLIAMS, R. W. 2009. Genetic modulation of striatal volume by loci on Chrs 6 and 17 in BXD recombinant inbred mice. *Genes Brain Behav,* 8**,** 296-308.

ROSEN, G. D. & WILLIAMS, R. W. 2001. Complex trait analysis of the mouse striatum: independent QTLs modulate volume and neuron number. *BMC Neurosci,* 2**,** 5.
ROSS, C. A. & TABRIZI, S. J. 2011. Huntington's disease: from molecular pathogenesis to clinical treatment. *Lancet Neurol,* 10**,** 83-98.
ROTHWELL, N. J. & LUHESHI, G. N. 2000. Interleukin 1 in the brain: biology, pathology and therapeutic target. *Trends Neurosci,* 23**,** 618-25.
RUBINSZTEIN, D. C. 2002. Lessons from animal models of Huntington's disease. *Trends Genet,* 18**,** 202-9.
SCHULZ, J. B., WELLER, M. & MOSKOWITZ, M. A. 1999. Caspases as treatment targets in stroke and neurodegenerative diseases. *Ann Neurol,* 45**,** 421-9.
SEN, R. & BALTIMORE, D. 1986a. Inducibility of kappa immunoglobulin enhancer-binding protein Nf-kappa B by a posttranslational mechanism. *Cell,* 47**,** 921-8.
SEN, R. & BALTIMORE, D. 1986b. Multiple nuclear factors interact with the immunoglobulin enhancer sequences. *Cell,* 46**,** 705-16.
SHI, J., HE, Y., HEWETT, S. J. & HEWETT, J. A. 2016. Interleukin 1beta Regulation of the System xc- Substrate-specific Subunit, xCT, in Primary Mouse Astrocytes Involves the RNA-binding Protein HuR. *J Biol Chem,* 291**,** 1643-51.
SHIH, A. Y., IMBEAULT, S., BARAKAUSKAS, V., ERB, H., JIANG, L., LI, P. & MURPHY, T. H. 2005. Induction of the Nrf2-driven antioxidant response confers neuroprotection during mitochondrial stress in vivo. *J Biol Chem,* 280**,** 22925-36.
SHIH, V. F., TSUI, R., CALDWELL, A. & HOFFMANN, A. 2011. A single NFkappaB system for both canonical and non-canonical signaling. *Cell Res,* 21**,** 86-102.
SIMS, J. E. & SMITH, D. E. 2010. The IL-1 family: regulators of immunity. *Nat Rev Immunol,* 10**,** 89-102.
SIPIONE, S. & CATTANEO, E. 2001. Modeling Huntington's disease in cells, flies, and mice. *Mol Neurobiol,* 23**,** 21-51.
SOLLE, M., LABASI, J., PERREGAUX, D. G., STAM, E., PETRUSHOVA, N., KOLLER, B. H., GRIFFITHS, R. J. & GABEL, C. A. 2001. Altered cytokine production in mice lacking P2X(7) receptors. *J Biol Chem,* 276**,** 125-32.
SOROLLA, M. A., REVERTER-BRANCHAT, G., TAMARIT, J., FERRER, I., ROS, J. & CABISCOL, E. 2008. Proteomic and oxidative stress analysis in human brain samples of Huntington disease. *Free Radic Biol Med,* 45**,** 667-78.
SPENCER, P. S. & SCHAUMBURG, H. H. 1977. Ultrastructural studies of the dying-back process. IV. Differential vulnerability of PNS and CNS fibers in experimental central-peripheral distal axonopathies. *J Neuropathol Exp Neurol,* 36**,** 300-20.
SQUITIERI, F., BERARDELLI, A., NARGI, E., CASTELLOTTI, B., MARIOTTI, C., CANNELLA, M., LAVITRANO, M. L., DE GRAZIA, U., GELLERA, C. & RUGGIERI, S. 2000. Atypical movement disorders in the early stages of Huntington's disease: clinical and genetic analysis. *Clin Genet,* 58**,** 50-6.
TABRIZI, S. J., CLEETER, M. W., XUEREB, J., TAANMAN, J. W., COOPER, J. M. & SCHAPIRA, A. H. 1999. Biochemical abnormalities and excitotoxicity in Huntington's disease brain. *Ann Neurol,* 45**,** 25-32.
THORNBERRY, N. A., BULL, H. G., CALAYCAY, J. R., CHAPMAN, K. T., HOWARD, A. D., KOSTURA, M. J., MILLER, D. K., MOLINEAUX, S. M., WEIDNER, J. R., AUNINS, J. & ET AL. 1992. A

novel heterodimeric cysteine protease is required for interleukin-1 beta processing in monocytes. *Nature,* 356**,** 768-74.

TREHARNE, A. C., OHLENDORF, D. H., WEBER, P. C., WENDOLOSKI, J. J. & SALEMME, F. R. 1990. X-ray structural studies of the cytokine interleukin 1-beta. *Prog Clin Biol Res,* 349**,** 309-19.

TROY, C. M., STEFANIS, L., PROCHIANTZ, A., GREENE, L. A. & SHELANSKI, M. L. 1996. The contrasting roles of ICE family proteases and interleukin-1beta in apoptosis induced by trophic factor withdrawal and by copper/zinc superoxide dismutase down-regulation. *Proc Natl Acad Sci U S A,* 93**,** 5635-40.

TUNEZ, I., TASSET, I., PEREZ-DE LA CRUZ, V. & SANTAMARIA, A. 2010. 3-Nitropropionic acid as a tool to study the mechanisms involved in Huntington's disease: past, present and future. *Molecules,* 15**,** 878-916.

VIGERS, G. P., ANDERSON, L. J., CAFFES, P. & BRANDHUBER, B. J. 1997. Crystal structure of the type-I interleukin-1 receptor complexed with interleukin-1beta. *Nature,* 386**,** 190-4.

VIGUERA, E., CANCEILL, D. & EHRLICH, S. D. 2001. Replication slippage involves DNA polymerase pausing and dissociation. *Embo j,* 20**,** 2587-95.

VONSATTEL, J. P., KELLER, C. & CORTES RAMIREZ, E. P. 2011. Huntington's disease - neuropathology. *Handb Clin Neurol,* 100**,** 83-100.

VONSATTEL, J. P., MYERS, R. H., STEVENS, T. J., FERRANTE, R. J., BIRD, E. D. & RICHARDSON, E. P., JR. 1985. Neuropathological classification of Huntington's disease. *J Neuropathol Exp Neurol,* 44**,** 559-77.

WALKER, F. O. 2007. Huntington's disease. *Lancet,* 369**,** 218-28.

WANG, C. E., LI, S. & LI, X. J. 2010. Lack of interleukin-1 type 1 receptor enhances the accumulation of mutant huntingtin in the striatum and exacerbates the neurological phenotypes of Huntington's disease mice. *Mol Brain,* 3**,** 33.

WANG, X., BARONE, F. C., AIYAR, N. V. & FEUERSTEIN, G. Z. 1997. Interleukin-1 receptor and receptor antagonist gene expression after focal stroke in rats. *Stroke,* 28**,** 155-61; discussion 161-2.

WILSON, K. P., BLACK, J. A., THOMSON, J. A., KIM, E. E., GRIFFITH, J. P., NAVIA, M. A., MURCKO, M. A., CHAMBERS, S. P., ALDAPE, R. A., RAYBUCK, S. A. & ET AL. 1994. Structure and mechanism of interleukin-1 beta converting enzyme. *Nature,* 370**,** 270-5.

WYTTENBACH, A., SAUVAGEOT, O., CARMICHAEL, J., DIAZ-LATOUD, C., ARRIGO, A. P. & RUBINSZTEIN, D. C. 2002. Heat shock protein 27 prevents cellular polyglutamine toxicity and suppresses the increase of reactive oxygen species caused by huntingtin. *Hum Mol Genet,* 11**,** 1137-51.

YAKES, F. M. & VAN HOUTEN, B. 1997. Mitochondrial DNA damage is more extensive and persists longer than nuclear DNA damage in human cells following oxidative stress. *Proc Natl Acad Sci U S A,* 94**,** 514-9.

YANG, G. Y., LIU, X. H., KADOYA, C., ZHAO, Y. J., MAO, Y., DAVIDSON, B. L. & BETZ, A. L. 1998. Attenuation of ischemic inflammatory response in mouse brain using an adenoviral vector to induce overexpression of interleukin-1 receptor antagonist. *J Cereb Blood Flow Metab,* 18**,** 840-7.

YOON, S. R., DUBEAU, L., DE YOUNG, M., WEXLER, N. S. & ARNHEIM, N. 2003. Huntington disease expansion mutations in humans can occur before meiosis is completed. *Proc Natl Acad Sci U S A,* 100**,** 8834-8.

VITA

NAME OF AUTHOR: Matthew Frederick Allen

HOMETOWN: Huddersfield, England

EDUCATION

B.Sc. (Hons) Medical Genetics	2015	The University of Huddersfield, Huddersfield, UK.

TEACHING EXPERIENCE

2015 – 2017	Fall semesters:	BIO477 Biochemistry 1
	Spring semesters:	BIO305 – Integrative Laboratory Techniques

CORRESPONDENCE: mfallen@syr.edu